Aus dem Institut für Kardiovaskuläre Physiologie und Pathophysiologie
Walter Brendel Zentrum für Experimentelle Medizin
Institut der Ludwig-Maximilians-Universität München
Direktor: Prof. Dr. Christian Wahl-Schott

The molecular insights into the pathogenesis of myocarditis

Dissertation
zum Erwerb des Doktorgrades der Naturwissenschaften
an der Medizinischen Fakultät der
Ludwig-Maximilians-Universität München

vorgelegt von

Felicitas Adelheid Böhm

aus Fürth

2023

Mit Genehmigung der Medizinischen Fakultät

der Universität München

Betreuer:	Prof. Dr. rer. nat. Alexander Bartelt
Zweitgutachter(in):	Prof. Dr. rer. nat. Jörg Renkawitz
Dekan:	Prof. Dr. med. Thomas Gudermann

Tag der mündlichen Prüfung: 12. Februar 2024

Table of content

Table of content ..... **V**

Zusammenfassung ..... **IX**

Abstract ..... **XI**

List of figures ..... **XII**

List of tables ..... **XIV**

List of abbreviations ..... **XV**

1. Introduction **19**

1.1 Human myocarditis 19

1.1.1 Etiology 19

1.1.2 Clinical presentation and diagnosis of myocarditis 20

1.1.3 Therapeutic approach 21

1.1.4 Pathophysiology 22

1.1.4.1 Acute phase 24

1.1.4.2 Subacute phase 24

1.1.4.3 Chronic phase 24

1.2 Immune system 25

1.2.1 Neutrophils (PMN) 25

1.2.1.1 The leukocyte recruitment cascade 25

1.2.1.2 Neutrophil extracellular traps (NETs) 26

1.2.2 Plasmacytoid dendritic cells (pDC) 28

1.2.2.1 Functions of pDCs 29

1.2.2.2 IFN-I signaling pathway 30

1.2.2.3 pDCs as IFN-I producing cells 31

1.2.2.4 IFN-I and diseases 34

1.2.3 T cells 34

1.3 Myocarditis mouse model 36

1.3.1 The EAM model 37
1.3.2 Time course of the EAM 37
1.3.3 Cellular infiltrate of EAM 38
1.3.4 Cytokines involved during EAM 39
1.4 Break of tolerance - autoimmune myocarditis 40
1.5 Midkine 41

2. Aim 43

3. Material and Methods 44

3.1 Cells 44
3.2 Animals 44
3.3 Experimental autoimmune myocarditis (EAM) mouse model 44
3.3.1 Immunization of mice 44
3.3.2 Histology and heart body weight ratio 45
3.3.3 Whole blood count 45
3.3.4 Serum analysis 46
3.3.5 Flow cytometry 46
3.3.5.1 Tissue sample preparation 46
3.3.5.2 Cell surface marker staining 47
3.3.5.3 Intracellular cytokine staining 47
3.3.6 Multiplex Elisa 48
3.3.7 Quantitative polymerase chain reaction 49
3.3.7.1 RNA Isolation 49
3.3.7.2 gDNA digestion and reverse transcription 50
3.3.7.3 Quantitative real-time PCR (qRT-PCR) 50
3.3.8 Echocardiography 51
3.3.9 Masson trichrome staining 52
3.4 Mouse treatment experiments 53
3.4.1 Treatment with receptor associated protein (RAP) 53

3.4.2 Treatment with a monoclonal Anti-IFNAR blocking Ab 54
3.4.3 Treatment with DNase and Chloridamidine 55
3.5 Immunofluoresence 55
3.6 Statistics 57
4. Results 58
4.1 Mice develop EAM 58
4.2 The Role of the MK-LRP1-NET-axis 61
4.2.1 MK gene expression is upregulated during EAM 61
4.2.2 LRP1 is critical for the pathogenesis of EAM 61
4.2.3 MK-mediated NET formation is LRP1 dependent *in vitro* 62
4.3 Targeting NETs as a therapeutic intervention of myocarditis on day 63 64
4.4 The role of IFN-I during EAM 66
4.4.1 The role of pDCs during EAM 67
4.4.2 IFN-I pathway genes are upregulated during EAM 67
4.4.3 Blocking IFNAR until day 14 does not alter leukocyte composition in the heart during EAM 70
4.4.4 Blocking IFNAR reduced infiltration of leukocytes into the cardiac tissue on day 21 after the onset of EAM 76
5. Discussion 82
5.1 EAM model 82
5.2 MK-LRP1 axis plays a role during EAM 83
5.3 MK mediates NET formation via LRP1 *in vitro* 84
5.4 Blocking NETs has no therapeutic intervention 85
5.5 The IFN-I pathway plays a role during EAM 87
5.5.1 IFN-I pathway genes during EAM 87
5.5.2 The role of pDCs for EAM 88
5.5.3 Role of IFN-I on leukocytes during EAM 89
5.5.4 Role of IFN-I for inflammatory cytokines 92
5.5.5 Clinical relevance of the results 92

6. Conclusion 94

References 96

Acknowledgements 120

Publications 121

Affidavit 122

Zusammenfassung

Die Myokarditis ist eine entzündliche Herzerkrankung, die häufig durch kardiotrope Viren ausgelöst wird. Während die myokardiale Entzündung bei der Mehrzahl der Patienten spontan abklingt, kann die akute Entzündung in eine subakute und chronische Phase übergehen, die schließlich zu kardialem Remodeling und Herzversagen führen kann. Im Gegensatz zum adaptiven Immunsystem ist die Rolle der angeborenen Immunität bisher noch nicht ganz aufgeklärt worden. Ziel dieses Projektes ist es, den Pathomechanismus während der Herzmuskelentzündung weiter zu untersuchen und somit neue Angriffspunkte zur Behandlung der Myokarditis zu identifizieren.

Um Einblicke in die zugrundeliegenden Mechanismen der postinfektiösen Myokarditis und Kardiomyopathien zu erhalten, wurde ein experimentelles Autoimmunmyokarditis Mausmodell (EAM) verwendet. In diesem Modell wird die Herzmuskelentzündung durch die Gabe eines kardialen Peptids zusammen mit *Complete Freund's Adjuvant* in Mäusen induziert. Die akute Phase des EAM-Modells ähnelt der postviralen Erkrankung nach dem Übergang zur Autoimmunmyokarditis, einem klinischen Szenario, das viele Patienten mit chronischer Myokarditis betrifft.

Wir konnten beobachten, dass das Zytokin Midkine (MK) während der kardialen Entzündung im Herzgewebe im EAM-Modell hochreguliert wird. *In vivo* Experimente identifizierten außerdem eine kritische Rolle für den Low-Density-Lipoprotein-Rezeptor-Protein 1 (LRP1) Rezeptor. *In vitro* Experimente bestätigten zudem, dass LRP1 den funktionell relevanten Rezeptor für MK bei der Bildung von Neutrophilen extrazellulären Traps (NETs) in Neutrophil-ähnlichen Hoxb8-Zellen darstellt. Die gezielte Bekämpfung von NETs nach Beginn der EAM ab Tag 21 durch die Applikation von DNase oder Cl-Amid als therapeutische Intervention hat jedoch keinen Einfluss auf die Myokarditis an Tag 63.

Es konnte auch gezeigt werden, dass plasmazytoide dendritische Zellen (pDCs), an Tag 21 im Herzgewebe der Mäuse während der EAM eingewandert sind. pDCs stellen die Hauptquelle von Interferon Typ I (IFN-I) dar. IFN-I ist für eine Vielzahl von Genen verantwortlich, die in aktivierten pDCs exprimiert werden (IFIT1, IFIT3, IRF3, IRF7, IRF8 und ISG15). Weiterhin sind sie dafür bekannt, eine Vielzahl von pro-inflammatorischen Zytokinen (CXCL10 und IL-6) zu sezernieren. Die Ergebnisse zeigten, dass IFN-I, die Interferon-regulierenden Faktoren, die Interferon-stimulierenden Gene und Chemokine an Tag 14 und 21 in Mäusen mit EAM hochreguliert sind. Bei Experimenten, indem der Interferonrezeptor blockiert wurde, konnte zudem eine reduzierte Infiltration von Leukozyten (Neutrophile, T-Zellen und pDCs) in das kardiale Gewebe an Tag 21 nach Induktion der EAM festgestellt werden.

Dies unterstreicht deutlich die Bedeutung von IFN-I während der kardialen Entzündung.

Zusammenfassend postuliert diese Arbeit, dass die MK-LRP1-NET-Achse sowie der IFN-I Weg eine entscheidende Rolle während der Herzmuskelentzündung spielt. Somit könnte der Interferon Signalweg ein neuartiges therapeutisches Ziel für die Behandlung der kardialen Entzündung darstellen.

Abstract

Myocarditis is an inflammatory disease which is often triggered by cardiotropic viruses. Whereas myocardial inflammation resolves spontaneously in the majority of patients, acute inflammation can progress to subacute and chronic inflammation finally resulting in cardiac remodeling and heart failure. In contrast to the adaptive immune system, the role of innate immunity remains have not been elucidated so far. In this project, the aim is to discover detailed pathomechanisms during cardiac inflammation and identify new targets to treat myocarditis.

To gain insights into the underlying mechanisms of post-infectious myocarditis and cardiomyopathy an experimental autoimmune myocarditis (EAM) murine model was used. In this model, mice are immunized with epitopes of α myosin heavy chain together with complete Freund´s adjuvant. The acute phase of the EAM model resembles post-viral disease after transition to autoimmune myocarditis, a clinical scenario affecting many patients developing chronic myocarditis.

In this thesis, it is demonstrated that the cytokine Midkine (MK) is upregulated during cardiac inflammation in the inflamed heart. In vivo experiments identified a critical role for the low-density lipoprotein receptor-related protein 1 (LRP1). *In vitro* experiments showed that LRP1 acts as the functionally relevant receptor to MK for NET formation in neutrophil-derived Hoxb8 cells. However, targeting NETs after the onset of EAM with the application of DNase or Cl-Amid as a therapeutic intervention has no impact on myocarditis during the chronic phase at day 63.

It could be also shown that a new key player between the innate and adaptive immune system, so called plasmacytoid dendritic cells (pDCs), are present on day 21 in the cardiac tissue of mice during EAM. pDCs represent the main source of interferon type I (IFN-I). Therefore, IFN-I accounts for a lot of genes expressed in activated pDCs (IFIT1, IFIT3, IRF3, IRF7, IRF8 and ISG15). pDCs are also known to secret a variety of pro-inflammatory cytokines (CXCL10 and IL-6). It could be reported for the first time IFN-I, interferon regulatory factors, and interferon stimulated genes and chemokines are all upregulated in EAM mice on day 14 and 21. This significant upregulation on day 14 and 21 of genes involved in the IFN-I pathway highlights the importance of IFN-I during cardiac inflammation. Interferon receptor blocking experiments showed a reduced infiltration of leukocytes (neutrophils, T cells and pDCs) into the cardiac tissue on day 21 after the onset of EAM.

In conclusion, this work postulates that the MK-LRP1-NET axis as well as the IFN-I pathway play a crucial role during EAM. Thus, the IFN-I pathway may represent a novel therapeutic target for the treatment of cardiac inflammation.

List of figures

Figure 1-1 Pathogenic mechanism involved in myocarditis. 23

Figure 1-2 The leukocyte recruitment cascade. 26

Figure 1-3 Schematic mechanism of NET release. 27

Figure 1-4 Functions of pDCs. 29

Figure 1-5 Schematic presentation of type I interferon (IFN) signaling. 31

Figure 1-6 Signaling pathway specific for pDCs 33

Figure 1-7 Development of T cells. 36

Figure 1-8 The phases of experimental autoimmune myocarditis (EAM) in the mouse model 38

Figure 1-9 Schematic figure of the possible role of Midkine in leukocyte recruitment 42

Figure 3-1 Evaluation of the fibrotic tissue in the myocardium. 53

Figure 3-2 Experimental protocol for blocking LRP1 during EAM *in vivo* 54

Figure 3-3 Experimental protocol for blocking the interferon receptor (IFNAR) using a blocking antibody (Ab) during EAM *in vivo*. 54

Figure 3-4 Experimental protocol for inhibiting NETs during EAM *in vivo*. 55

Figure 4-1 Balb/c WT mice develop experimental autoimmune myocarditis 60

Figure 4-2 MK gene expression is altered during EAM in the cardiac tissue and spleen on day 21 61

Figure 4-3 LRP1 is critical for the pathogenesis of EAM 62

Figure 4-4 MK induced NET formation via LRP1 *in vitro* 64

Figure 4-5 Targeting NETs after onset of EAM did not impact fibrosis or systolic function 66

Figure 4-6 Quantitative analysis of the infiltration of activated pDCs into the cardiac tissue at day 14 67

Figure 4-7 Gene expression of genes involved in the IFN-I pathway. 69

Figure 4-8 Blocking IFNAR from day 7 until 14 has no impact on the outcome of myocarditis 71

Figure 4-9 Gating strategy for heart infiltrating cells after blocking IFNAR until day 14 72

Figure 4-10 Blocking IFNAR does not alter leukocyte composition of heart infiltrating cells on day 14 73

Figure 4-11 Gating strategy for heart infiltrating cells after blocking IFNAR until day 14. 74

Figure 4-12 Quantitative analysis of infiltrating T cells into the cardiac tissue on day 14 75

Figure 4-13 Quantification of cytokines in the serum after blocking IFNAR on day 14 after the induction of EAM 76

Figure 4-14 Blocking IFNAR from day 7 until 21 has no impact on the outcome of myocarditis 78

Figure 4-15 Targeting the interferon receptor (IFNAR) reduces leukocyte infiltration into the cardiac tissue on day 21 79

Figure 4-16 Quantitative analysis of infiltrating T cells into the cardiac tissue on day 21. 81

Figure 5-1 Mode of action of IFNAR blocking antibody on day 21 91

Figure 6-1 Proposed mechanism of IFN-I and immune cells during myocarditis. 95

List of tables

Table 1 Overview of possible causes of myocarditis. 20

Table 2 Antibody cocktail for cell surface staining 47

Table 3 Antibody cocktail for cell surface marker 48

Table 4 Antibody cocktail for cytokine staining 48

Table 5 Primer sequences for qPCR. 51

Table 6 Protocol for qRT-PCR 51

Table 7 Buffer used for Immunofluorescence staining. 56

Table 8 Primary antibodies used for Immunofluorescence staining. 57

Table 9 Secondary antibodies used for Immunofluorescence staining. 57

List of abbreviations

Ab	Antibody
αMyhC	Alpha Myosin heavy chain
ADM	Adhesion medium
APC	Antigen presenting cells
BW	Body weight
BSA	Bovine serum albumin
CAR	Coxsackievirus adenoviral receptor
CD	Cluster of differentiation
CD8+	Cytotoxic CD8 positive T cells
CD4+	CD4 positive T cells
CFA	Complete Freund´s Adjuvant
Cl-Amid	Chloridamide
CTTP	Cytoplasmic transductional-transcriptional processor
CVB3	Coxsackievirus B3
DAMPs	Damage-associated molecular patterns
DC	Dendritic cell
DCM	Dilated cardiomyopathy
DN	Double negative
DNA	Desoxyribonucleic acid
DP	Double positive
Ds	Double stranded
EAM	Experimental autoimmune myocarditis
EC	Endothelial cell
EDTA	Ethylenediamine-tetraacetic acid
EMB	Endomyocardial biopsy
FACS	Fluorescence-activated cell sorting

FCS	Fetale bovine serum
HEPES	4-(2-hydroxyethyl)-1-piperazineethanesulfonic acid
HEV	High endothelial venules
HW	Heart weight
HW/BW	Heart weight/body weight
ICAM-1	Intercellular adhesion molecule-1
IgG	Immunoglobulin G
IL	Interleukin
IFN	Interferon
IFN-I	Type I Interferon
IFNAR	Interferon type I receptor
IRAK	IL-1 receptor associated kinase
IRF	Interferon regulatory factors
ISG	Interferon stimulated genes
ISGF	Interferon stimulated gene factor
ISRE	Interferon stimulated response element
i.p.	Intraperitoneal
JAK	Janus kinase
KO	Knockout
LFA-1	Lymphocyte function associated antigen-1
LPS	Lipopolysaccharide
MAC-1	macrophage antigen-1
MAPK	Mitogen-activated protein kinases
MHC	Major Histocompatibility complex
MK	Midkine
MPO	Myeloperoxidase
MyD88	Myeloid differentiation factor 88
NADPH	Nicotinamide adenine dinucleotide phosphate

NE	Neutrophil Elastase
NETs	Neutrophil extracellular trap
NF-κB	Nuclear factor kappa-light chain-enhancer of activated B cells
PAD4	peptidyl arginine deiminase 4
PAMPs	Pathogen associated molecular pattern
PBS	Phosphate buffered saline
PCR	Polymerase chainreaction
pDC	Plasmacytoid dendritic cells
PFA	Paraformaldehyde
PMA	Phorbol-12-myristate-13-acetate
PRR	Pattern-recognition receptor
PSGL-1	P-selectin glycoprotein ligand-1
RA	Rheumatoid arthritis
RNA	Ribonucleic acid
PMN	Polymorphonuclear neutrophils
ROS	Reactive oxygen species
RPMI	Roswell Park Memorial Institute 1640
s.c.	subcutaneous
SEM	Standard error of mean
SLE	Systemic Lupus Erythematosus
SP	Single positive
ss	Single stranded
STAT	Signal transducers and activators of transcription
TAE	Tris base acetic acid and EDTA
TBS	Tris buffered saline
TBST	Tris buffered saline with Tween20
TCR	T cell receptor
Th-cells	T helper cells

TNFα	Tumor necrosis factor α
TLR	Toll-like receptor
TRAF	TNF receptor-associated factor
T-reg	Regulatory T cells
TYK	Tyrosine kinase
WT	Wildtype

1. Introduction

1.1 Human myocarditis

In 1995 the World health organization defined myocarditis as the inflammation of the myocardial tissue[1]. The term myocarditis was first introduced at the beginning of the 19th century and described a disease of the heart[2]. Now the term myocarditis refers to acute and chronic inflammatory responses of the heart mostly triggered by a viral infection or a postviral immune response. However, it can also be idiopathic, toxic or a result of an autoimmune disease which will be further introduced in the next chapters.[1,3,4] Pathologically, myocarditis is identified as an infiltration of focal or diffuse mononuclear cells to the myocardium if over 14 leukocytes per 1 mm² are visible in the heart by histology with immunohistochemical techniques[4]. It can be divided into acute, subacute, or chronic state and can be either focal or affect more parts of the muscular wall of the heart called myocardium[4]. Clinically a wide variability of symptoms occurs from almost asymptomatic to patients with acute heart failure[5]. Because of the unclear pathophysiology and inadequate therapy options myocarditis and its consequences remain a challenge for diagnosis and therapy.

1.1.1 Etiology

The term myocarditis is a collective term for an inflammatory disease of the heart muscle and combines a wide variety of etiologies. Until now it is known that myocarditis is caused by the interaction between the environment and genetic factors of the patient[4]. Environmental triggers include infectious causes like bacteria, fungi or viruses as well as non-infectious causes such as immune-mediated ones like allergens or autoantigens. Moreover, toxic causes like drugs, hormones or physical agents can also be triggering factors (Table 1)[4].

Infectious causes	Bacterial	*Staphylococcus, Streptococcus, Chlamydia, Mycoplasma, Mycobacteria*
	Fungal	*Aspergillus, Candida*
	Parasitic	*Trichinella spiralis, Toxoplama gondii*
	Viral	Enteroviruses (Coxsackie A/B), HIV Adenovirus, Parvovirus B19, Coronavirus

Non-infectious - immune mediated causes	Allergens	Vaccines, drugs (penicillin, tetracycline)
	Alloantigens	Heart transplant rejection
	Autoantigens	cardiac antigens (aMyHC)
	Associated with Autoimmune diseases	Systemic Lupus Erythematosus (SLE), giant cell myocarditis
Non infectious - toxic causes	Drugs	Amphetamines, cocaine, ethanol, clozapine
	Heavy metals	Copper, iron, arsenic
	Physical agents	Radiation, electric shock

Table 1: Overview of possible causes of myocarditis. Modified from Caforio et al. and Kindermann et al.[4,6].

Viral infections and their postinfectious immune response is the most common cause of myocarditis in western industrialized nations and geographical differences of triggers could be shown[7]. In France, enteroviruses are most common[8] whereas Parvovirus B19 and human herpesvirus 6 is most common in Germany[9–11]. In addition, there are also numerous non-viral infections inducing myocarditis. Most common triggers in developing countries are bacterial pathogens such as Chlamydia and Mycobacterium, fungi, and parasites[12]. Besides infectious causes, myocarditis can also occur due to non-infectious causes. These include agents (vaccines, heavy metals, physical agents), hypersensitivity disorders following drug administration, certain vaccinations or autoimmune diseases such as systemic lupus erythematosus or rheumatoide arthritis[6].

1.1.2 Clinical presentation and diagnosis of myocarditis

The heterogeneous appearance of myocarditis is also reflected in its clinical presentation. The symptoms of myocarditis range from asymptomatic states with hardly any signs and symptoms to flu like symptoms including fever, mild dyspnea or chest pain and can develop into life-threatening disease such as angina pectoris or cardiac rhythmic disorder[4,13]. Symptoms can resolve without any treatment, however, it can lead to cardiogenic shock or sudden death. Patients suffering from DCM show reduced heart pump action, blood clots and arrhythmias leading to heart and organ failures[14].

The incidence of myocarditis is around 1.5 to 1.8 million in the whole world per year[15,16]. In 2013 22 per 100,000 people suffered from myocarditis whereas nowadays it is 10.2 to 105.6 per 100,000 worldwide[17,18] whereas men have a higher incidence rate than women[19]. Myocarditis is slightly more common in men than in female patients due to sex hormones which influence the reaction of the heart in the event of an injury [20,21]. In young competitive athletes myocarditis is the third leading cause of sudden cardiac death as the American Heart Association publishes[22]. Young men suffer more frequently from heart muscle inflammation with highest occurrence between 16 and 20 years of age[21]. Female patients on the other hand have an lower incidence rate than male but develop more severe cases, including life threatening cardiac arrhythmias, heart failure and death, at an older age of 56 to 60[19,20].

An early clinical diagnosis is more difficult due to the heterogeneous presentation of a subclinical progress of myocarditis dysfunction and the associated delayed first presentation at the clinic or the cardiologist[6]. Therefore, myocarditis remains undetected in a lot of cases. The first instrument of choice for the detection of myocarditis is the echocardiogram (ECG). It can detect abnormalities in the contractile function and helps in early diagnosis by identifying deformation of the cardiac chamber of the myocardium[23]. Additionally, magnetic resonance imaging (MRI) gained interested because it can measure the function and the structure of the heart and detects wall abnormalities or thickening in case of myocarditis[13,24]. Another noninvasive technique is the examination of biomarkers in the serum, such as cardiac Troponin T which is elevated in the blood during heart damage[25].

For final diagnosis endomyocardial biopsy (EMB) is another option. It remains the gold standard for diagnostic confirmation. In 1986 the Dallas criteria were established to define myocarditis by histopathological characterization. Here, Dallas criteria define myocarditis due to inflammatory infiltrate in the myocardium accompanied by necrosis (acute myocarditis) or degenerative changes of the surrounding cardiomyocytes without necrosis (borderline myocarditis)[26]. In EMBs, DCM is manifested as the replacement of cardiac cells with fibrotic tissue and deposition of collagen[4]. However, higher diagnostic and prognostic relevance of modern immunohistochemical methods, the Dallas criteria are no longer adequate[27].

1.1.3 Therapeutic approach

So far there are no therapeutic approaches established that abolish myocarditis entirely. In case of suspected myocarditis or validated by histopathology the international guidelines advise patients to reduce physical activity for at least three to six months until the inflammation has disappeared and the cardiac function has

normalized[28]. Furthermore, patients receive standard medications to treat heart failure. The standard drug therapy currently used includes angiotensin include angiotensin-converting enzyme (ACE) inhibitors, angiotensin receptor blockers, beta-receptor blockers and diuretics[29]. Furthermore the use of defibrillators and cardiac resynchronization therapy are used for cardiac function support[6]. In addition, small studies have shown success with causal therapeutic approaches such as IFNβ but these have not yet found their way into clinical practice clinical practice as they show mixed results. Patients, diagnosed with viral myocarditis, have been shown to eliminate the virus within six months of IFNβ therapy and improve left ventricular function of the heart[30]. A follow up on these patients showed that treatment of IFNβ and therefore eradicating the virus showed a significant higher survival rate than patients with a persisting virus[31]. However, in a recently published study there was no relevant hemodynamic difference in a larger patient population compared to the placebo group[33]. A long term follow up of patients with idiopathic dilated heart muscle diseases or myocarditis were treated with IFNα. 81% of the patients showed improved ejection fraction at 2 year follow up[32]. For some patients, immunosuppressive therapy to treat myocarditis, is an option to cure myocarditis[4].

Because the causes and mechanisms of myocarditis are not fully understood due to the unknown pathomechanism, research on myocarditis is an important topic to find the best therapy options.

1.1.4 Pathophysiology

In summary myocarditis results from the interaction of an external pathogen with the immune system of the host[34]. Both, non-infectious and infectious triggers can lead to myocardial damage and the exposure of to the immune system which can result in an autoimmune response against the heart (Fig 1-1). In the majority of patients (40-60%) spontaneous healing of cardiac inflammation occurs with a complete recovery and heart function[35,36]. Nonetheless, in up to 30% of patients the acute phase can progress to a subacute stage followed by a chronic stage finally resulting into cardiac remodeling, fibrosis and loss of myocardial architecture. This latter chronic phase can lead to the major long-term consequence dilated cardiomyopathy (DCM) leading to acute heart failure. DCM is characterized by the dilatation of the left heart chamber with impaired emptying of the left ventricle causing heart pump weaking. It is manifested by cardiac remodeling with massive replacement of muscle cells with fibrotic tissue and collagen in the heart (fibrosis). DCM is being the main reason for heart transplantation these days.[4,14,35,37–39] In up to 50% of DCM patients, myocarditis is the underlying reason for DCM in Europe and North America[40]. Up to now it is

known that a heart-specific autoimmune mechanism is also involved in the development and/or progression of myocarditis[41]. In 30% of myocarditis and DCM patients high amounts of heart-reactive autoantibodies were detected in the blood[42] and the autoantigen cardiac myosin heavy chain (MyHC) was detected in the sera[43].

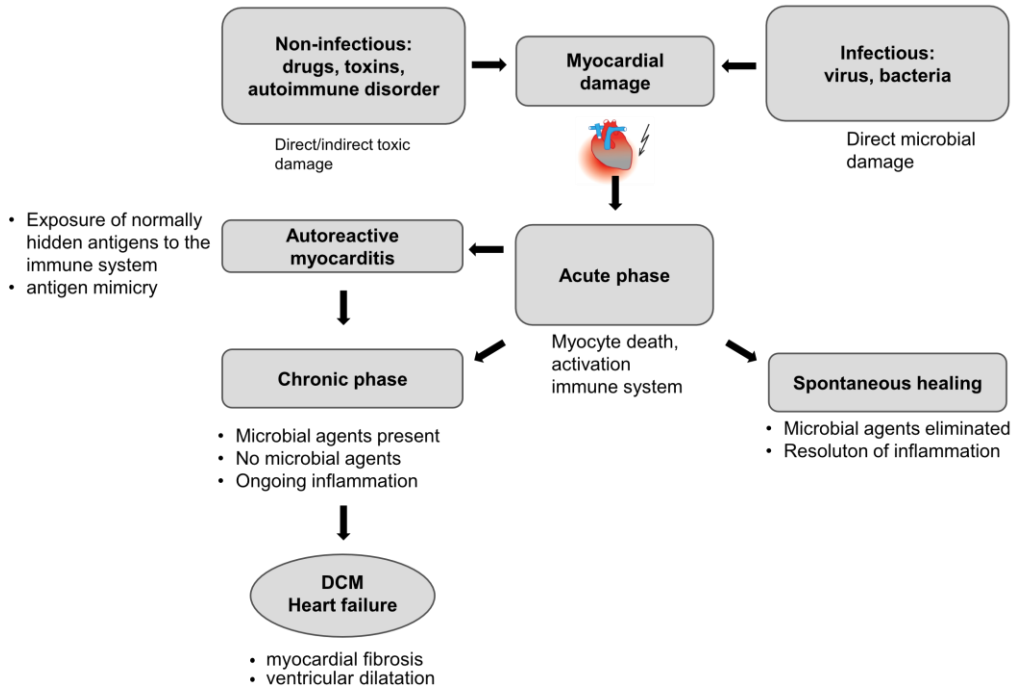

Figure 1-1 Pathogenic mechanism involved in myocarditis. Modified from Caforio et al.[4]

The pathophysiology of cardiac inflammation in humans is incompletely known and continues to raise scientific questions. The immune system makes an important contribution to cardiac inflammation. After infection, large numbers of immune cells such as natural killer cells, macrophages, neutrophils and T cells infiltrate cardiomyocytes at different time points during myocarditis, where they participate in different activities such as removal of dying tissue, removing pathogens or promote healing. However, failing of immune cells leads to damage of the heart including heart failure[44]. The most important insights into pathophysiological processes of myocarditis have been obtained with the help of different mouse models (see Chapter 1.3).

Myocarditis can be divided into three phases: Phase one (acute phase) is characterized by damage of the myocard followed by a first reaction of the innate immune system. Phase two, the subacute phase, is featured by components of the innate immune system and the immune response occurs. Patients resistant may recover without transition to phase three. However, persistent immune response and permanent damage to the heart may occur in the further chronic phase 3 leading to heart failure with fibrosis and dilatation of the heart in susceptible people.[45]

1.1.4.1 Acute phase

The first phase is characterized by myocardial damage and the activation of the innate immune system[46]. If myocarditis is mediated by a virus which enters the host via the gut (Enterovirus) or through the respiratory tract (Enterovirus and Adenoviruses) it is called acute viral myocarditis[47]. The virus hides in immune cells of lymphatic organs escaping the immune clearance and is then transported via blood vessels through the blood or lymphatic system to secondary organs, where it reaches its target organ[48]. The virus infiltrates the heart muscle cells via specific receptors[34]. After the virus entered the cardiomyocytes, virus replication takes place leading to myocardial injury[49]. As a result, cardiomyocytes undergo apoptosis and autophagy. Following damage of the cardiac tissue and death of cardiomyocytes, cardiac self-antigen protein fragments, such as cardiac myosin, are released and exposed to the innate immune system. Toll-like receptors (TLR) on macrophages get activated exclusively by cardiac myosin and invade the heart[50]. Clinically, this phase is often missed by clinicians since this phase last only a few days.

1.1.4.2 Subacute phase

The second phase is manifested by acute inflammation and uncontrolled innate immune response even after virus resolution and takes place weeks to month[6,49]. The immune signaling leads to a change in the host cells cytoskeleton with an increased entry of the virus into its target cells[34]. Virus specific T lymphocytes, natural killer cells and neutrophils infiltrate the heart tissue to fight inflammation[6,51]. Additionally high levels of cytokines are produced during myocardial injury[52] and can lead together with autoantibodies produced by B-cells to further tissue damage of the heart leading to impaired systolic function[38]. If the immune system is still active despite elimination of the virus, an autoimmune response follows.

1.1.4.3 Chronic phase

Important for the patients outcome is the balance of the immune system by its host. The immune response needs to be activated to eliminate virus infected cells but it also needs to turn the immune response off when appropriate because ongoing inflammation leads directly to tissue damage and organ dysfunction[34]. If the virus is eliminated efficiently, hearts normally heal spontaneously. In up to 40% of the patients the immune response is regulated and heart function is improved without any noticeable consequential damages[5]. However, it can happen that the persistence of the virus leads to a chronic autoantigen-driven response with a massive infiltration of heart reactive CD4+ T cells, leading to DCM with heart failure or death. This immune

reaction is often directed against organ specific antigens such as cardiac Myosin and thus has an autoimmune character. Overreaction of the immune system can cause heavy tissue damage to the heart resulting in fibrosis and dysfunction[15].

1.2 Immune system

Under steady state conditions all classes of leukocytes, such as neutrophils, B and T cells, are present in the heart of mice. Here, they are resident or circulate the blood[44]. Hearts of mammalians use both of the immune systems to respond to tissue injury resulting from different triggers. Leukocyte infiltration represents a key feature of cardiac inflammation. So far the role of the adaptive immune system in myocarditis has been widely investigated[53]. In contrast to the adaptive immune system, the role of innate immunity, especially of polymorphonuclear neutrophils (PMN) and plasmacytoid dendritic cells (pDCs) remain largely unclear. Therefore, the most relevant cell components of the innate and the adaptive immune system for this thesis will be described in the next chapters.

1.2.1 Neutrophils (PMN)

When myocarditis occurs, neutrophils are often recruited to the affected area as part of the immune response. Neutrophils help to combat pathogens and clear cellular debris at the site of inflammation. However, in the case of myocarditis, an excessive or prolonged activation of neutrophils can contribute to tissue damage. PMN are described as the first cells at the site of inflammation and have a rather short life span in the circulating blood[54]. They respond to altered conditions by producing cytokines, which recruits further immune cells, and can alter their gene expression during inflammation and aging[55]. At the site of inflammation neutrophils undergo a strictly regulated mechanism called the leukocyte recruitment cascade to invade the inflamed tissue.

1.2.1.1 The leukocyte recruitment cascade

Upon infection or inflammation PMN have the ability to migrate through the endothelium to get to the site of inflammation[56]. This process is initiated by tissue resident macrophages or dendritic cells. These cells recognize pathogen-associated molecular patterns (PAMPs) and tissue damage is recognized by damage-associated molecular patterns (DAMPs). The release of proinflammatory cytokines (TNFα, IL-1β) of these immune cells leads to the activation of the endothelium and it's adhesivity for circulating PMN[57,58]. This follows a tightly regulated multistep cascade including capturing, fast and slow rolling, firm adhesion, adhesion strengthening, spreading,

intraluminal crawling, transmigration, abluminal crawling, which all depend on β2 integrins and interstitial migration to the site of inflammation (Fig 1-2)[59,60].

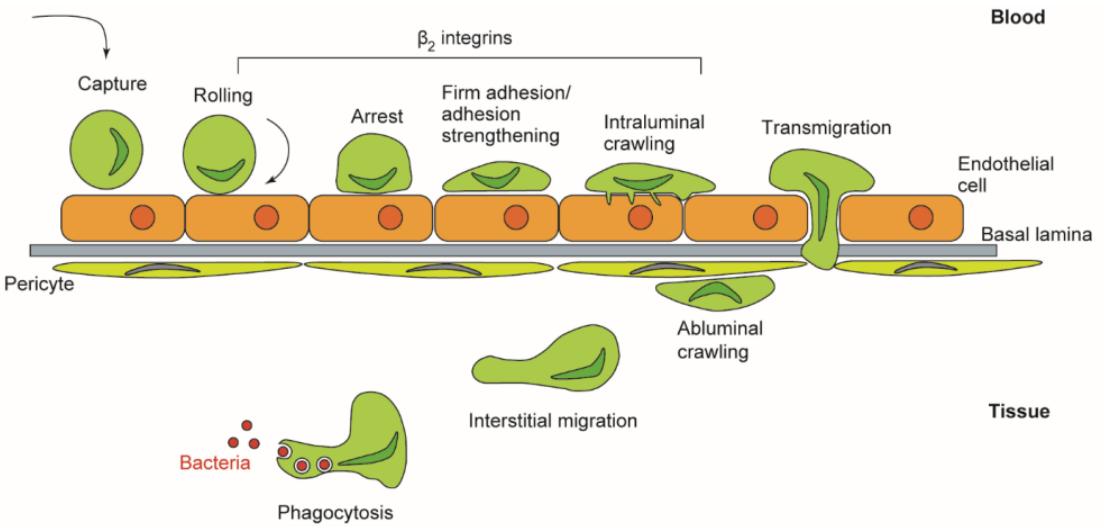

Figure 1-2 The leukocyte recruitment cascade. Upon inflammation neutrophils migrate from the blood stream to the site of injury and migrate into the inflamed tissue. They undergo a tightly regulated multistep cascade including capturing, fast and slow rolling, firm adhesion, adhesion strengthening, spreading, intraluminal crawling, transmigration, abluminal crawling, which all depend on β2 integrins and interstitial migration to the site of inflammation. At the site of inflammation neutrophils undergo phagocytosis or NETosis to eliminate pathogens. Modified from Schymeinsky et al.[60]

The initial capturing and rolling on the vessel wall is mediated by the reversible interactions of neutrophil expressed selectins with their ligands[56]. L-selectin and P-selectin glycoprotein ligand-1 (PSGL-1) on neutrophils bind to P- and E-selectin expressed on the inflamed endothelium despite constant blood flow[61]. Firm adhesion of neutrophils is facilitated by additional support of adhesion molecules of the β2 Integrin family, presented by PMN. The interaction of PSGL-1 on PMN with selectins on the inflamed endothelium triggers a signaling cascade in PMN leading to the activation of β2 Integrins. Activated β2 Integrin's allows PMN to bind to intercellular adhesion molecules (ICAM-1) on EC resulting in firm adhesion[62]. Following adhesion, neutrophils finally migrate into the inflamed tissue where they undergo either phagocytosis or NETosis.

1.2.1.2 Neutrophil extracellular traps (NETs)

At the site of inflammation neutrophils eliminate pathogens by phagocytosis and degranulation of antimicrobial proteins[63]. In 2004, NETs as a novel mechanism of neutrophil defense against pathogens have been described for the first time[64]. NETs are formed during the cell death of PMN called NETosis[65] and are formed after microorganism or endogenous stimuli, such as immune complexes, bind and

neutrophils adhere[66]. The formation of NETs can be triggered by LPS, small microorganisms or DAMPs and activates downstream effector proteins. Within 60 min after stimulation the chromatin starts to decondense in the cell nuclei while the cell membrane remained completely intact. This is accompanied by a progressive separation of the inner and outer nuclear membranes. Finally the cells round off before the cell membrane ruptures and the cell content is released into the extracellular space.[65] NETs are structures of chromatin filaments coated with histones, proteases and granular proteins such as Myeloperoxidase (MPO), Neutrophil Elastase (NE) and the antimicrobial peptide LL-37 which are expelled into the extracellular space[64]. An important role in this process seems to play the protein peptidyl arginine deiminase 4 (PAD4)[67]. After induction of NETs, PAD4 citrullinates histones by converting Arginine into Citrulline and therefore leads to decondensation of the chromatin[68,69]. Furthermore, reactive oxygen species (ROS) generated by the nicotinamide adenine dinucleotide phosphate (NADPH)-oxidase, stimulates MPO to translocate NE from the granule into the nucleus to help also decondensate chromatin by processing histones[65,70] (Fig 1-3). Following this, the nuclear membrane ruptures and decondensed chromatin is released into the cytosol. Via Gasdermin D (GSDMD), a protein which forms pores, NETs are released into the extracellular space[71].

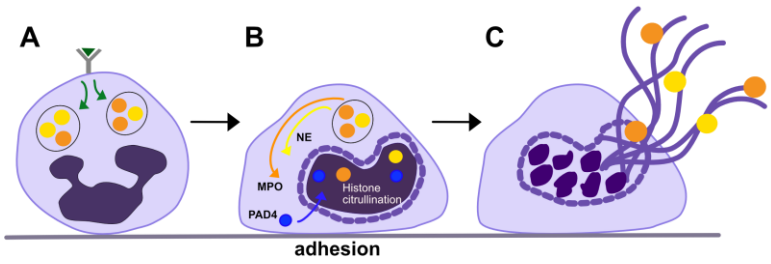

Figure 1-3 Schematic mechanism of NET release. A) Stimulation with different inflammatory triggers (virus, bacteria or inflammatory mediators) leads to neutrophil adhesion. B) Neutrophils mobilize granule components, including NE and MPO leading together with peptidylarginine deiminase 4 (PAD4), which promotes citrullination of histones, to chromatin decondensation. C) Finally, the cell membrane ruptures and NETs are released.

NETs are known to help neutrophils to immobilize, target and kill bacteria by possessing antimicrobial components such as histones, NE, MPO and LL37[72]. When encountering a microbe, PMN decide whether or not to induce NETs depending on the size of the pathogen[73]. In contrast to large microbes, small ones hardly trigger NET formation. However, if dysregulated NETs can occur in a non-infectious, sterile inflammation[74–76], such as SLE[77], rheumatoid arthritis (RA)[78], vascular stroke[79] or Wiskottich-Aldrich syndrome[80]. By releasing NETs, PMN externalize citrullinated autoantigens implicated in autoimmune diseases. Recently, our working group could show for the first time NETs in EMBs of patients with acute myocarditis[51]. NETs also

have an impact on other immune cells. NETs can activate CD4+ T cells by reducing the activation threshold in vitro linking the innate and the adaptive immune system[81]. LL37 for example, forms a complex with self-DNA from NETs, which are taken up by pDCs, and promote a strong IFNα response leading to proliferation and activation of Th1 cells[82]. NETs taken up by endothelial cells (EC) can induce a type I IFN signature leading to the induction of IFN-I stimulated genes (ISGs)[83]. Furthermore, increased NETs can modulate immune response by activating the IFN-I pathway in pDCs in SLE[84,85] and Wiskott-Aldrich Syndrome[80]. This shows that NETs have a positive effect by eliminating pathogens. However, the activation and persistence of NETs can lead to autoimmunity triggering diseases.

1.2.2 Plasmacytoid dendritic cells (pDC)

pDCs were described 50 years ago[86] and are a subtype of dendritic cells (DC). They originate in the bone marrow from lymphoid precursor cells[87,88] and are known to be main producers of IFN-I. IFNα is essential for the survival , activation and migration of pDCs in vivo[89]. By producing IFNα they promote an antiviral state by enhancing immune response of innate immunity[90]. However, pDCs also play a role in producing pro-inflammatory cytokines and act as antigen presenting cells. Therefore, they are a new key player of immune cells linking the innate and the adaptive immune system.

pDCs are present in the human peripheral blood and lymphoid tissue at very low levels, accounting for 0.2% to 0.5% of all peripheral blood mononuclear cells[91]. Under homeostatic conditions pDCs circulate in the blood and migrate into lymph nodes via high endothelial venules (HEV)[92]. To successfully migrate into lymph nodes circulating pDCs express high levels of the chemokine receptor CXCR4 and integrins and bind to adhesion molecules ICAM 1 and to the CXCR4 ligand CXCL12 expressed by HEV[93–95]. Additionally to remaining in primary and secondary lymphoid organs, pDCs are difficult to detect in most peripheral tissues, but are detectable in some tissues, such as small intestine[96]. During pathological conditions pDCs migrate from the bone marrow or the circulation to the site of infection, where they secrete large amounts of IFN-I. Large numbers of pDCs have been found in autoimmune and inflammatory diseases such as the skin of lupus erythromatosus[97] and lichen planus patients[98] or in inflamed synovia of patients with RA[99], in the intestine of an inflammatory mice model[96] or in coronary artery lesions of a murine model mimicking coronary arteritis[100]. Migration of pDCs to the site of inflammation involves adhesion molecules and chemokines. The receptor CXCR3, which is upregulated during inflammatory conditions on pDCs is required to migrate into the inflamed tissue[94]. Here, CXCR3 binds to the ligand CXCL10 produced in the inflamed tissue. However,

only response to both CXCR4 and CXCR3 and their ligands CXCL12 and CXCL10 respectively, induces pDC migration into the inflamed tissue and cluster formation in the inflamed lymph node[95,101].

1.2.2.1 Functions of pDCs

Because of the production of IFNα, pDCs link the innate and the adaptive immunity. Whereas, the production of TNFα is independent of IFNα, the activation of the interferon type I receptor (IFNAR) signaling pathway serves as an amplifier for TLR activation and thus allowing pDCs to produce high levels of CXCL10[102]. TNFα leads to the differentiation of pDCs into mature antigen-presenting cells, whereas IL-6 together with IFNα induces the differentiation of B cells in antibody (Ab) secreting plasma cells, secreting IgG[103]. The secretion of CXCL10 in pDCs is able to recruit activated T cells and other immune cells to the site of inflammation[104]. IFN-I release can lead to CD4+ T cell activation by upregulating CD69[90] and differentiation into Th1 subtype[105]. It directly affects T cell response by the secretion of IL-17 of Tcells[106]. Furthermore, pDCs express major histocompatibility complex (MHC) II molecules and T cell- co-stimulatory molecules and can therefore present antigens to CD4+ T cells[107]. Moreover, they have found to promote B cell activation together with IL-6[103]. IFN-I acts as an immune adjuvant and promotes the maturation of DCs, polarization of Th cells in to Th1 and activation of cytotoxic T cells (Fig 1-4)[108,109].

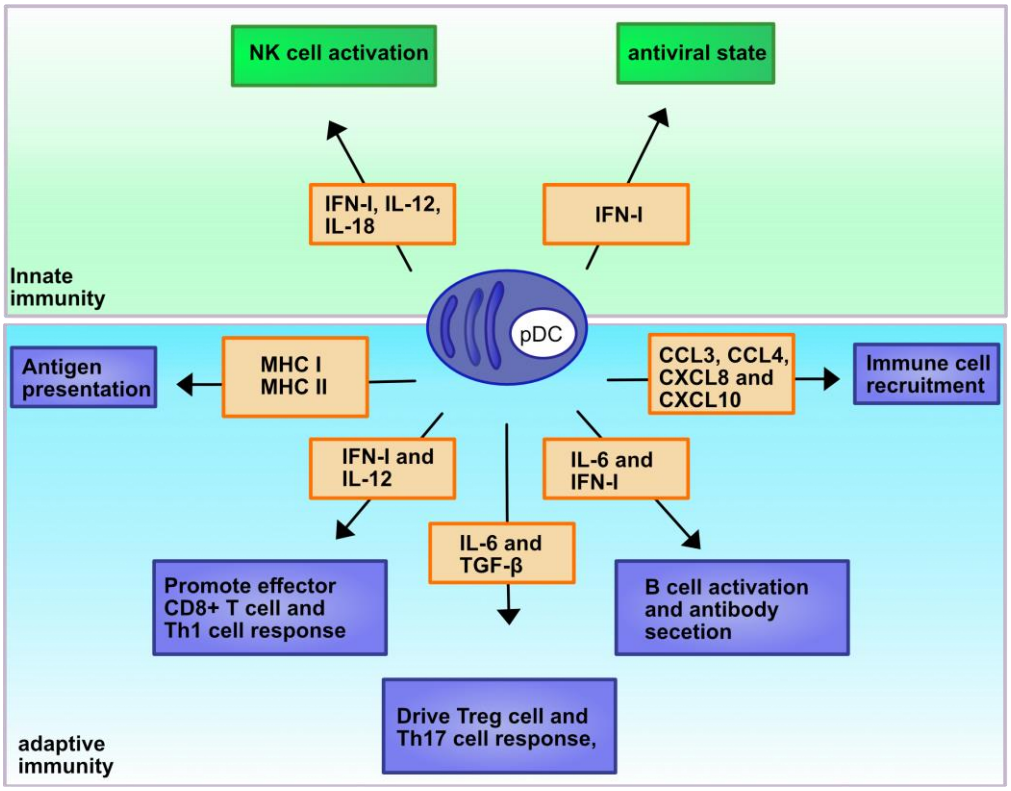

Figure 1-4 Functions of pDCs. pDCs link the innate and the adaptive immunity by producing IFN-I and proinflammatory cytokines (CXCL10, IL-6) leading to the

recruitment of further immune cells, promoting CD8+ T cell and Th1 cell response and B cell activation. Furthermore, they provide an antiviral state and activate natural killer cells (NK).

1.2.2.2 IFN-I signaling pathway

IFN is a special cytokine, which consists of three classes IFN type I, II and III. IFN-I consists of IFNα, which is divided into 13 subtypes, IFN β, IFNδ, IFNε, IFNκ, IFNτ, IFNω and is produced by innate immune cells[110]. pDCs are specialized to produce large amounts of IFN-I after viral infections[108]. However, macrophages, fibroblasts, endothelial cells[111] and neutrophils[112,113] also produce IFN-I. IFN-I binds to their specific ubiquitously expressed receptor, composed of IFNAR1 and IFNAR2, activating the Janus kinase (JAK)/signal transducers and activators of transcription (STAT) pathway. Type II only consists of IFNγ and binds to its IFNGR receptor, composed of IFNGR1 and IFNGR2. Type II is induced by NK cells, macrophages and activated T cells. Besides Type I and II, type III acts mainly on epithelial cells binding to its receptor with the IL10R2 and IFNLR1 chain[114].

Under steady state conditions IFN-I production is restricted, however in response to sensing of microbial patterns (PAMPs) by pattern-recognition receptors (PRRs) and cytokines, IFN-I production is induced in mainly all cells[115]. It is dependent on interferon regulatory factor (IRF)3 or IRF7. IRF3 is constitutively expressed in mostly every cell and is not induced further after virus infection, however IRF7 is cell type specific with constitutive expression in pDCs[116] and therefore can immediately express large amounts of IFNα after TLR signaling[117]. Upon virus detection all infected cells detect cytosolic ribonucelic acid (RNA) or desoxyribonuleic acid (DNA) and phosphorylates IRF3, which is translocated into the nucleus to promote the expression of Type I IFN[114]. Type I IFN in turn induces more IRF7 leading to a positive feedback loop thus leading to even more IFN[118]. IFN-I then binds to its receptor, which is ubiquitously expressed on all cells[119]. Binding of IFN-I can promote an autocrine (on the secreting cell) and paracrine (on bystander cells) signaling pathway. For both pathways, binding of IFN-I to IFNAR leads to the activation of the JAK/STAT pathway. IFNAR1 activates JAK1 and Tyrosine kinase (TYK) 2, which are constitutively associated with the receptor, leading to the phosphorylation and activation of STAT1 and STAT2 by JAK.[114,120–122] STAT1 and STAT2 recruit IRF9 and they assemble to the IFN-stimulated gene factor 3 (ISGF3) complex. ISGFR3 and STAT proteins bind to IFN-stimulated response element (ISREs), acting as transcription factors and translocate to the nucleus to induce expression of ISGs[123]. ISGs provide an antiviral state in infected and neighboring cells inhibiting viral replication (Fig 1-5)[115].

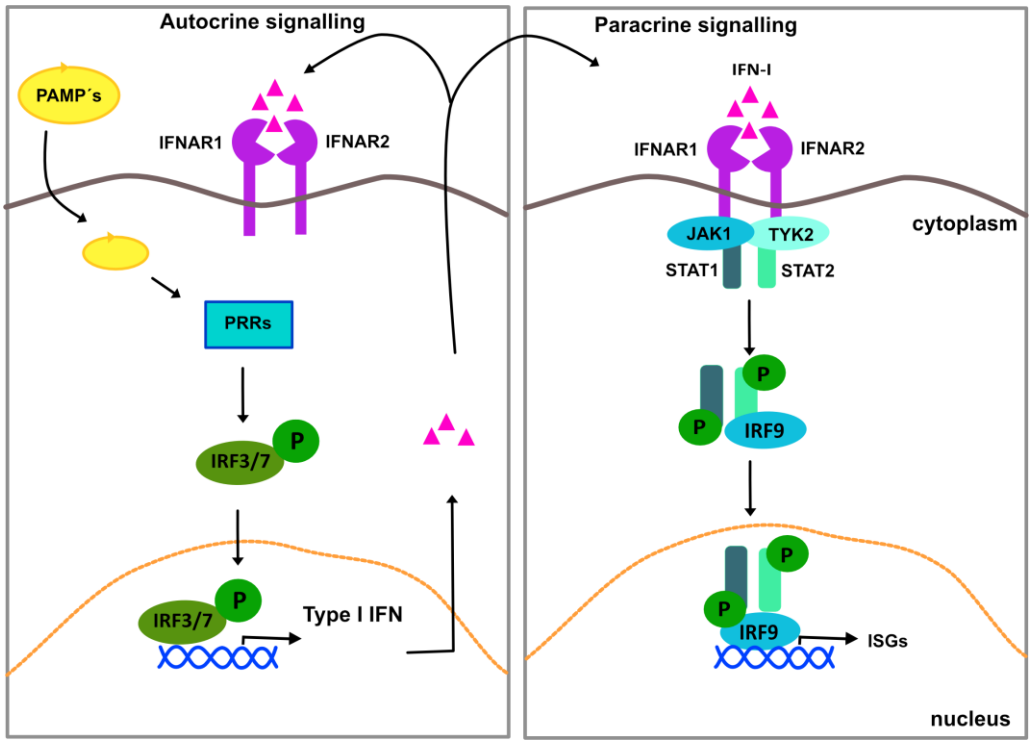

Figure 1-5 Schematic presentation of type I interferon (IFN) signaling. PAMP´s, genomic material, get recognized by PRR´s leading to the activation and phosphorylation of interferon regulatory factor (IRF)3 and/or IRF7. IRF3/7 translocate to the nucleus to promote the production of IFN-I. IFN-I can act in an autocrine and paracrine manner. Upon binding of IFN-I to IFNAR1/2 receptor leads to activation of JAK1/TYK2 leading to the phosphorylation of Stat1/2. Stat1/2 lead together with IRF9 to the ISGF3 complex. The complex translocate to the nucleus driving the expression of interferon regulated genes (ISG).

1.2.2.3 pDCs as IFN-I producing cells

pDCs can produce IFNα systemically measurable in response to a wide range of DNA and RNA viruses, whereas the virus is either enveloped or non-enveloped. Next to IFNα they are also able to produce IFNβ but to a lower extent[124]. Besides endocytosis of the virus, different cell surface receptors recognize pathogens and mediate the uptake of the virus into the target cell. Human pDCs express Fc receptor for IgG (FCyRII), Siglec-5 and CD36, whereas murine pDCs exclusively express SiglecH[125]. After binding to the receptor, a receptor-mediated endocytosis, followed by the acidification of the compartments activates the fusion of the virus into the cytoplasm[124]. Toll-like receptors (TLRs) are important for innate response and of the known TLRs, TLR 7 and 9 are uniquely expressed in pDCs[126]. TLRs reside in the endoplasmic reticulum and are translocated via a chaperone to the endosome after virus activation. They expose their ligand-binding domain by cleavage in the endosome. Both receptors are transmembrane receptors and bind their ligands within endosomes[127]. Therefore, the virus has to enter the endosome via receptor-mediated endocytosis or direct fusion with the endosomal membrane. The endocytosed virus

gets uncoated in the acidic endosome and pDCs get activated by their respective ligand pairs via endosomal TLR7/9.[124] TLR9 detects double stranded (ds) DNA containing CpG rich sequences, whereas TLR7 senses single stranded (ss) RNA, such as Coxsackievirus B.[82,128–130] The activation of TLR´s lead to an intracellular multifaced signal cascade involving different molecules and is specifical for pDCs. In mice IFN-I production is dependent on IRF7 acting as the master regulator of IFN-I dependent immune response in pDCs[131]. Following detection of endocytosed nucleic acid ligands, the adapter molecule myeloid differentiation factor 88 (MyD88) is recruited to TLR 7/9 by its C-terminal Toll-interleukin-receptor protein domain[132,133]. Then a complex called cytoplasmic transductional-transcriptional processor (CTTP) is built[134]. Here, MyD88 forms a complex with IL-1 receptor-associated kinase (IRAK)-4 and (IRAK)-1 through its death domain, a serine/threonine kinase, the ubiquitin ligase TNF receptor-associated factor (TRAF 6) and IRF7[134,135]. IRAK4 phosphorylates IRAK1, which is the kinase to phosphorylate IRF7. IRF7 translocates to the nucleus to act as a transcription factor where it promotes the expression of IFN-I.[133,134,136] Because IRF7 is constitutively expressed in pDcs it allows a fast assembly of the complexes described above and therefore a fast amount of IFN-I production[137]. Expressed IRF8 seems to act as a positive stimuli[138], controls the survival and function[139] and is essential for the development of pDCs as studied in IRF8 KO mice[140]. Downstream of TLR signaling, IRF5 interacts with the CTTP[124], gets activated by MyD88 and TRAF6 and is translocated to the nucleus, where it induces the production of pro-inflammatory cytokines such as IL-6 or TNFα[141,142].

Furthermore pDCs sense via TLR7/9 and activate downstream the MyD88/ nuclear factor kb (NFκB) cascade[143]. This pathway is well conserved between humans and mice. Here, MyD88, IRAK4, IRAK1 and TRAF6 build a complex[134] and TRAF6 ubiquitinylates TAK1 inducing the expression of mitogen-activated protein kinases (MAPKs) and directly phosphorylates IKK-β of the IKK complex consisting of IKK-a, IKK-β and IKK-γ[138]. The activated IKK complex permits NF-κB to enter the nucleus[89,144]. NF-κB and MAPKs induce the production of proinflammatory cytokines (TNFα, IL-6, IL-12, IL-1β)[102] and chemokines (CXCL10)[145] (Fig 1-6).

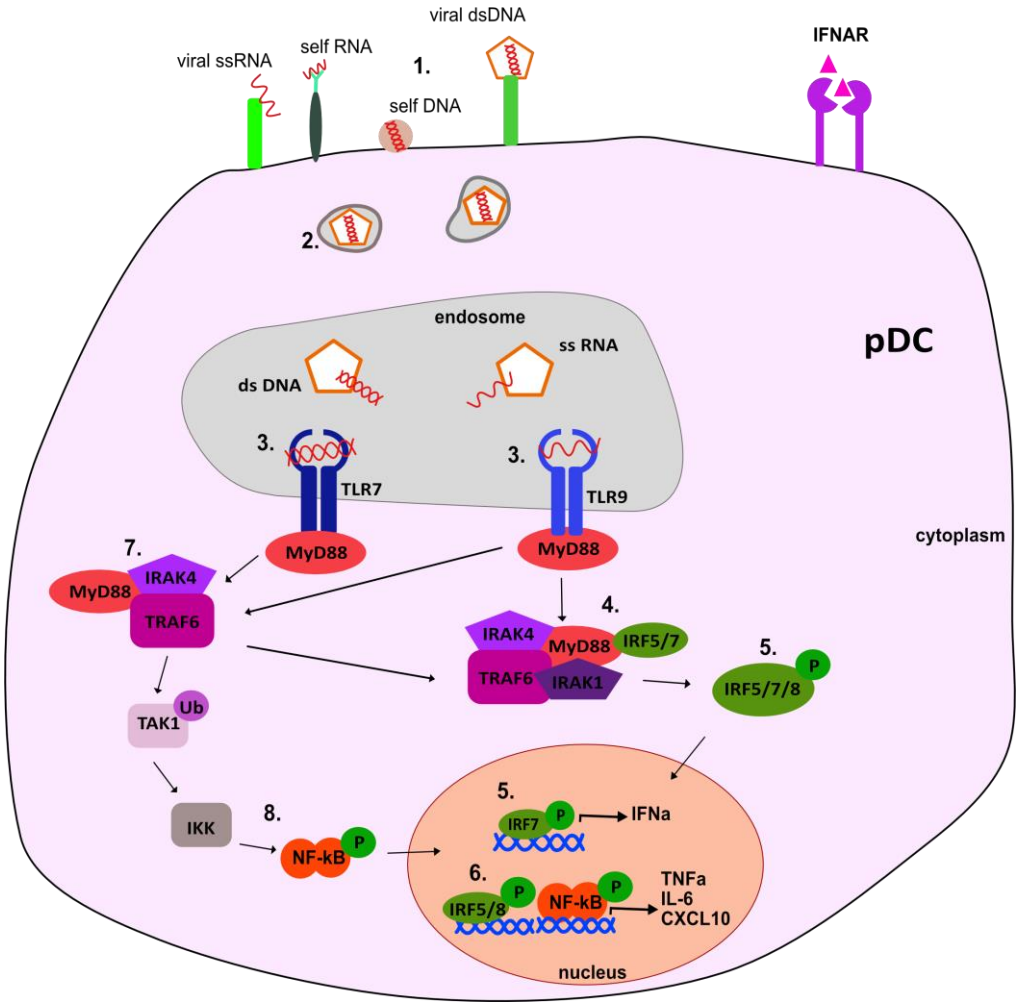

Figure 1-6 Signaling pathway specific for pDCs. 1) The virus enters the target cell by binding to specific receptors, followed by a receptor-mediated endocytosis. Acidification of the endosomal compartments activates the fusion of the virus with endosomal membranes and release of the virus into the cytosol. 2) DNA or RNA is transported to the endosome via vesicles 3) Here, they bind TLR7 or 9. This hence allows downstream signaling via the adaptor molecule MyD88. 4) MyD88 forms a complex with IRAK4 and IRAK1, TRAF 6 and IRF7. IRAK 4 phosphorylates IRAK1, which is the kinase to phosphorylate IRF7. 5) IRF7 translocates to the nucleus to promote the expression of IFN-I. 6) Phosphorylated IRF5/8 induces the expression of cytokines. Furthermore pDCs sense via TLR7/9 and activate downstream the MyD88/NFκB cascade. 7) MyD88, IRAK4, IRAK1 and TRAF6 build a complex and TRAF6 ubiquitinylates TAK1 which directly phosphorylates the IKK complex. 8) The activated IKK complex permits NF-κB to enter the nucleus and induces the production of proinflammatory cytokines (TNFα, IL-6) and chemokines CXCL10.

1.2.2.4 IFN-I and diseases

However, pDCs also play a predominant role during viral infections and autoimmunity. During viral infections, pDCs first produce large amounts of IFNα at the site of virus replication, whereas antigen presentation occurs in a latter stage[146]. IFN-I production of pDCs contributes to a variety of autoimmune diseases. In the autoimmune disease SLE, self-nucleic acid from NETs of PMN are responsible for pDC activation and inducers of IFN-I[84,147]. The DNA-Ab complex binds FCRIIa on pDCs and is translocated to endosomal compartments, acting in a TLR9 dependent manner to induce IFNα[148]. In this disease there is evidence for a direct activation of pDCs through IFNα[109]. During psoriasis pDCs initiate disease progression via IFNα production by infiltrating the skin of these patients[149]. It is known that IFN-I can inhibit CVB3 replication *in vitro* and CVB3-induced myocarditis mice treated with IFN-I ameliorated the effect and prevented mice from early death due to CVB3 infection[150]. Recently a group could show an important function of the IFN-IRF3 axis during a myocardial infarction model. Interruption gave rise to reduced levels of chemokines, inflammatory cytokines, or inflammatory cell infiltration in cardiac tissue, but also improved cardiac function[151]. Furthermore excessive IRF3 activation and IFN-I causes autoinflammatory conditions[152].

1.2.3 T cells

As T cells play a crucial role during all phases of myocarditis, a better understanding of T cells is necessary. T cells are part of the adaptive immune system, which is extremely specific and the response is very efficient. It takes about two weeks to develop its potential but it can acquire a memory to recognize pathogens even faster after the second infection. T cells can be classified by their cluster of differentiation (CD) markers and play a role during promotion of inflammation through cytokine production, killing unwanted target cells and regulate immunosuppressive response.[153]

They originate from a hematopoetic stem cell which differentiates into a multipotent progenitor cell and into the common lymphoid progenitor cell in the bone marrow[154]. Lymphoid progenitor cells enter the circulation and migrate from the bone marrow to the thymus, where T cells develop[154]. In the thymus, they undergo T cell receptor (TCR) arrangement and selection (Fig 1-6). Early T cells are double negative (DN) thymocytes because they lack the expression of TCR, CD4 and CD8[153]. T cells progress through four states of double negativity DN1 to DN4 where a rearrangement of TCRα and β chains take place until they reach double positive (DP) transition with a complete TCR receptor (CD4+/CD8+)[155]. Before DP cells get released in the

periphery, they are tested whether TCR is functional or tested for self-reactivity in the cortex and medulla of the thymus[156]. Therefore, DP thymocytes meet cortex-specific self-antigens bound to myosin heavy chain (MHC) I or II molecules on the surface of cortical epithelial cells in the thymus[157]. DP thymocytes with a high affinity for the presented antigen by the MHC class undergo apoptosis, whereas DP thymocytes with an intermediate affinity for the presented antigen undergo survive (positive selection)[157]. Positive selection also coincides with the development of DP thymocytes into single positive (SP) cells. DP thymocytes binding to MHC class I develop into CD8+ and binding to MHC class II develop into CD4+ SP cells[157]. To ensure self-tolerance SP thymocates move to the medulla. Thymocytes cells binding with a high affinity for the presented antigen undergo apoptosis (negative selection) whereas low affinity leads to näive SP CD4+ or CD8+ cells[158].

After their development and selection in the thymus SP naïve T cells migrate to secondary lymphoid organs, such as lymph nodes or the spleen. Here, they circulate until they meet antigen presenting cells (APCs) with matching antigens and get primed. Antigens presented via MHC I molecules, such as intracellular peptides from pathogens, activate näive T cells to become a CD8+ cytotoxic cell, whereas antigens presented via MHC II, activate näive T cells to develop into CD4+ T cells[155,159].

Afterwards they migrate into the inflamed tissue where they receive additional signals from APCs and local cytokines to carry out their effector function. CD8+ T cells secrete enzymes that will kill target cells directly such as cancer cells or virus. The activation of CD4+ T cells leads to a differentiation into subsets and is dependent on the cytokine milieu, such as IL-6 and IL-1β, and antigenetic stimulation with different cytokine release and aims to act. Th1 produce IFNγ, activate macrophages and eliminate pathogens and is essential in the regulation of inflammatory responses in autoimmune diseases. Th2 stimulate B-cells, mast cells, eosinophils and produce large amounts of IL4 whereas Th17 recruits neutrophils and promote autoimmune inflammation by secreting IL-17 (Fig 1-7)[160].

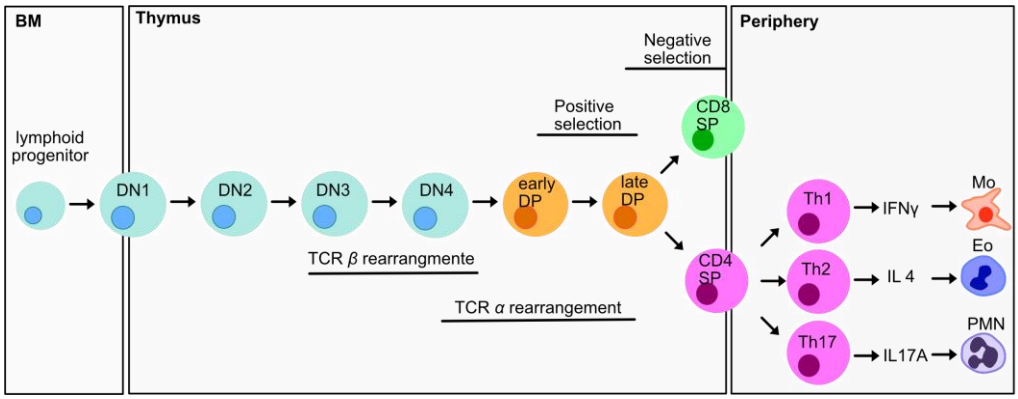

Figure 1-7 Development of T cells. Lymphoid progenitor cells migrate from the Bone marrow (BM) to the thymus where they undergo T cell receptor rearrangement to develop into double positive cells (DP). DP cells ensure MHC restriction (positive selection) and self-tolerance (negative selection) to differentiate into CD4 and CD8 single positive (SP) cells-CD4 and CD8 naïve T cells enter LN and spleen to get activated. CD4+ naïve cells differentiate into Th1, Th2 and Th 17 subsets with secreting IFNγ, IL-4 and IL-17, respectively to attract further immune cells, such as Macrophages (Mo), Eosinophils (Eo) or Neutrophils (PMN) to fight pathogens.

1.3 Myocarditis mouse model

The pathophysiology of cardiac inflammation in humans is incompletely known and continues to raise scientific questions. The most important insights into pathophysiological processes of myocarditis have been obtained with the help of different mouse models. Mouse models represent an excellent way to study pathologies due to the genetic homologies between human and mice[161]. Different mouse models giving insights into the underlying mechanism of post-infectious myocarditis and cardiomyopathy were described in the literature so far. There are two models which have a huge impact on the understanding of myocarditis. The first one is induced by the infection with CVB3 and the other one by the immunization with a cardiac peptide elusively expressed in the cardiac tissue called cardiac myosin[162].

The CVB3 model shows the transition into a second phase after an acute phase, with left ventricle dysfunction of viral myocarditis in certain mouse strains such as A/J and Balb/c. This chronic phase is characterized by fibrosis, cell necrosis and DCM without a virus detection in this phase[163]. The advantage of this virus-induced myocarditis mouse model is the realistic similarity to the human myocarditis which is mainly induced by a virus as well. However, myocarditis is the result of not only a immune response against a virus but also a consequence of a boosted heart-specific autoimmune response[164]. Here, cardiac myosin is one of the main antigens, only present in the heart[165,166], to mediate a heart-specific autoimmune mediated immune response during the chronic phase in the CVB3 model[167]. Disadvantage of the CVB3

model is the complexity of handling the virus, therefore the EAM mouse model used during this PhD project will be described in more detail the following chapter.

1.3.1 The EAM model

The EAM model does not rely on an infection and therefore gives insights in an isolated manner into the latter phase of myocarditis. The chronic phase of the CVB3 model can be simulated by immunizing mice with pure cardiac myosin derived from α-cardiac myosin heavy chain. Here, mice are exposed to cardiac self-antigen peptide. Neu et al. described in 1987 the immunization with a cardiac myosin together with the T cell activator Complete Freund´s adjuvant (CFA) in different mouse strains[168]. Here, myocarditis is driven by heart-reactive T cells without a pathogen. Due to genetic susceptibility only few strains develop myocarditis therefore we used Balb/c mice[168,169]. The fact that the adoptive transfer of purified T cells from mice with acute myocarditis to healthy control mice transferred the disease and depletion of CD4+ T cells, provided evidence that myosin-induced myocarditis is a primarily T cell driven disease[170,171]. Studies to investigate the pathomechanism of the induction and maintenance of EAM suggest that both the innate and the adaptive immune systems are important in the development of the disease. Important key players of myocarditis are so far: autoreactive T cells[170], heart specific autoantibodies[43,172], different cytokines and chemokines[52,173].

1.3.2 Time course of the EAM

Since inducing EAM and investigating different time points was an essential part of this thesis, this chapter will give more detail about the different phases of the EAM. Mice get immunized by the application of CFA together with cardiac myosin twice in eight days[39]. The emulsion of cardiac myosin and CFA triggers an autoimmune response by a massive infiltration of immune cells into the heart in susceptible mouse strains, reaching its peak of infiltration on day 21[174]. Furthermore antibodies against myosin reaches its peak in murine sera on day 21[175]. Three phases can be observed: first the induction phase with priming from day 0-10, second the effector or progression phase starting around day 7-10 by the infiltration of immune cells and last the remodeling or late phase lasting until day 60 leading to DCM with fibrosis and heart failure (Fig 1-8)[175,176].

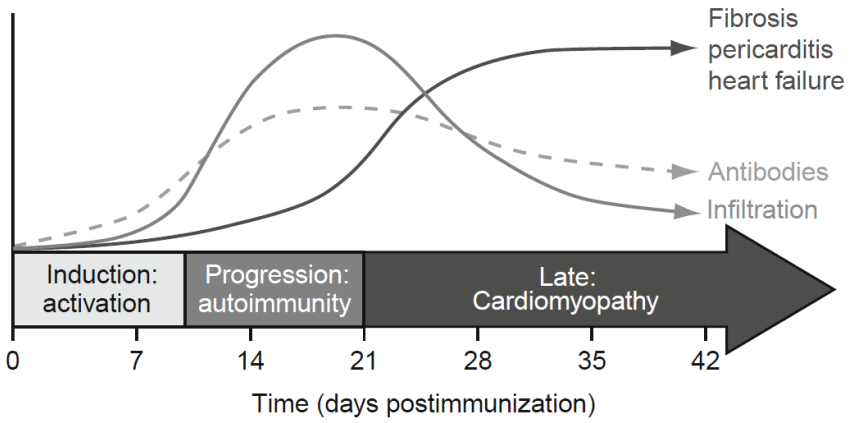

Figure 1-8 The phases of experimental autoimmune myocarditis (EAM) in the mouse model according to Cihakova and Rose[175].

1.3.3 Cellular infiltrate of EAM

As described above the exposure to cardiac self peptide αMyhC and the adjuvant CFA induce the early immune response. TLR receptors on immune cells and cardiac cells get activated. Innate immune cells and cardiac cells release cytokines, chemokines and interferons. Il1β induces the production of monocytes and macrophages in the bone marrow. These cells get released and migrate to lymphoid organs such as spleen. Afterwards these immune cells home from the spleen to the heart. Until day 7 mice showed histological evidence of acute inflammation as indicated by the infiltration of a first wave of mononuclear and polynuclear cells such as monocytes, natural killer cells and macrophages[173,177]. Additionally macrophages digest dead cardiomyocytes and migrate to the draining lymph nodes[44]. In the lymph nodes dendritic cells present the cardiac myosin to naïve T cells. A heavy infiltration of mixed inflammatory cells and the recruitment of specific CD4-positive (CD4+) T cells, which get activated by the cardiac myosin, to the lymph node follows between day 7 and 14 after immunization, marking the second wave of inflammatory heart infiltration in mice with EAM[6,38]. These activated CD4+-T cells migrate from the peripheral lymph node organs to the myocardium, where they infiltrate the cardiac tissue. This correlates with histopathological methods shown by Afanasyeva et al. who examined the different subpopulations infiltrating the heart showing CD45+ leukocytes peaking between day 15 and 21 after immunization in EAM mice compared to control mice[174]. Furthermore increased numbers of CD3+ (T cells), CD4-positive (CD4+) T cells, CD8-positive (CD8+) T cells, CD19 (B-cells), CD11b+/Gr-1-(Macrophages) and (CD11b/Gr1+ (neutrophils) infiltrated the heart during

myocarditis[174]. Furthermore, activated B-cells generate antibodies. These myosin reactive antibodies are measurable in the serum with increasing inflammation between day 10 and 21. 21 days postimmunization less immune cells infiltrate the heart, inflammation decreases, and the heart tissue is starting to become fibrotic[175,178]. In the chronic phase of myocarditis (day 21-63) a correlation between the proportion of CD4+ T cells and cardiac functional parameters, such as increased end-diastolic volume and reduced ejection fraction leading to decreased pump function is observable[174].

T cells play a crucial role for the development of cardiac inflammation and different subsets play distinct roles in EAM. It could be shown via flow cytometry that myocarditis is a T cell driven process and the heart infiltrate consists of CD4+ T cells and CD8+ T cells[170,179]. CD4+ T cells initiate the disease and CD4+ T cell depletion completely prevented EAM in mice[170]. While CD4+ T cells appear to be critical for the development of EAM, the role of CD8+ T cells is less clear. Depletion of CD8+ T cells reduced the severity of inflammation but did not prevent induction of myocarditis[170,171]. CD4+ T cell subsets contribute differently to the outcome of myocarditis. Th1 not only initiates tissue damage but also protects the myocardium from excessive inflammation. Basically, the differentiation of T helper cells in EAM shows a dominance of the Th2 subtype as well as Th17 T cells[180,181]. Th17 T cells infiltrate the heart during EAM and are a major regulator in late and chronic phase of the disease[182–184].

1.3.4 Cytokines involved during EAM

Upon activation, macrophages, neutrophils and other innate immune cells secrete pro-inflammatory cytokines. Their general role is to mediate the recruitment of neutrophils and macrophages to the site of inflammation. They also induce the expression of cellular components that help to eliminate the pathogen.[185] Prominent ones are the interleukin family such as Interleukin1 (IL-1), Interleukin6 (IL-6) and TNFα acting locally as well as systemically. TNFα and IL-1β are crucial for myocarditis as blocking these cytokines during the onset ameliorates myocarditis[186]. IL1 and TNFα are necessary at the time of infection for the transition to an autoimmune myocarditis. Cytokines released by T cells such as IFNγ (Th1), IL-4 (Th2) and IL-17 (Th17) play a crucial role during cardiac inflammation and can either diminish or ameliorate the effect[173,182]. Here, cardiac fibroblasts mediate the progression to inflammatory DCM[184]. IL-17-deficient animals are protected from the progression of EAM to DCM[182]. Missing both, IFNγ and IL-17, leads to an even more severe and fatal autoimmune inflammation with poor survival in EAM[187]. When IFNy, released by Th1

subtype, is overexpressed in mice it induces chronic myocarditis[188]. In a transgenic mouse model of spontaneous EAM, knocking out the IFNγ receptor reduced cardiac inflammation, indicating that IFNγ promotes cardiac inflammation[189]. However, other studies show that IFNγ deficiency is associated with cardiac dysfunction and severe myocarditis in a mouse model[180,190–192]. Here, IFNγ protects mice to develop myocarditis. One mechanism for this double-edged sword mechanism of IFNγ is based on findings that IFNγ signaling promotes macrophages to generate nitric-oxide and in consequence limiting autoreactive T cell-proliferation leading to a protection of myocarditis[193]. IL-6 has been shown to be critical for the induction of EAM[194]. Blocking IL-6 with an Ab protected mice from heart failure hence IL-6 is necessary during EAM to develop DCM[195]. Here, IL-6 mediated the induction of EAM by the initiation of Th17 cells[196]. Furthermore, the level of IL-1β and IL-17a have also been shown to induce cardiac remodeling in the mouse model and are essential for the development of DCM[46,182,184].

1.4 Break of tolerance - autoimmune myocarditis

As described above the role of the immune system is to destroy, isolate and remove pathogens or toxic agents which may harm the homeostasis of the host. However, it occurs that the immune system fails and reacts against the host itself. Failure in the immune system can lead to autoimmune mediated myocarditis. The adaptive immunity underlies a strict regulation to maintain homeostasis. As described above, CD4+ T cells are the main drivers of heart-specific autoimmunity in myocarditis. The alpha isoform of myosin heavy chain (αMyhC), encoded by the Myh6 gene, is the known autoantigen for CD4+ T cells in the EAM model. Normally Mhy6 genes and therefore aMyhC are absent in the medullary thymic epithelial cells, which mediate central tolerance, in mice and human and therefore T cell education fails[197]. In mice and human, a high number of näive αmyhC CD4+ T cells circulate the body and therefore facilitate the expansion of heart-specific effector CD4+ T cells. However, this high frequency of the cells is due to a defect in the negative selection in the thymes[198]. Here, the cardiac tissue is damaged by any cause and releases cardiac self-antigens. Additionally the activation of self-antigen presenting dendritic cells in the draining lymph nodes may lead to a breakdown in heart specific tolerance[199]. As a consequence, this triggers the cell expansion of heart-reactive CD4+ T cells and therefore autoimmunity. Furthermore, auto-reactive T cells can be activated due to the structural similarity between microbial and self-antigens, known as molecular mimicry. Lately it could be shown, that cardiac myosin reactive T cells enter the

myocardium, which were primed by myosin-peptide mimics derived from commensal *Bacteroides* species in the gut[200].

1.5 Midkine

The growth factor midkine (MK) is a heparin-binding growth factor predominantly important during embryonic development and was first described in the 1980ies[201]. Together with Pleiotropin they form a family which are structurally unique[202]. Under physiological conditions MK expression is highly restricted, however during pathological conditions MK is highly expressed. Here, it is mainly expressed in the mid-gestation stage, which gave it the name MIDkine[203]. It is overexpressed in cancer cells, but not in blood-derived normal cells including lymphocytes or activated T lymphocytes and is associated with a poor prognosis of these patients[204]. Furthermore MK is expressed in the cerebral cortex[205] and under hypoxic conditions it is expressed in neutrophils, monocytes and endothelial cells[206]. However only ECs secrete MK under hypoxic conditions[206]. In addition, there is growing evidence that MK may also be important during inflammatory processes giving hint as a potential therapeutic target[207]. Another role was shown during pathological kidney conditions[208], RA[209], autoimmune disease such as multiple sclerosis[210,211] and inflammatory bowel disease[212]. Since it is secreted during various diseases, MK can act as a biomarker[213,214]. However, the source of MK remains elusive.

The human MK gene is located on chromosome 11 and encodes a 13 kDA protein rich in basic and cysteine amino acids[203]. The protein consists of a signal peptide for secretion. Followed by an N-Domain and C-Domain held together by disulfide linkages. Whereas the C-Terminal domain is responsible for MK activation, the N-terminal Domain is required for dimerization[202].

So far, MK is one of many ligands known to bind to the low density lipoprotein receptor-related protein1 (LRP1)[215]. Here, MK binds LRP1 and mediates neural cell survival[216]. Previously, LRP1 has been described to associate with the alpha chain of the β2 Integrin macrophage antigen-1 (MAC-1)[217] and regulates β2 integrin-mediated leukocyte adhesion[218]. Lately it was shown that MK supports neutrophil trafficking during the acute inflammation process by promoting adhesion via β2 integrins[219]. Here, MK may mediate PMN adhesion by binding to LRP1 interacting with β2-integrins (Fig 1-9)[219].

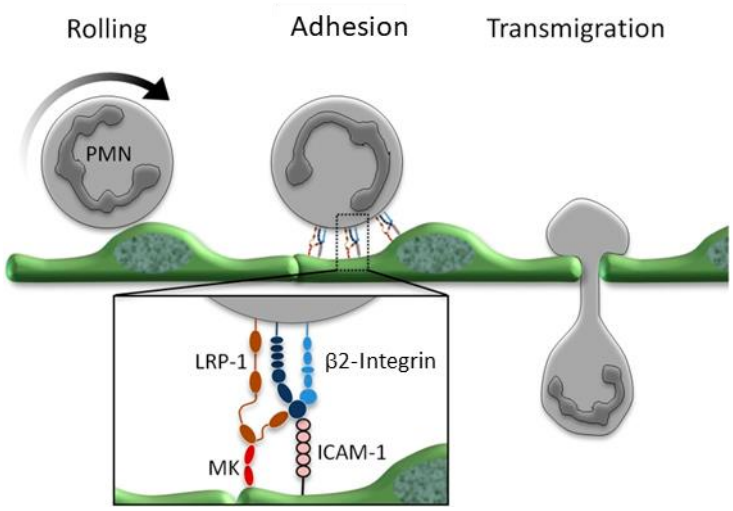

Figure 1-9 Schematic figure of the possible role of Midkine in leukocyte recruitment. After rolling, neutrophils arrest on the inflamed endothelium mediated by MK binding to LRP1 following a change in the confirmation of LFA-1 to the high affinity state. This step requires the firm binding to ICAM-1 on the activated endothelium. Afterwards neutrophils transmigrate through the endothelium. Modified from Herter & Manyadas[220].

A study had been shown that MK derived from CD4+ T cells can activate T cells themselves and induce Th1 differentiation *in vitro*[221]. Furthermore, blocking MK reduced the severity of experimental autoimmune encephalomyelitis through the expansion of regulatory T cells (T-reg) in peripheral lymph nodes and reduced infiltration of Th1 and Th17 cells into the central nervous system indicating a critical role of MK as a suppressor of Tregs[210]. So far, the role of MK during cardiac inflammation remains elusive.

2. Aim

Myocarditis is a disease, which is the third common cause of death in Germany. Until now, the pathogenesis of myocarditis remains largely unknown. Although there are many studies about the adaptive immune system during myocarditis, the role of the innate immunity remains largely unknown, especially the link between the innate and the adaptive immune system. Therefore, we wanted to identify and understand how the immune system influences the manifestation of myocarditis. To investigate myocarditis in vivo, an often described mouse model, the EAM model, was applied. Despite intensive research lately, the exact role for the innate immune system remains largely elusive. It has been previously shown that neutrophils and their formation of NETs are present in the cardiac tissue of patients with acute myocarditis. Furthermore, the cytokine MK was shown to mediate neutrophil trafficking by promoting adhesion via β2 integrins during acute inflammation. Therefore, the first aim of this study was to characterize the role of the MK-LRP1-NET axis *in vivo* using a mouse model of myocarditis and *in vitro* using neutrophil-derived Hoxb8 cells.

In a second part the link between the innate and adaptive immune system for cardiac inflammation in myocarditis was investigated in particular. The IFN-I pathway plays a crucial role for diseases and links the innate and adaptive immune system. As pDCs are the main IFN-I producing cells during viral infection, we secondly aimed to elucidate whether the IFN pathway and pDCs play a role during myocarditis. To be able to address this point, we used an IFNAR blocking Ab blocking the IFN-I pathway during cardiac inflammation *in vivo* until day 14 and 21.

In summary, this study will not only improve the understanding of the molecular insights into myocarditis mbut may provide new concepts of therapeutic strategies in the treatment of cardiac inflammation.

3. Material and Methods

3.1 Cells

Hoxb8 cells were generated from LRP1$^{fl/fl}$vav^{cre} WT and KO mice by Annette Zehrer AG Walzog. Cells lacking LRP1 are referred to as Hoxb8LRP1^{ko} and LRP1 WT cells as Hoxb8LRP1^{wt}.[51]

3.2 Animals

All experiments were conducted from 2018 until 2021 at the Walter Brendl Centre of Experimental Medicine of the LMU at the Biomedical Center München (Munich, Germany). All animal experiments were approved by the Regierung von Oberbayern, Germany (TV: 55.2-1-54-2532-200-2016). For the experimental autoimmune myocarditis mouse model, 6 - 8-week-old male WT mice on a Balb/c background were obtained from Charles River Laboratories (Sulzfeld, Germany). Animals were housed at the biomedical medicine centre (Munich, Germany) under standard conditions (22 ± 2 °C, 30 – 60 % humidity, 12 h light/dark cycle, lights on at 7 am) and fed a standard chow diet and water *ad libitum*.[51]

3.3 Experimental autoimmune myocarditis (EAM) mouse model

To investigate myocarditis in vivo a myocarditis mouse model called experimental autoimmune myocarditis mouse model (EAM) was applied in all experiments. Therefore mice get immunized and after immunization mice develop acute myocarditis with a massive infiltration of leukocytes until day 21 which marks the peak of inflammation. The acute phase is followed by a chronic stage of the disease. Until day 63 mice develop fibrosis and systolic dysfunction which resembles the latter phase of the disease.

3.3.1 Immunization of mice

Induction of Myocarditis was induced in Balb/c WT mice with the purified synthetic peptide of a cardiac α myosin heavy chain (αMyHC, Ac-RSLKLMATLFSTYASADR-OH, Caslo, Lyngby, Demark) together with complete Freund´s adjuvant (CFA, Sigma Aldrich, St.Louis, Missouri, USA) on day 0 and day 7 via a subcutaneous injection. Therefore, the peptide was dissolved in phosphate buffered saline (PBS, Biochrom,

Berlin, Germany) sonificated with a sonicator and mixed with an equal volume of CFA until it was completely emulsified. Each mouse was injected with a final concentration of 200µg/mouse of the emulsion. Sham control mice were treated with equal volumes of CFA and PBS without cardiac peptide.[51]

3.3.2 Histology and heart body weight ratio

To study leukocyte infiltration into the cardiac tissue, mice were sacrificed at day 21 after the induction of EAM and hearts were rinsed using PBS. Afterwards tissue was placed in a tube and fixed with 4% paraformaldehyde (PFA, Sigma Aldrich) for at least 24 h. To determine the heart weight/body weight ratio (HW/BW ratio), connective tissue was removed and hearts were weighed and the following calculation for HW/BW ratio was used: HW/BW*100. For histology, hearts were deparaffinized and dehydrated in a series of ethanol (EtOH, Th. Geyer, Germany) starting from 2x 70%, 3x 96%, 3x 100%, 2x xylol (Sigma Aldrich), 2x paraffin (Sigma Aldrich). Afterwards each heart was cut into three to four cross sections and embedded into paraffin blocks. After cooling at RT until the next day, paraffin blocks were cut at 4µM thickness and paraffin ribbons were placed in a water bath at 40°C. Sections were mounted onto glass slides and placed at RT overnight before staining. For hematoxylin & eosin (H&E) staining heart sections were dewaxed in xylol for 15 min. For rehydration sections were placed in 100% EtOH, 96% EtOH and 70% EtOH each 2x for 5 min and rinsed with Aqua dest. for 10 min followed by 5 min with PBS. Hematoxylin (Sigma Aldrich) staining was performed for 7 min with water rinse for 5 min before staining for 3 min with Eosin (Sigma Aldrich). Afterwards dehydration was performed using 100% EtOH twice for 1 min before placing into xylol for 3 min. Coverslips were mounted with Roti-mounting medium (Carl Roth, Karlsruhe, Germany). EAM Score was applied to evaluate the infiltration of leukocytes into the cardiac tissue. Therefore leukocytes were counted of each heart section in a fully blinded manner using a Leica M205 FA stereo microscope.: 0, no inflammatory infiltrates; 1, small foci of <100 inflammatory cells between myocytes; 2, larger foci of >100 inflammatory cells; 3, >10% of a cross section shows infiltration of inflammatory cells; 4, >30% of a cross section shows infiltration of inflammatory cells.

3.3.3 Whole blood count

Mice were euthanized under anesthesia with 1% isoflurane CP (CP-Pharma, Burgdorf, Germany) and blood was harvested directly from the heart into tubes filled with Ethylenediamine-tetraacetic acid (EDTA, microvetten) on day 21. Whole blood

was counted using a ProCyte DX™ blood counter (IDEXX, Laboratories, Hoofddorp, Netherlands).

3.3.4 Serum analysis

Mice were euthanatized under anesthesia with 1% isoflurane and blood was harvested directly from the heart into tubes (Eppendorf, Hamburg, Germany) at day 14 or 21. To collect serum, blood was left for 30 minutes to clot at RT and centrifuged for 10 min at 2000xg at 4°C. Supernatant was collected and used for further analysis.

3.3.5 Flow cytometry

For analysis of myocardial leukocyte infiltration, flow cytometry was performed from hearts of mice.

3.3.5.1 Tissue sample preparation

Mice were euthanized under anesthesia with 1% Isoflurane and hearts were perfused with PBS to get rid of the blood at day 14 or 21. Hearts were placed into a 24 well plate filled with 1 mg/ml collagenase type II (PAN Biotech, Aidenbach Germany) diluted in RPMI medium (PAN Biotech, Aidenbach, Germany). Hearts were then cut into small pieces with dissecting utensils and incubated for 30 min at 37°C in a shaker with 180 RPM. Afterwards hearts were crushed through a 70µM cell strainer (Corning, USA) over a 50 mL Falcon tube (Corning, USA), rinsed with 50mL of PBS and centrifuged at 800xg for 5 min at 4°C. After centrifugation cell pellets were resuspended in 1mL FACS Buffer, PBS containing 0.4% EDTA (AppliChem, Darmstadt, Germany) and 1% Fetal calf serum (FCS, Biochrom, Berlin, Germany) (Table 1), and then 300 µL were transferred either into a new tube for RNA isolation or FACS tubes for flow cytometry staining. For RNA extraction, tubes were centrifuged at 300xg for 5min at 4°C and the cell pellet was resuspended with 1 mL of TRIzol reagent (Thermo Fisher Scientific, Waltham, Massachusetts, USA). Samples were immediately immersed in liquid nitrogen and stored at -20°C until further usage. For cell surface marker staining, cells were transferred into facs tubes and centrifuged at 300xg for 5 min at 4°C before Ab staining. For intracellular cytokine staining, tubes were centrifuged at 800xg for 5 min at 4°C.

Name	Ingredients	Company
FACS Buffer	PBS+ 0.04% EDTA 1% FCS	Biochrome, Germany AppliChem, Germany Biochrome, Germany

Table 2 FACS Buffer

3.3.5.2 Cell surface marker staining

After centrifugation cells were resuspended in 100 µL PBS containing the Ab cocktail described in Table 3 and were incubated for 30 min at 4°C in the dark. Cells were centrifuged at 300xg for 5 min and resuspendend in 300µL PBS. For cell counting, cells were supplemented with 100 µL of 1:10 diluted 123 count eBeads™counting beads (Thermo Fisher Scientific) right before recording at the Beckman Coulter Cytoflex (Krefeld, Germany). Data were analyzed using FlowJo 9 software (Becton Dickinson GmbH, Heidelberg, Germany).

Antigen	Fluorochrome	Dilution	Company
CD45	APC- Cy7	1:300	Biolegend (London, UK)
B220	FITC	1:300	Biolegend (London, UK)
TCRβ	PE	1:400	Biolegend (London, UK)
SiglecH	PerCp Cy5.5	1:300	Biolegend (London, UK)
Ly6G	BV421	1:600	Biolegend (London, UK)
CD69	PE-Cy7	1:300	Biolegend (London, UK)
Live/Dead	Zombie	1:2000	Thermo Fisher Scientific, Germany

Table 3 Antibody cocktail for cell surface staining.

3.3.5.3 Intracellular cytokine staining

After centrifugation cells were resuspended in 100µL Roswell Park Memorial Institute 1640 (RPMI) medium (Biochrom, Berlin, Germany) + 10% FCS. For stimulation, cardiac peptide was diluted to a concentration of 2 µg/mL cardiac peptide α-MyhC and 100 µL were added to 100 µL cell suspension. Cells were placed at 37°C and 5% CO2. After 1 hour 1 µL/mL Brefeldin A (GolgiPlug, BD Bioscience, Franklin Lakes, New Jersey, USA) inhibiting the intracellular protein transport from the endoplasmic reticulum to the Golgi complex and therefore resulting in the accumulation of the cytokines in the Golgi complex, was included for the last 3 hours. After 4 hours of stimulation cells were centrifuged at 1500rpm for 6 min at 4°C and placed into a 96 well u- bottom well plate. Before staining, cells were centrifuged at 1500 rpm for 3 min at 4°C and supernatant was removed. Cells were resuspended in 50µL PBS containing cell surface marker and live dead staining (Table 4) was applied. Staining

was performed for 30 min at 4°C and washed three times with FACS buffer (Table 1). Each centrifugation step in between was performed at 1500rpm for 3 min at 4°C. Afterwards cells were fixed in 100µL BD cytokine fixation/permeabilization solution (BD Bioscience) for 20 min at 4°C. After washing the cells two times with BD Perm/wash buffer (BD Bioscience) at 1500rpm for 3 min at 4°C, cytokine staining was performed in 100µL BD Perm/wash buffer for 30 min at 4°C in the dark (Table 5). Cells were washed three times with BD Perm/wash buffer and resuspended in 300µL PBS. For cell counting, cells were supplemented with 100 µL of 1:10 diluted 123 count eBeads™counting beads right before recording at the Beckman Coulter Cytoflex. Data was analyzed using FlowJo software.

Antigen	Fluorochrome	Dilution	
CD45	BV421	1:300	Biolegend (London, UK)
CD4	Alexa Fluor eF710	1:300	Biolegend (London, UK)
TCRβ	PE	1:400	Biolegend (London, UK)
Live/dead		1:2000	Thermo Fisher Scientific, Germany

Table 4 Antibody cocktail for cell surface marker.

Antigen	Fluorochrome	Dilution	
IL17A	AF647	1:300	Biolegend (London, UK)
IFNy	FITC	1:300	Biolegend (London, UK)
IL4	PECy7	1:300	Biolegend (London, UK)

Table 5 Antibody cocktail for cytokine staining.

3.3.6 Multiplex Elisa

To study cytokine concentration in the serum of mice, serum was collected as described before (3.3.4). The frozen serum was thawed and LEGENDplex™ mouse Anti-virus response panel (BioLegend, San Diego, California, USA) was performed according to the manufacture´s protocol. In short, serum was diluted 1:2 with assay buffer and Standard was diluted in 125µL Assay Buffer, representing top standard C7. For a standard dilution series seven tubes were named C0-C7 and each tube (C0-C6) was filled with 37.5µL of Assay buffer. Afterwards 12.5µL of top standard C7 was transferred to C6 and mixed well. In the same manner, C6 to C1 were processed. This dilution standard ranged from 10000 pg/mL (C7) to 0 pg/mL (C0). 12.5µL of the standard dilution was added to the first row of a v-bottom plate and mixed with 12.5µL of MatrixA. Samples were also added to the v bottom plate and diluted with 12.5µL of Assay buffer. Afterwards 12.5µL of the premixed beads were added to each well to

reach a total of 37µL in each well. The plate was sealed and covered with aluminum foil to protect from light and placed on a shaker at 800rpm for 2 hours at RT. After centrifugation at 1050rpm for 5 min, the supernatant was removed using a multichannel pipette. Washing was performed with 1x wash buffer by dispensing 200µL into each well and 12.5µL of detection antibodies were added to the plate. After shaking for 1 hour at RT on a shaker with 800rpm, 12.5µL of Streptavidin-phycoerythrin was added and placed on a shaker for 30 min. Before reading the plate on a flow cytometer, washing was performed and samples were resuspended in 75µL PBS. Cytokine concentration was analyzed using Bio-Legend´s LEGENDplex™ Analysis software and was calculated from the standard curves using linear regression.

3.3.7 Quantitative polymerase chain reaction

3.3.7.1 RNA Isolation

For RNA extraction, whole hearts from mice were harvested after flushing hearts with PBS to remove whole blood on day 7, 14 and 21. Hearts were immediately snap frozen in liquid nitrogen or, alternatively 300µL of whole heart suspension after collagenase type II treatment (3.2.5.1) was immediately added to 1mL TRIzol (Thermo Fisher Scientific, Germany) and stored at -20°C until further usage. Whole hearts were stored at -80°C until further usage. At the day of isolation, 1mL TRIzol was added to whole hearts and transferred into round bottom tubes and immediately homogenized mechanically using an Ultra-Turrax T8 homogenizer (IKA Labortechnik, Germany). RNA isolation was performed according to the manufacturer´s protocol. Therefore, hearts were left at RT for 5 min for complete dissociation before adding 200µL of chloroform (Sigma Aldrich, Germany). Samples were vortexed for at least 15 sec and incubated for 2 min at RT. Solution was centrifuged for 18 min at 13000 rpm at 4°C and the aqueous solution was carefully transferred into a new tube. 500µL of isopropanol (Propan-2-ol, AppliChem, Germany) was added, vortexed for 15 sec and left at RT for 10 min for RNA precipitation. Samples were centrifuged for 10 min at 13000rpm at 4°C until RNA pellet was visible. The RNA pellet was washed with 75% EtOH and centrifuged at 10000rpm for 8 min at 4°C. Supernatant was removed and RNA pellet was air dried at RT for 5-10 min. Finally, RNA was diluted with 20µL RNAse-free H2O (Thermo Fisher Scientific, Germany) and the concentration as well as the A260/280 ratio was analyzed using Nanodrop™ 2000 spectrometer (Life Technologies, Germany). Only RNA with an A260/280 ratio of at least of 1.8 was used for further analysis.

3.3.7.2 gDNA digestion and reverse transcription

For gDNA digestion 1µg RNA was digested according to the manufacturer´s protocol using the DNAse I Amplification Grade Kit (Thermo Fisher Scientific, Germany). Afterwards 1µg total RNA was transcribed into cDNA using the iScript cDNA synthesis Kit (Bio-Rad Laboratories, California, USA). The master mix contained 1µg total RNA, 4µL of 5x iScript Reaction mix, 1µL of reverse transcription in a total volume of 20µL, filled up with nuclease-free water. The PCR was performed at 5 min at 25°C (for annealing), followed by 30 min at 42°C (reverse transcription step) and a denaturation step for 5 min at 85°C. cDNA was diluted to a final concentration of 10ng/µL and stored at -20°C.

3.3.7.3 Quantitative real-time PCR (qRT-PCR)

To quantify expression levels of mRNA, cDNA was used for quantitative real time PCR (qRT-PCR) analysis. The increase of fluorescence signal can be monitored in real time with SYBR green (Bio-Rad). Therefore 20 ng of cDNA (2µL) was mixed with 1µL 10µM reverse Primer, 1µL 10 µM forward Primer (Metabion, Planegg, Germany) (table 5), 10µL SYBR green and filled up to a total of 20µL with Nuclease free water. The PCR plate was centrifuged for 2 min at 300xg at RT. Samples were applied to a 96 well plate and the run was performed using StepOnePlus System (Thermo Fisher Scientific, Germany) according to the protocol in Table 6. As reference gene, the housekeeping gene Hypoxanthin-Guanin-Phosphoribosyl-Transferase (HPRT), was used. Results were analyzed using StepOne Software v2.3 (Thermo Fisher Scientific, Germany) and data were analyzed by the 2−ΔΔCt method of comparing threshold cycles first to *Hprt* expression, and then ΔCt of target genes in sham controls[222].

Primer	Sequence (5´- 3´)
mMDK FV	GTC AAT CAC GCC TGT CCT CT
mMDK RV	CAA GTA TCA GGG TGG GGA GA
mHPRT FV	ACA GGC CAG ACT TTG TTG GAT
mHPRT RV	ACT TGC GCT CAT CTT AGG CT
mIRF3 FV	GGC TTG TGA TGG TCA AGG TT
mIRF3 RV	CAT GTC CTC CAC CAA GTC CT
mIRF7 FV	CTG GAG CCA TGG GTA TGC A
mIRF7 RV	AAG CAC AAG CCG AGA CTG CT
mIRF8 FV	GAC CGA AGT TCC TGA GAT GG

mIRF8 RV	TGG GCT CCT CTT GGT CAT AC
mIFIT1 FV	TAC AGG CTG GAG TGT GCT GAG A
mIFIT1 RV	CTC CAC TTT CAG AGC CTT CGC A
mIFIT3 FV	CTG AAG GGG AGC GAT TGA TT
mIFIT3 RV	AAC GGC ACA TGA CCA AAG AGT AGA
mISG15 FV	GGT GTC CGT GAC TAA CTC CAT
mISG15 RV	TGG AAA GGG TAA GAC CGT CCT
mIFNα FV	TAATTCCTACGTCTTTTCTTT
mIFNα RV	TATGCCTGATCCCTGAACAGT
mIFNβ FV	AAGAGTTACACTGCCTTTGCCATC
mIFNβ RV	CACTGTCTGCTGGTGGAGTTCATC

Table 6 Primer sequences for qPCR. FV indicates forward, RV reverse.

Step	Temperature	Time	Cycle
Initial denaturation	95°C	10 min	1x
Denaturation	95°C	15 sec	40x
Annealing	60°C	1 min	
Melt curve	95°C	15 sec	1x
	60°C	1 min	
	95°C	+ 0.7°C/min	

Table 7 Protocol for qRT-PCR.

3.3.8 Echocardiography

To study systolic function of hearts using Echocardiography on day 63, mice were anesthetized with 2% Isoflurane and placed on a heated platform to ensure stable body temperature of 35.5 – 36.5°C. To maintain anesthesia mice were treated with 3% isoflurane. Transthoracic echocardiographic short-axis M-mode images were obtained with a Vevo2100 imaging system (VisualSonics, Toronto, Canada) using a 40MHz transducer. Parasternal long-axis M-mode was used to standardize transducer positioning for short-axis M-mode imaging. For evaluation of cardiac

function, 3 consecutive cycles were measured and averaged. Left ventricular end diastolic (EDV) and systolic (ESV) volumes were calculated using the formulae 7*LVID;d^3/(2.4+LVID;d) and 7*LVID;s^3/(2.4+LVID;s). Calculation of left ventricular ejection fraction (in %) was conducted via the formula ((EDV-ESV)/EDV)*100. Cardiac index was defined as cardiac output divided by body weight (BW).[51]

3.3.9 Masson trichrome staining

To analyse fibrosis in the cardiac tissue, Masson Trichrome staining was applied on day 63 after the induction of EAM. This is a histological method to stain for muscle tissue and collagen in the tissue. Mice were sacrificed on day 63 after induction of EAM and hearts were deparaffinized, dehydrated and cut in sections as described under 3.2.2. For Masson Trichrome staining, heart sections were dewaxed in xylol for 15 min. For rehydration, sections were placed in 100% EtOH, 96% EtOH and 70% EtOH each for 5 min and rinsed with Aqua dest. together with a final concentration of 0.03% H_2O_2 (Sigma Aldrich), for 5 min followed by 5 min with PBS. Then Masson Trichrome staining was performed as written in the manufacturer´s protocol (Bio-Optica, Milano, Italy). Shortly sections were rinsed with distilled water and Weigert´s iron hematoxylin were put on the section for 10 min. Without washing, picric acid alcoholic solution was applied for 4 min. After washing for 3-4 sec in distilled water, Ponceau staining was applied for 4 min. After washing, Phosphomolybdic acid solution was applied for 10 min. Then, without washing, Masson aniline blue was put on the sections for 5 min. Afterwards slides were washed in distilled water and rapidly dehydrated in 100% EtOH and 96% EtOH and 1 min in 70% EtOH. Samples were cleared in xylene and mounted using mounting medium. Heart sections were analyzed in a fully blinded manner using a Leica M205 FA stereo microscope with 12x magnification. To evaluate the percentage of fibrotic tissue in the whole heart Image J software was used. Therefore, the area (mm^2) of the fibrotic tissue (2) and the area (mm^2) of the myocardium (3) of one heart section (1) was calculated (Fig-3-1). This was done for all sections for one heart and the following calculation was used: area (mm^2) of fibrotic tissue/area (mm^2) of myocard*100.[51]

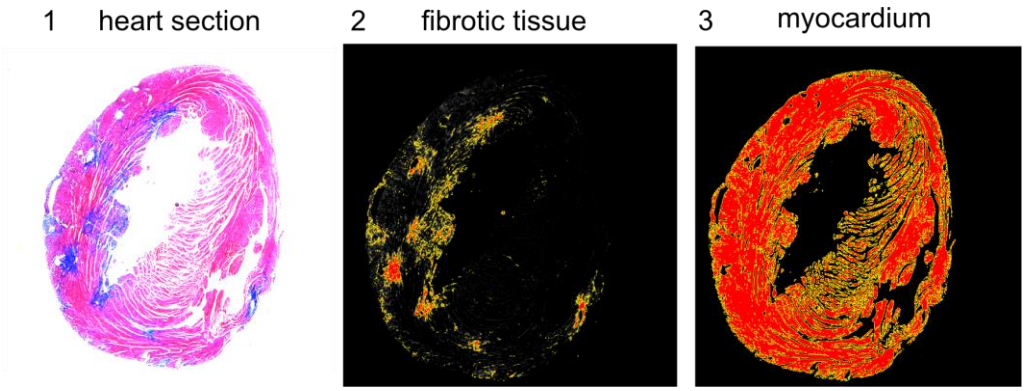

Figure 3-1 Evaluation of the fibrotic tissue in the myocardium. Masson Trichrome staining for one heart section. To calculate the percentage of fibrotic tissue in the whole heart (1) fibrotic area (mm²) (2) is divided through (3) the whole area of the myocardium (mm²).

3.4 Mouse treatment experiments

3.4.1 Treatment with receptor associated protein (RAP)

To study the role of Low Density Lipoprotein Receptor-related Protein 1 (LRP1) during myocarditis, mini osmotic pumps (Alzet model 2004, Charles River, USA) filled with the receptor associated protein RAP (provided by D.K. Strickland, Center for Vascular and Inflammatory Disease, Departments of Surgery and Physiology, University of Maryland School of Medicine, Baltimore, MD) or PBS as a control were implanted into the back of mice. Therefore, lyophilized RAP was dissolved in PBS at a concentration of 112µM one day prior to the experiment and filled into mini-osmotic pumps. Mice were anesthetized with 200µL MMF (Fentanyl 0,05mg/kg, Midazolam (5mg/kg) and Medetomidin (0,5mg/kg)) i.p., the back was shaved and a small cut was made. The pump was implanted into the back and the back was sutured. Mini osmotic pumps constantly released RAP in PBS or PBS as a control at a constant rate of 0.25µL/h, achieving RAP plasma levels of 5-10nM. Afterwards, mice were immunized as described under 3.3.1 and placed on a heating mat until they were awake. On day 21, mice were euthanized under anesthesia by cervical dislocation, hearts were flushed with PBS and placed in 4% PFA. H&E staining was performed as described under 3.3.2.[51]

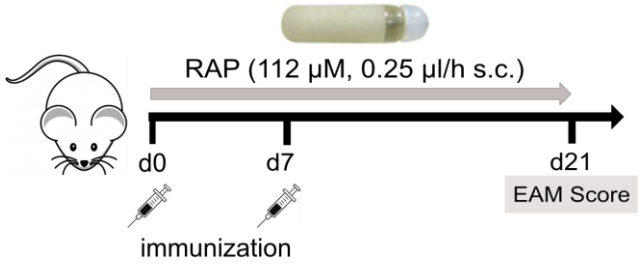

Figure 3-2 Experimental protocol for blocking LRP1 during EAM *in vivo.* Mini osmotic pumps constantly releasing RAP were implanted over 21 days. On day 21, mice were sacrificed and EAM Score was calculated.

3.4.2 Treatment with a monoclonal Anti-IFNAR blocking Ab

After Induction of EAM, mice were treated with a monoclonal blocking IFNAR Ab of mouse origin (IFNAR1, MAR1-5A3, BioLegend) or isotype control (mouse IgG1 κ, BioLegend). Mice were injected i.p. with 500µg for 3 consecutive days from day 8 followed by 500µg three times a week until the end of the experiment on day 14 or 21. BW was measured on each injection day and expressed in % of the initial BW. On day 21, mice were sacrificed and blood was taken as described under 3.3.4, spleen weight was measured, flow cytometry analysis were done as described under 3.3.5, cytokine concentration in the serum as described in 3.3.6. and HW/BW ratio was calculated as described under 3.3.2.

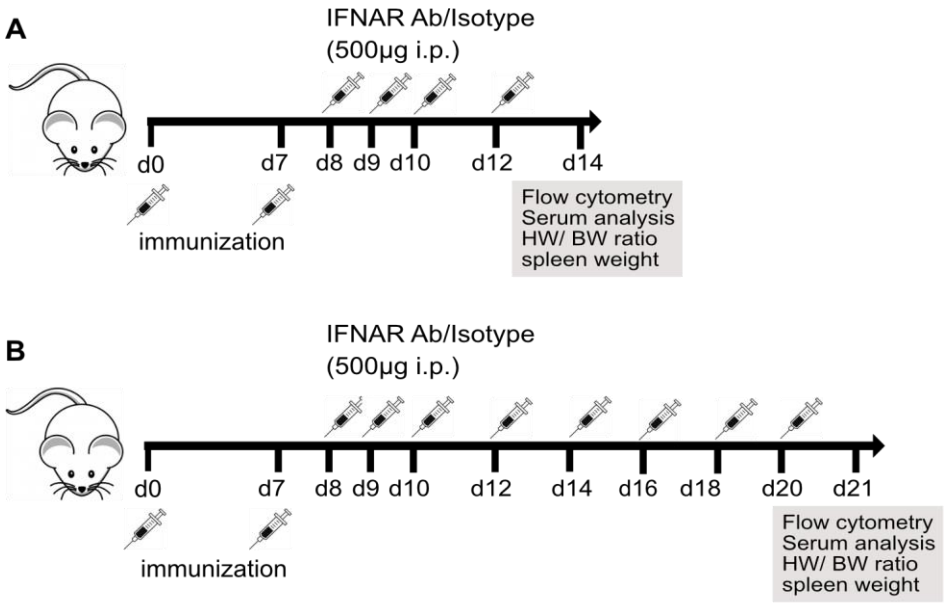

Figure 3-3 Experimental protocol for blocking the interferon receptor (IFNAR) using a blocking antibody (Ab) during EAM *in vivo*. A+B) Mice were immunized and treated with 500µg/mouse IFNAR Ab or Isotype control until day 14 and 21 respectively. A) On day 14 and B) day 21, mice were sacrificed and cytokine concentration in the serum was measured, spleen weight was calculated as well as HW/BW ratio and leukocyte infiltration was analyzed using Flow cytometry.

3.4.3 Treatment with DNase and Chloridamidine

After induction of EAM, mice were injected i.p. with either 50µg/mouse DNAse (Pulmozyme, Roche, Basel, Switzerland) twice a day or 250µg/mouse Chloridamidine (Cl-Amid, Merck, Darmstadt, Germany) once a day from day 21 until day 63. As control, 50µL PBS was applied to EAM and sham mice daily. On day 63 echocardiography was conducted as described in 3.3.8 and mice were sacrificed to stain hearts for Masson-Trichrome staining as described in 3.3.9.

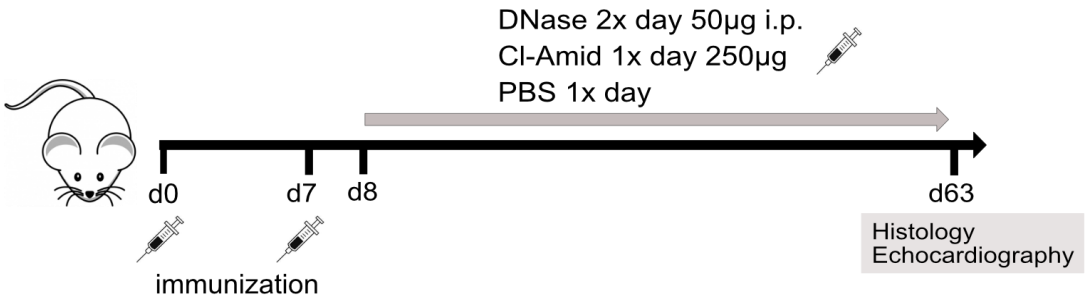

Figure 3-4 Experimental protocol for inhibiting NETs during EAM *in vivo*. Mice were immunized and treated with DNase twice a day and Cl-Amid once a day or PBS as a control. On day 63 echocardiography was conducted and mice were sacrificed for histology of the heart.

3.5 Immunofluoresence

Immunofluorescence staining was performed using Hoxb8 cells from LRP1^{ctrl} (Hoxb8LRP1^{ctrl}) and LRP1^{KO} (Hoxb8LRP1^{KO}) mice. Hoxb8 cells were cultured using Hoxb8-SCF cells culture medium (Table 8). For immunofluorescent staining, Hoxb8 cells were differentiated into neutrophils four days prior the experiment. Therefore Hoxb8 cells were incubated in 10 mL differentiation medium (Table 8) in a 10 cm² culture dish until day of experiment. Immunofluorescent staining was performed in IBIDI chambers coated with 20µg/mL rMK (PeproTech, New Jersey, USA) or 100 µg/mL mFibrinogen (PeproTech) at 4°C overnight. On the next day the chamber was washed thoroughly with PBS after coating. dHoxb8 cells were seeded in adhesion medium (ADM, Table 8) at a concentration of 2x10^5 in a 12 well chamber and were incubated with either 100 nm phorbol myristate acetate (PMA, Merck) as a positive control or left untreated as a control for 12 to 16 h at RT. Before fixation non adherent cells were gently discarded. Fixation was done using freshly diluted 4 % PFA in PBS for 4 minutes. Cells were washed 3x with PBS + 0.1% Tween20 (Sigma Aldrich) for 5 min each and were blocked with blocking solution (Table 8) on a shaker for 1 hour at RT. Cells were incubated with primary antibodies and isotype control (Table 9) were diluted in blocking solution on a shaker for 1 h at RT. After three times of washing with

PBS+0.1%Tween20 for 5 minutes each, cells were incubated with appropriate secondary antibodies (Table 10) diluted in 1% bovine serum albumin (BSA) in PBS for 1 hour at RT in the dark. Staining of the nucleus was performed using Hoechst 1:1000 (Table 10). Before mounting, cells were washed three times with 0.1%Tween20 in PBS for 5 minutes. Chambers were covered with ProLongTM Gold antifade reagent (Thermo Fisher Scientific) and coverslips. Images were taken at the Bioimaging core facility of the Biomedical Center Munich (Dr. Steffen Dietzel) using a Leica SP8X WLL upright confocal microscope and lasers with an excitation wavelength of 405 nm, 488 nm and 546 nm.[51]

Name	Ingredients	Company
Hoxb8-SCF cells culture medium	RPMI 1640 + 10% FCS + 1% Penicillin/Streptomycin (P/S) + 4% stem cell factor (SCF) containing CHO supernatant + 30 µM beta 2-mercaptoethanol + 10 µM β-Estradiol	Biochrome, Germany Biochrome, Germany Biochrome, Germany Sigma Aldrich, Germany Sigma Aldrich, Germany
Differentiation medium	RPMI 1640 + 10% FCS + 1% P/S + 4% SCF containing CHO supernatant + 20 ng/ml G-CSF	 Sigma Aldrich, Germany Sigma Aldrich, Germany
Adhesion Medium	pH 7.4 HBSS + 1.2 mM Ca2 + 1 mM Mg2 + 0.25 % Bovine serum albumin (BSA) + 0.1 % glucose + 20 mM Hepes	Biochrom AppliChem, Germany AppliChem, Germany Sigma Aldrich, Germany AppliChem, Germany Sigma Aldrich, Germany
Blocking solution	PBS + 1 % BSA + 10% goat serum	Biochrome, Germany Sigma Aldrich, Germany Carl Roth, Germany

Table 8 Buffer used for Immunofluorescence staining.

Antigen	Reactivity	Dilution	Clone	Company
Neutrophil Elastase NE	rat α-mouse IgG2α	2,5µg/ml (1:200)	Klon 887105	R&D Systems, USA
Histone H3	rabbit α-mouse IgG	5 µg/ml (1:200)	-	Abcam, UK
Isotype control	rat IgG2α, κ	2,5µg/ml (1:200)	eBR2a	Thermo Fisher Scientific, Germany
Isotype control	Rabbit IgG	5µg/ml (1:600)	-	Thermo Fisher Scientific, Germany

Table 9 Primary antibodies used for Immunofluorescence staining.

Antigen	Dye	Reactivity	Dilution	Company
Hoechst 33342	-	-	1:1000	Thermo Fisher Scientific, Germany
Secondary Ab	AF 546	goat α-rabbit	1:200	Life technologies, Germany
Secondary Ab	AF 488	goat α-rat	1:200	Cell signaling, UK

Table 10 Secondary antibodies used for Immunofluorescence staining.

3.6 Statistics

All data were analyzed using GraphPad Prism 9 software (GraphPad Software, San Diego, California, USA) and represented as mean ± SEM. For pairwise comparison an unpaired t test with Welch correction was used. For multiple comparison with one variable, ANOVA on ranks followed by Dunn´s post hoc test was performed. For multiple comparison with more than one variable, a 2-way ANOVA with Tukey´s comparison test was used. Significant outlier are excluded using GraphPad Prism outlier calculator. Statistical significance was assessed as *$p<0.05$, **$p<0.01$ ***$p<0.001$ and ****$p<0.0001$.

4. Results

Parts of the following data are published in “Midkine drives cardiac inflammation by promoting neutrophil trafficking and NETosis in myocarditis” by Weckbach LT.,.., **Boehm F**., et al. (2019) in the journal of experimental medicine (JEM)[51].

4.1 Mice develop EAM

To study myocarditis *in vivo*, the EAM model was used for experiments which resembles human myocarditis. Due to genetic differences only a few mouse strains are susceptible to the EAM model. In the present study Balb/c WT mice which are known to develop EAM were choosen[223]. To check whether Balb/c WT are the right experimental setup, mice were immunized s.c. with the cardiac peptide αMyHc (Ac-RSLKLMATLFSTYASADR-OH) together with Complete Freund´s Adjuvant (CFA) on day 0 and 7. As a control, sham-treated animals received PBS and CFA on day 0 and 7. On day 21, mice were sacrificed and hearts were removed for histological examination (Fig 4-1A).

When analyzing the BW of both groups, it was observed that the EAM as well as the sham-treated control group gained weight (105%) until the second immunization on day 7. Until day 21 sham-treated control mice constantly gained weight with about 15% (115%) increase in BW compared to initial BW (100%). However, mice treated with αMyHc showed a significant weight loss until day 14 (95%) after the induction of EAM compared to sham-treated control mice which did not receive the cardiac peptide. Nevertheless, EAM mice gained weight until day 21 (Fig 4-1B).

Myocarditis is characterized by the presence of foci of myocardial infiltration and cardiomyocyte death in histological sections. To investigate leukocyte infiltration into the cardiac tissue mice were sacrificed at day 21 which marks the peak of inflammation and hearts were stained with hematoxylin for the cell nuclei (blue) and Eosin for the extracellular matrix and cytoplasm (pink)[180]. Histological sections of the myocardium showed more leukocyte infiltration into the tissue in EAM mice (right) compared to sham-treated control mice (left) as indicated by the arrows (Fig 4-1C).

Next spleen weight and HW/BW ratio, which is known to be an indicator of cardiac hypertrophy and an important parameter for cardiac function[224], was analyzed on day 21. Spleen weight of mice treated with the peptide was significantly elevated compared to that of sham-treated control mice. HW/BW ratio was significant higher between HW/BW of EAM treated mice compared to sham-treated control mice (Fig 4-1D).

To analyze whether the spleen weight and the HW/BW ratio are depending on the degree of leukocyte infiltration, referred to as EAM Score, in the cardiac tissue, Hematoxylin and Eosin (H&E) staining was applied. Here, mice with an EAM Score of 4, meaning over 30% of the heart is infiltrated by leukocytes, showed a higher spleen weight as well as a higher HW/BW ratio compared to sham-treated control animals. Whereas mice without any leukocyte infiltration in the heart, indicated by an EAM score of 0, showed similar results as sham-treated control mice (Fig 4-1E). These data indicate a direct link between the degree of inflammation and spleen weight or HW/BW ratio.

Furthermore, blood was harvested on day 21 after the induction of EAM and analyzed using flow cytometry. A significant increase in the number of leukocytes, neutrophils, lymphocytes and monocytes in EAM-treated mice compared to sham-treated control mice was observed indicating an ongoing inflammation process (Fig 4-1F).

All results collected suggest that the EAM model is a perfect experimental setup to further investigate the molecular insights into myocarditis *in vivo*. The data reveal specificity of organ hypertrophy in EAM treated mice.

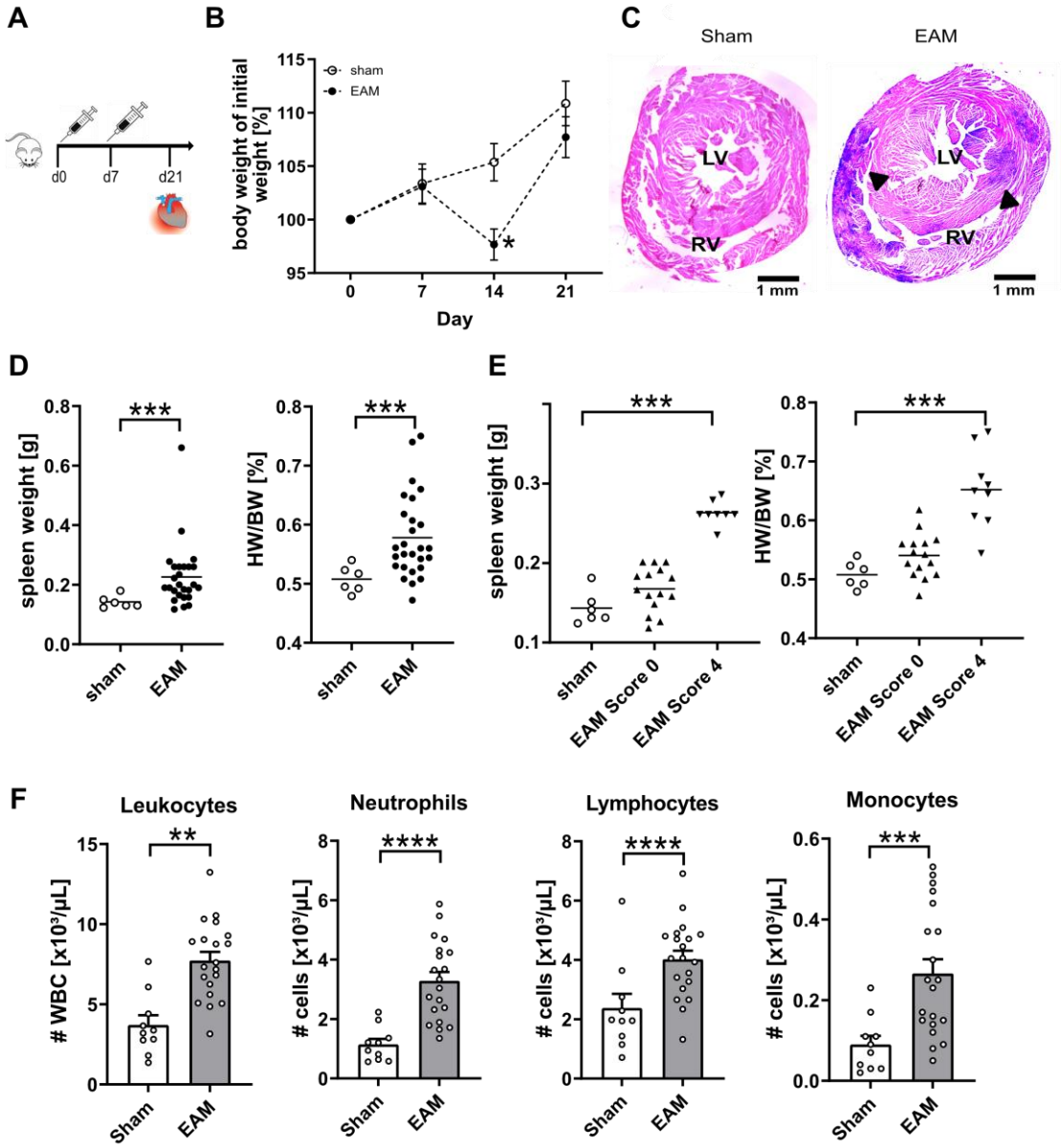

Figure 4-1 Balb/c WT mice develop experimental autoimmune myocarditis. A) Mice were immunized with the alpha myosin heavy chain peptide on day 0 and 7 and sacrificed on day 21 after the induction of EAM. B) Body weight from the initial weight was measured on day 0, 7, 14 and 21 starting from the first day of immunization of EAM mice compared to sham-treated mice. C) Representative cross sections of heart tissue of EAM or sham immunization on day 21 using Hematoxylin/Eosin staining. Scale bar: 1 mm. D+E) Spleen weight and HW/BW (heart weight/body weight) ratio were analyzed on day 21 after the induction of EAM**.** n=6 for sham; n=26 for EAM. F) Blood was harvested on day 21 and overall cell numbers and leukocyte subset counts were measured. n=10 for sham; n=20 for EAM. To determine P values, a 2-way ANOVA was performed for A, a student's t test was used to compare sham and EAM for D+F and ANOVA on ranks with Dunn´s multiple comparison test for E. For all panels, *p<0.05, **p<0.01, ***p<0.001, ****p<0.0001; n.s. not significant. Data are presented as mean ± SEM or mean ± individual data points. LV=left ventricle, RV=right ventricle. Arrows indicate foci of leukocyte infiltration.

4.2 The Role of the MK-LRP1-NET-axis

4.2.1 MK gene expression is upregulated during EAM

The cytokine MK could be shown to be critical for PMN adhesion and recruitment during the inflammatory process[225] and blocking MK during the acute phase of cardiac inflammation reduced leukocyte infiltration into the cardiac tissue on day 21[51]. To investigate, whether MK gene expression is also altered during cardiac inflammation in the EAM model real-time PCR of the cardiac tissue of EAM mice compared to sham-treated mice on day 21 was performed. MK gene expression was significantly upregulated in the heart during cardiac inflammation compared to mice which do not develop myocarditis (Fig 4-2B).

Since MK is known to be expressed in the kidney of mice fetuses, it was analyzed whether MK expression is altered in the kidney during inflammation in adult mice. MK was significantly increased in the kidney of mice with EAM in comparison to sham-treated mice (Fig 4-2A).

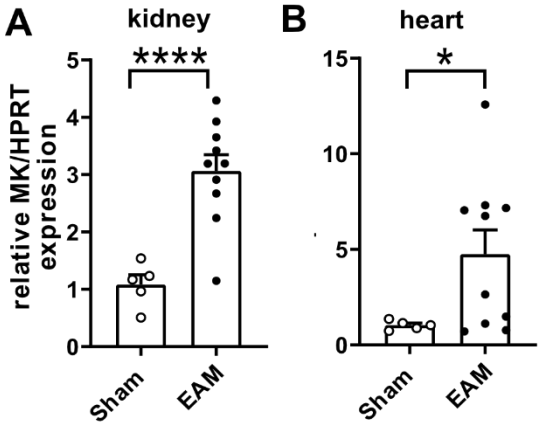

Figure 4-2 MK gene expression is altered during EAM in the cardiac tissue and spleen on day 21. A+B) Relative gene expression of MK in sham and EAM mice was determined by qPCR and normalized to housekeeping gene HPRT. A) Gene expression of MK in A) kidney and B) cardiac tissue. n=5 hearts for sham, n=10 hearts for EAM group. To determine P values, a student's t test was used to compare sham and EAM. *p<0.05, ****p<0.0001; n.s. not significant. Modified from Weckbach LT.,…,**Boehm F.** et al., 2019)[51]

4.2.2 LRP1 is critical for the pathogenesis of EAM

LRP1 is known to be the functional receptor for MK on PMN during the recruitment of Neutrophils[219]. To elucidate the role of LRP1 for the pathogenesis of EAM, LRP1 was targeted using the effective inhibitor receptor associated protein (RAP), which is known to block all members of the LDL receptor family[226]. Due to fast clearance of RAP mini osmotic pumps were implanted *s.c.* in the back of mice constantly releasing

112 µM of the inhibitor into the circulation over 21 days after the induction of EAM (Fig 4-3A).

EAM Score, where a score of 0 means no infiltration of leukocytes and a score of 4 30% of the heart is infiltrated, was used to evaluate leukocyte infiltration into the cardiac tissue. RAP administration from day 0 to 21 significantly reduced leukocyte infiltration into the cardiac tissue in the EAM model suggesting that LRP1 may play a role for leukocyte recruitment during cardiac inflammation in this model (Fig 4-3B).

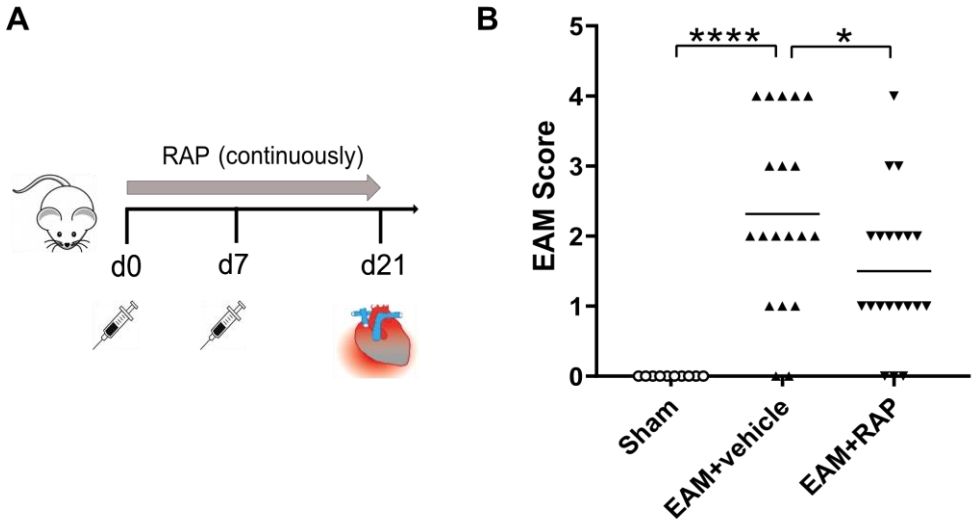

Figure 4-3 LRP1 is critical for the pathogenesis of EAM. A) Mini osmotic pumps were implanted in the back of mice constantly releasing RAP at a concentration of 112 µM into the circulation from day 0 until day 21 upon induction of EAM. B) Leukocyte infiltration using EAM Score was measured at day 21 after the induction of EAM in EAM mice compared to sham-treated mice. n=10 hearts for sham, n=20 hearts for EAM+vehicle group and n=20 for EAM+RAP group. To determine P values, ANOVA on ranks with Dunn´s multiple comparison test was performed. Data are expressed as mean ± SEM. *p<0.05, ****p<0.0001. (modified from Weckbach LT.,…, **Boehm F.** et al., 2019)[51]

4.2.3 MK-mediated NET formation is LRP1 dependent *in vitro*

Previous data could show that blocking MK with a blocking Ab over 21 days during EAM reduced the number of infiltrated neutrophils in the cardiac tissue *in vivo*[51]. Furthermore the reduced infiltrated neutrophils showed a reduced formation of NETs[51].

To further study whether MK is able to induce NET formation via LRP1 *in vitro*, NET formation using Hoxb8 cell-derived PMN generated from LRP1$^{fl/fl}$/vav-cre^{+} (dHoxb8-LRP1^{ko}) or LRP1$^{fl/fl}$/vav-cre^{-} (dHoxb8-LRP1^{ctrl}) was investigated. These cells were kindly generated by Annette Zehrer (AG Walzog) and are an easy tool to study

neutrophil function *in vitro*. Whereas PMN are short-lived cells which can not be manipulated genetically, a new murine cell system had been developed to study neutrophils *in vitro*. Here, a retrovirus encoding for the fusion protein of an estrogen-depending Hoxb8 (ER-Hoxb8) was transferred into isolated mouse bone marrow cells. These cells retain the potential to differentiate into myeloid and lymphoid cells but have lost the capacity to do it themselves. Binding to estrogen induces the transcription of proteins preventing differentiation into murine hematopoietic progenitor cells. Upon removal of estrogen the ER-Hoxb8 fusion protein becomes inactive and the progenitor cells can differentiate into mature neutrophils. The expansion *in vitro* with SCF influences the differentiation into neutrophils.[227,228]

Differentiated Hoxb8 cells (dHoxb8) were generated from the bone marrow of $LRP1^{ctrl}$ (dHoxb8$LRP1^{ctrl}$) and $LRP1^{fl/fl}$ (dHoxb8$LRP1^{KO}$) mice. Using immunofluorescence, these cells were stimulated in the presence of immobilized MK (iMK) or fibrinogen as a negative control. As a positive control, cells were treated with PMA. When staining for DNA and citrullinated H3 (H3Cit) no NET formation was observed when left untreated. PMA induced NET formation regardless of the presence of LRP1. In the presence of iMK, LRP1ctrl cells formed NETs as indicated by the colocolization of DNA and H3Cit. By using Hoxb8 cells lacking the LRP1 receptor (dHoxb8$LRP1^{ctrl}$) hardly any NET formation was observed (Fig 4-4A). The quantitative analysis revealed that MK-mediated NET formation was significantly reduced in the absence of LRP1 suggesting that MK mediates NET formation via LRP1 (Fig 4-4B).

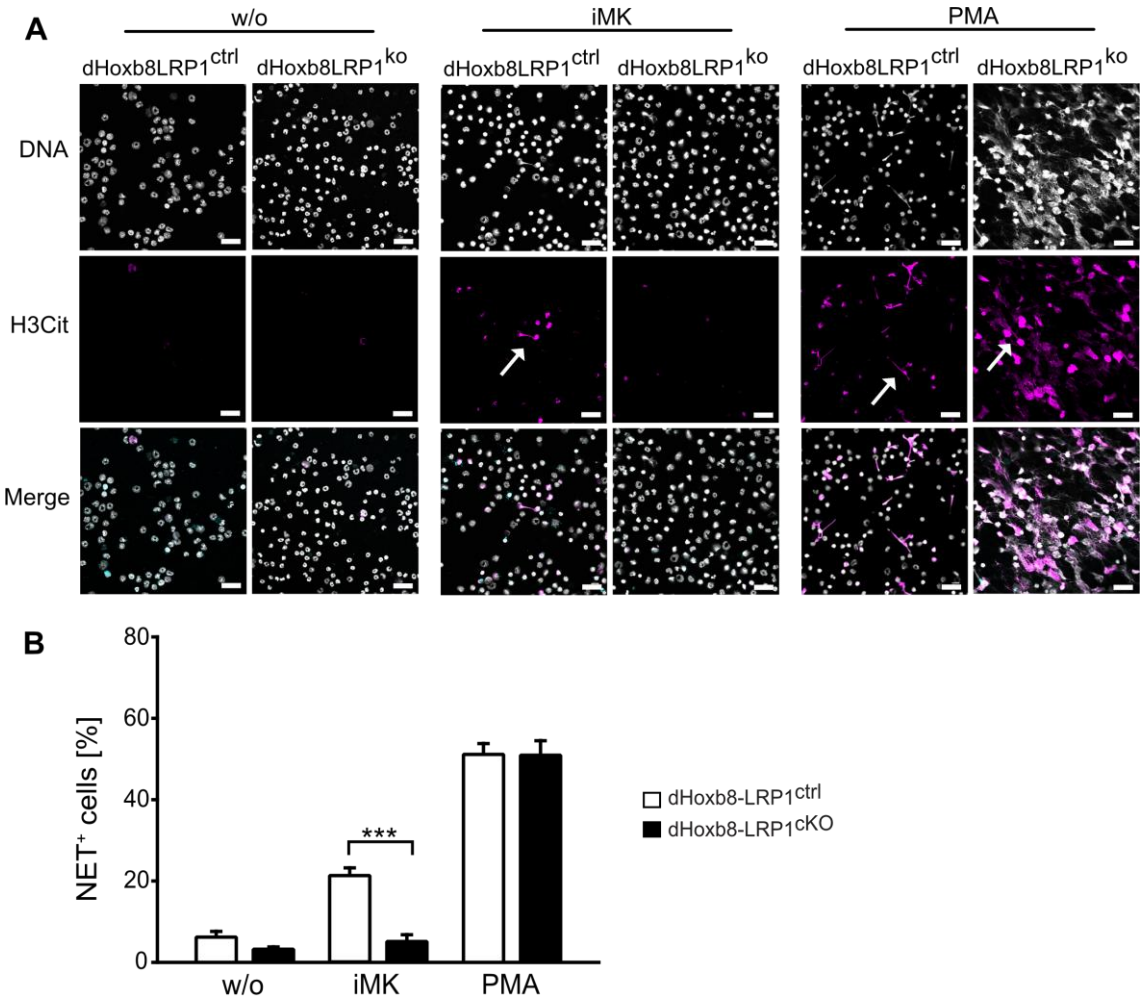

Figure 4-4 MK induced NET formation via LRP1 *in vitro*. A) Immunofluorescence images of dHoxb8-LRP1^{KO} and dHoxb8-LRP1^{ctrl} cells. Cells were treated with iMK, PMA or were left unstimulated (w/o) for control. Images show staining for citrullinated histone 3 (H3Cit) in magenta and DNA in grey. Scale bar: 20 µm. Arrows indicate the presence of NET formation. B) Quantitative analysis of NET formation in the presence of iMK, PMA or without stimulation. Data show the percentage of NET$^+$ cells of all dHoxb8 cells. n=3. To determine P values, a student's t test was used to compare sham and EAM. Data are presented as mean ± SEM. ***p<0.001. (modified from Weckbach LT.,…, **Boehm F**. et al., 2019)[51]

4.3 Targeting NETs as a therapeutic intervention of myocarditis on day 63

For the first time, it was recently demonstrated by Weckbach et al., that neutrophils play a crucial role during cardiac inflammation by inducing NETs[51]. NETs are present in the cardiac tissue of patients with acute myocarditis as well as in the cardiac tissue of mice on day 21 after the induction of EAM[51]. Using the EAM model Weckbach et al., showed that blocking NETs reduced inflammation during the acute phase of the disease[51].

Since NETs consist of DNA which can be teared down by desoxyribonucleases, recombinant DNase can be applied to degrade NETs and therefore have a regulatory effect on NET formation in neutrophils[77,229]. On the other hand, the inhibitor Cl-Amid inhibits NET formation by irreversibly inactivating peptidyl arginine deiminase 4 (PAD4) by modificating an active site of cysteine which is important for its catalytic activity[230].

Given that NETs play a crucial role during the acute phase of cardiac inflammation the question came up whether blocking NETs has an impact during the chronic phase and whether blocking may have a therapeutic impact on the outcome of myocarditis. To address these questions, mice were immunized on day 0 and 7 and two different substances were applied to block NETs. DNAse was administered twice a day and Cl-Amid once a day from day 21 until day 63 (Fig 4-5A).

First, the amount of fibrotic tissue using Masson-Trichrome staining as the amount of collagen in the cardiac tissue and stained for collagen (blue) and for cell nuclei (pink) was evaluated. Microscopic inspection of the heart sections demonstrated that immunized mice receiving PBS showed more fibrotic tissue in the myocardium than sham controls at day 63. Mice receiving DNAse or Cl-Amid showed no difference compared to EAM mice receiving only PBS from day 21 to 63 (Fig 4-5D). For quantitative analysis of the amount of fibrosis in the myocardium, a semiquantitative fibrosis score was used. Here, a score of one defines no fibrosis in the myocardium whereas a score of 5 means 5 % of the heart is fibrotic tissue. When analyzing the area of fibrosis compared to the whole myocardium using the fibrosis score no effect was observed for DNase or Cl-Amid-treated mice compared to PBS treated mice (Fig 4-5B).

To study cardiac function ejection fraction (EF) was measured using mouse echocardiography at day 63. This parameter describes the percentage of blood in the heart that is pumped out of the left ventricle into the body´s vascular system. Thus, EF is an important parameter for cardiac function. Significantly reduced systolic function of EAM mice compared to sham-treated control mice was observed at day 63, as expected. However, the data obtained revealed no improvement of the heart function after targeting NETs in EAM mice compared to EAM mice treated with PBS (Fig 4-5C).

Taken together, targeting NETs with the application of DNase or Cl-Amid as a therapeutic intervention has no impact on myocarditis at day 63.

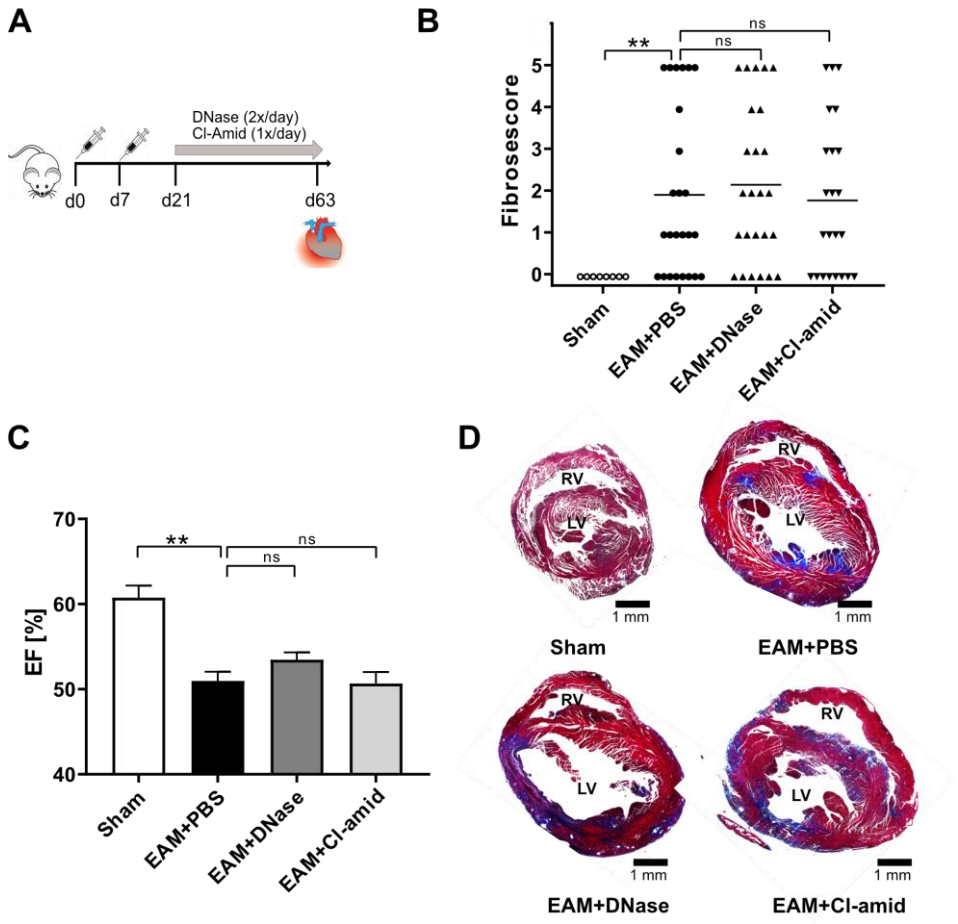

Figure 4-5 Targeting NETs after onset of EAM did not impact fibrosis or systolic function. A) Mice were sham-immunized (sham) or immunized (EAM) and were treated with either DNase or Cl-Amid from day 21 to 63. B) Degree of fibrosis in the cardiac tissue was measured using a semiquantitative fibrosis score. C) Echocardiographic evaluation of systolic function at day 63 after the induction of EAM. D) Representative images of a Masson´s Trichrome staining on heart sections of sham-treated, PBS treated EAM mice and EAM mice after DNAse or Cl-Amid treatment at day 63 after induction of EAM. Fibrotic tissue appears blue. Scale bar: 1 mm. LV=left ventricle, RV= right ventricle. n=8 for sham group and n=24-26 for EAM groups. To determine P values, ANOVA on ranks with Dunn´s multiple comparison test was performed. Data are presented as mean ± SEM. **p<0.01; n.s. not significant.

4.4 The role of IFN-I during EAM

As described above, myocarditis is a T cell mediated process and the link between the innate and the adaptive immune system during myocarditis remains largely elusive. To this end, it needs to be investigated whether the IFN-I pathway plays a role during myocarditis. Recently, plasmacytoid dendritic cells (pDCs) were described as a new key player between the innate and adaptive immune system[231].

4.4.1 The role of pDCs during EAM

To test whether pDC´s play a role during cardiac inflammation, digested hearts of EAM mice were stained for immune cell marker for pDCS, SiglecH, B220 and CD69 after the onset of EAM at day 14. A significant higher infiltration of activated pDCs (SiglecH+B220+CD69+) was observed compared to sham-treated mice into the cardiac tissue indicating that pDC´s may play a crucial role during cardiac inflammation (Fig 4-6).

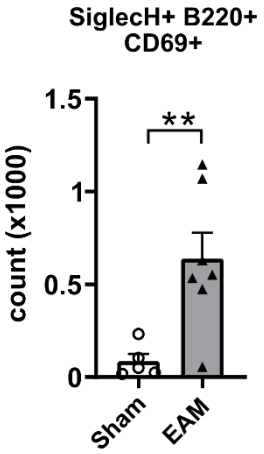

Figure 4-6 Quantitative analysis of the infiltration of activated pDCs into the cardiac tissue at day 14. Flow cytometry analysis of SiglecH$^+$B220$^+$CD69$^+$ on pDCs after the induction of EAM. n=5 for sham and n=7 for EAM. To determine P values, student´s t-test was performed. Data are presented as mean ± SEM. **p<0.01.

4.4.2 IFN-I pathway genes are upregulated during EAM

pDCs represent the main source of IFN-I. Therefore IFN-I accounts for a lot of genes expressed in activated pDCs (IRF3, IRF7, IRF8, interferon stimulated genes (IFIT)1, IFIT3 and ISG15). pDCs are also known to secret a variety of pro-inflammatory cytokines (CXCL10, CXCL8, CCL3 and CCL4). Thus, it was investigated whether IFN-I or genes involved in the IFN-I pathway may play a role during cardiac inflammation.

To address this question, mice were immunized, sacrificed at day 7, 14 or 21 and hearts were collected. Hence, mRNA levels for IFN-I (*Ifnα, β*), *Irf3*, *Irf7*, *Irf8*, *Ifit1*, *Ifit3* or *Isg15* were analyzed using quantitative real time PCR.

No altered relative gene expression was found in the cardiac tissue of EAM mice for all tested genes on day 7 (Fig 4-7A-D). However, increased levels of *Ifnα* and *Ifnβ* were observed, specifically on day 14 and 21 after the induction of EAM compared to day 7 in EAM treated mice. Additionally, gene expression was significantly upregulated on day 14 and 21 in EAM treated mice compared to sham-treated control mice (Fig 4-7A).

Irf3, *Irf7* and *Irf8* were significantly upregulated on day 21 in EAM mice compared to day 7 and 14. Furthermore a significantly upregulation of these genes could be observed between EAM treated mice and Sham control mice on day 14 and 21 (Fig 4-7B). The same effect of an upregulation of these genes on day 14 and 21 was observed for *Ifit1, Iift3* and *Isg15* (Fig 4-7C).

Next, altered gene expression of different chemokines (CXCL10, IL-6) was investigated, which can be induced after IFN-I stimulation. *Cxcl10* and *Il-6* were significantly upregulated on day 14 and 21 in EAM mice compared to day 7. Furthermore, a significantly upregulation of these genes could be observed between EAM treated mice and Sham control mice on day 14 and 21.

To conclude, IFN-I, IRFs, ISGs and chemokines are all upregulated in EAM mice on day 14 and 12 compared to sham-treated control mice. As expected, no difference was observed between EAM treated and sham-treated control mice on day 7. This significant upregulation on day 14 and 21 of genes involved in the IFN-I pathway highlights the importance of IFN during cardiac inflammation. These data suggest that IFN-I is activated during cardiac inflammation and may play a role during EAM.

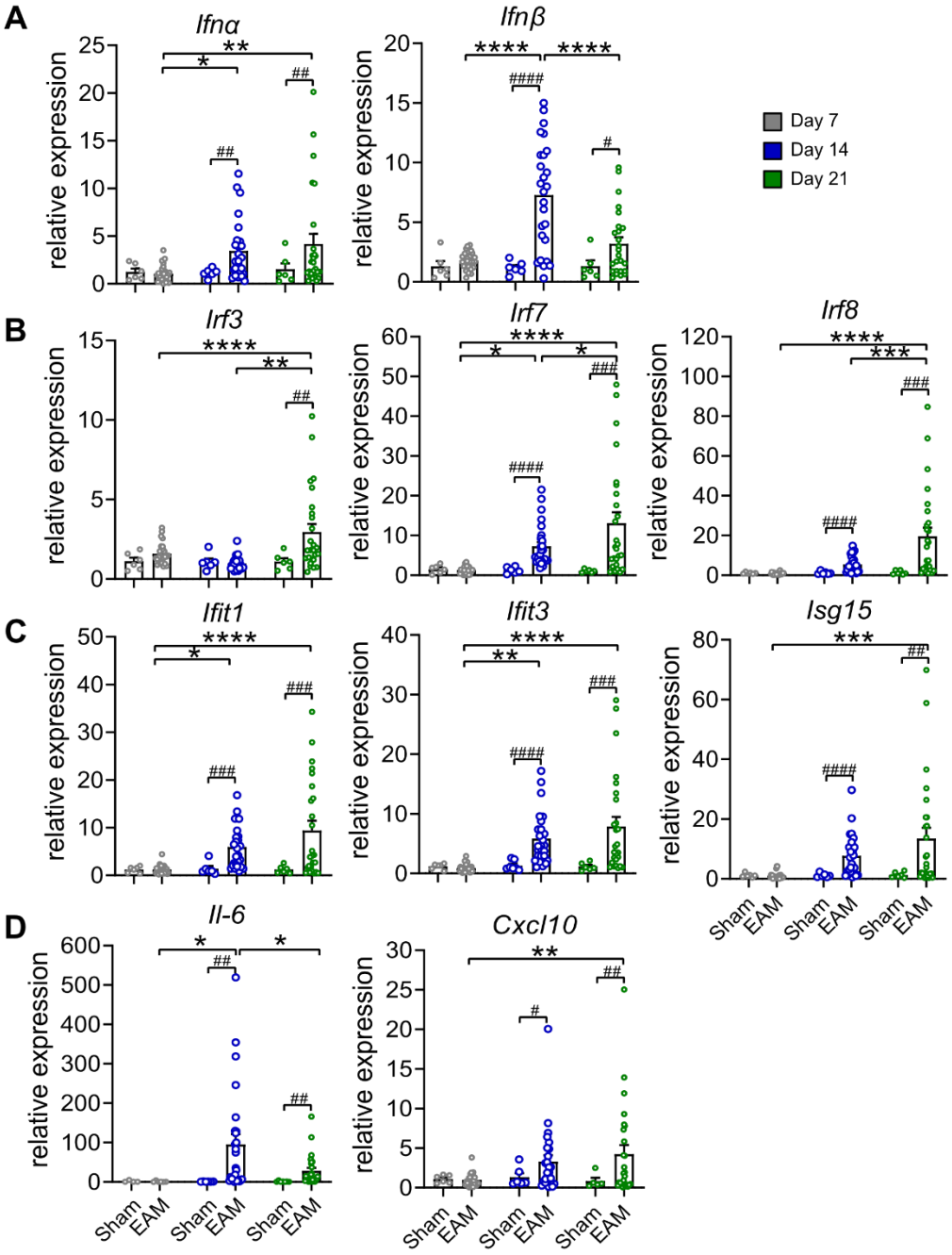

Figure 4-7 Gene expression of genes involved in the IFN-I pathway. A-D) Relative expression levels of mRNA in the cardiac tissue of EAM mice (EAM) compared to sham-treated mice (sham) at time point 7, 14 and 21 after the induction of EAM using quantitative real time PCR. Gene expression was normalized to housekeeping gene HPRT. n=6 hearts for sham, n=26 hearts for EAM group. To determine P values, a student's t test was used to compare sham and EAM (#), and a 2-way ANOVA with Tukey´s Post-hoc was used to compare time points (*). Data are presented as mean ± SEM. *p<0.05, **p<0.01, ***p<0.001, ****p<0.0001, # equivalent to *.

4.4.3 Blocking IFNAR until day 14 does not alter leukocyte composition in the heart during EAM

Since a shift in the upregulation of genes involved in the interferon pathway could be detected during cardiac inflammation, it was analyzed if IFN-I and genes involved in the IFN-I pathway might play a role during cardiac inflammation.

Therefore, IFNAR, which is ubiquitously expressed in all cells, was blocked by using an IFNAR Ab after the induction of EAM. Balb/c mice were treated with the IFNAR blocking Ab or isotype control from day 8 until day 14 after the induction of EAM. The treatment consisted of three consecutive injections daily with 500µg per mouse followed by 500µg three times a week until day 14 (Fig 4-8A).

By analyzing the BW in relation to the initial BW it was observed that each group gained weight from day 0 until day 7. After the second immunization on day 7 mice receiving the isotype control showed a significant reduced BW compared to sham-treated control mice. Mice treated with the IFNAR Ab showed a reduced BW compared to sham-treated control mice. However, there was no difference observed between isotype-treated EAM mice compared to IFNAR Ab-treated mice (Fig 4-8B).

Next, HW/BW of mice was analyzed on day 14. The HW/BW ratio was significantly higher in isotype-treated EAM mice compared with that of sham-treated control mice. However, the ratio of the mice treated with the IFNAR Ab did not differ from those of the isotype-treated mice (Fig 4-8C).

Additional data were obtained from the analysis of spleen and heart weight (HW) on day 14. As for the HW/BW ratio, a significant change was observed in spleen and HW for the isotype-treated group compared to sham-treated mice. However, a difference for heart and spleen weight was not detected in the IFNAR AB-treated group compared to those of the isotype-treated ones. No significant changes in the organ weight were observed between both groups (Fig 4-8D, E).

To sum up, isotype-treated mice showed changes in the HW, spleen weight and the HW/BW ratio compared to sham-treated mice indicating that mice treated with the cardiac peptide have been developing cardiac inflammation. However, no significant change for this parameter was observed in IFNAR Ab-treated mice.

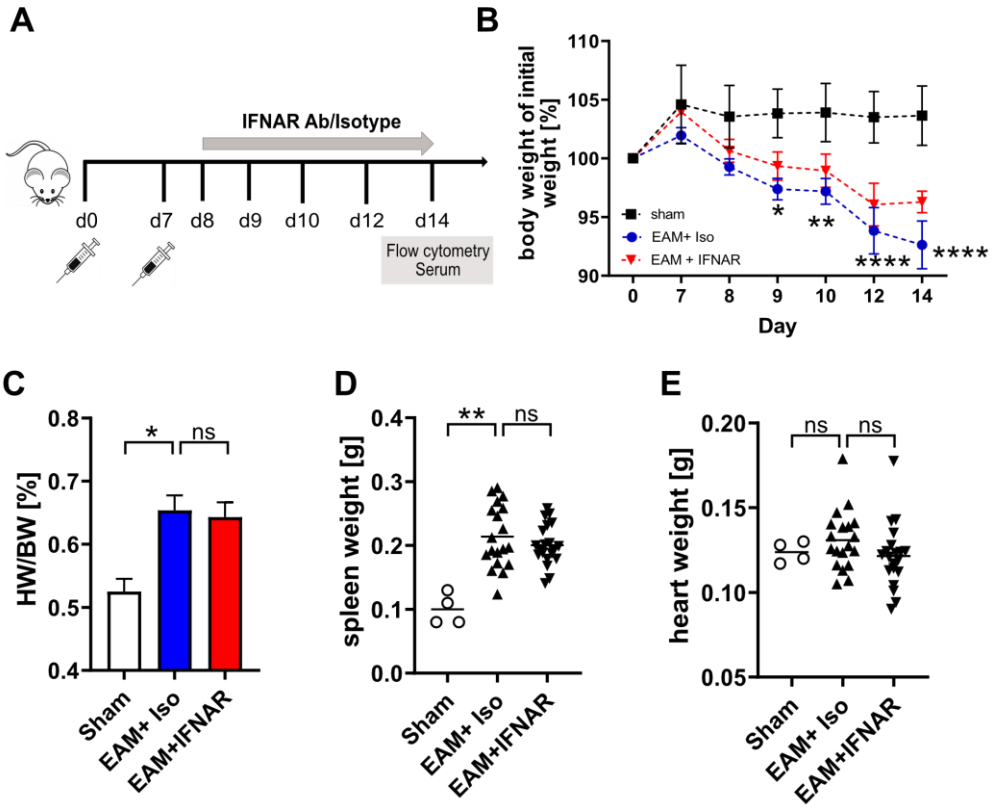

Figure 4-8 Blocking IFNAR from day 7 until 14 has no impact on the outcome of myocarditis. A) 500 µg of either control or IFNAR blocking Ab were injected three days in a row followed by 3 times per week until day 14. B) Body weight of mice was measured over 14 days. C) Evaluation of the heart weight/body weight (HW/BW) ratio, D) spleen weight and E) heart weight at day 14 after induction of EAM or Sham-treated mice. n=10 for Sham, n= 20 for EAM+ isotype and n=20 for EAM+IFNAR Ab**.** To determine P values, a 2-way ANOVA was performed for B and ANOVA on ranks with Dunn´s multiple comparison test for C-E. For all panels, *p<0.05, **p<0.01; n.s. not significant. Data are presented as mean ± SEM.

Next, altered leukocyte infiltration of specific leukocytes was investigated in the heart by IFNAR blockade on day 14. Therefore, digested whole hearts of EAM mice were analyzed upon administration of the IFNAR blocking Ab or isotype control treatment at day 14 after the induction of EAM using flow cytometry. Samples were stained for different markers such as the pan-leukocyte marker CD45, Ly6G, B220, SiglecH, live/dead, TCRβ and CD69. The gating strategy included initial gating on leukocyte population from the FSC versus SSC plot followed by gating on viable cells. Within the viable population, CD45 was plotted and within the CD45+ cells for Neutrophils (Ly6G), pDCs (B220 and SiglecH) and T cells (TCRβ). Each population was plotted against CD69 as an activation marker for cells (Fig 4-9).

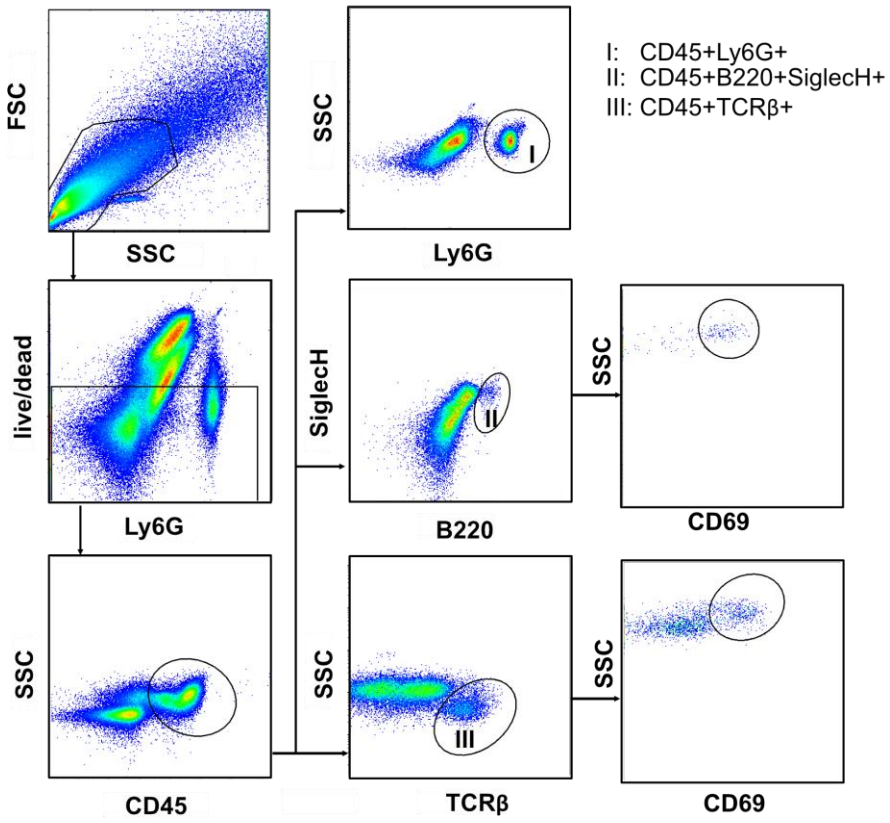

Figure 4-9 Gating strategy for heart infiltrating cells after blocking IFNAR until day 14. Mice were sacrificed at day 14 after immunization. Representative gating of heart-infiltrating inflammatory cells. An example of cell populations determined in the phenotyping analysis is shown.

Flow cytometry analysis revealed that EAM mice showed significant higher numbers of infiltrated cells stained with the pan leukocyte marker CD45+ in the heart compared to sham-treated control mice at day 14 after the induction of EAM. Moreover, a profound change was detected in the composition of infiltrating cells of Ly6G+, SiglecH+B220+ and activated SiglecH+B220+ and TCRβ CD69+ cells (Fig 4-10A-F). However, blocking IFNAR had a similar degree of inflammation and quantitatively comparable numbers of heart infiltrating CD45+cells as isotype controls (Fig 4-10A). There was a significant difference in the composition of infiltrating myeloid cells and-, specifically Ly6G+ neutrophils-, were diminished in IFNAR blocked mice in the cardiac tissue (Fig 4-10B). However, reduced infiltration of TCRβ and SiglecH was not affected by blocking IFNAR (Fig 4-10C, D). Moreover, no difference in the number of intracardiac cells was observed for activated TCRβ+CD69+ and SiglecH+B220+CD69+ cells (Fig. 4-10E, F).

Hence, IFNAR Ab treatment did not alter CD45 differences in the heart on day 14 and also showed no effect on the number of leukocytes in the heart. This indicates that blocking IFNAR until day 14 might not have a critical impact on cardiac inflammation.

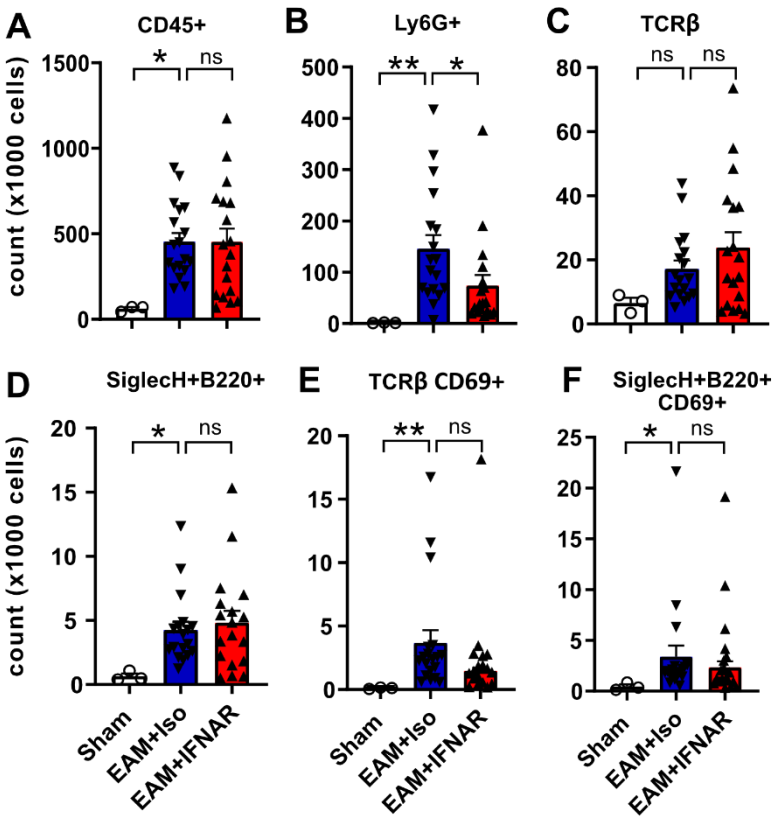

Figure 4-10 Blocking IFNAR does not alter leukocyte composition of heart infiltrating cells on day 14. EAM was induced and IFNAR blocking Ab or isotype were applied from day 8 until day 14. Mice were sacrificed 14 days after Immunization. (A-F) Flow cytometry analysis of the composition of heart infiltrating inflammatory cells. A) Total cell number of intracardiac CD45+ leukocytes, B) Intracardiac CD45+Ly6G+ neutrophils, C) intracardiac TCRβ+ T cells, D) SiglecH+ B220+ pDCs and E+F) activated T cells and pDCs. n=10 for Sham, n= 20 for EAM+ isotype and n=20 for EAM+IFNAR Ab**.** To determine P values, an ANOVA on ranks with Dunn´s multiple comparison test was performed. For all panels, *p<0.05, **p<0.01; n.s. not significant. Data are presented as mean ± SEM.

Since CD4+ T cells are the main drivers of cardiac inflammation, it was analyzed whether blocking IFNAR has an impact on the infiltration of inflammatory cells into the cardiac tissue on day 14. Therefore, cells were restimulated with the αMyHC peptide to see whether T cells are capable of producing cytokines *in vitro*. Afterwards cells were stained for cytokines IFNγ for Th1 subtype, IL4 for Th2 subtype and IL17A for Th17 subtype and analyzed using flow cytometry. The gating strategy included initial gating on leukocyte population from the FSC versus SSC plot followed by gating on viable cells. Within the viable population, CD45 was plotted and within the CD45+ cells for CD4+ T cells (TCRβ). Within CD4+ T cells were gated for cytokines (Fig 4-11).

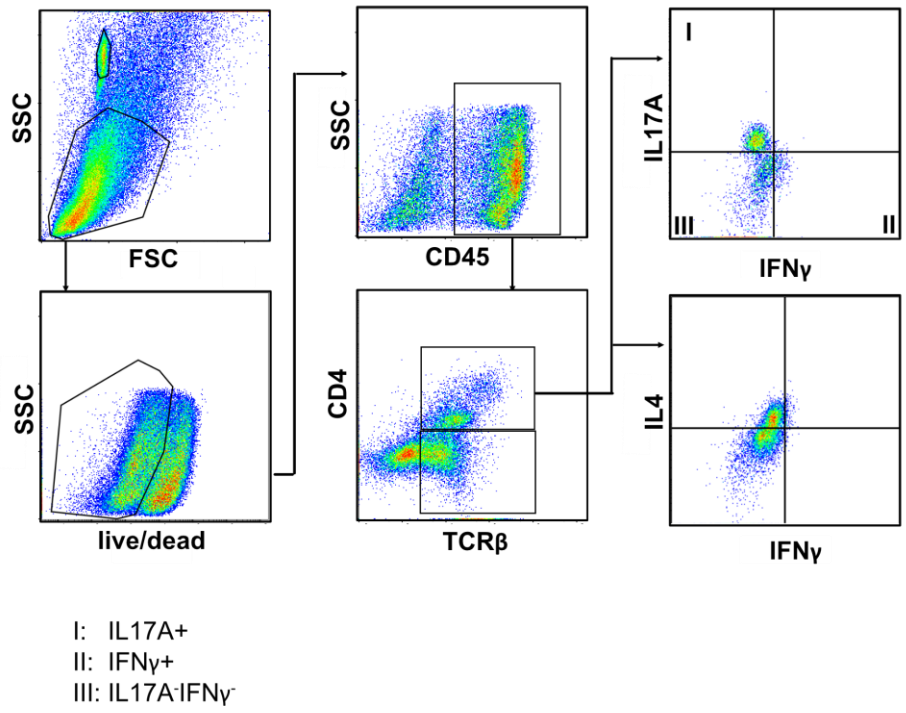

I: IL17A+
II: IFNγ+
III: IL17A$^-$IFNγ$^-$

Figure 4-11 Gating strategy for heart infiltrating cells after blocking IFNAR until day 14. Mice were sacrificed at day 14 after immunization. Representative gating of heart-infiltrating inflammatory cells. Sn example of cell populations determined in the phenotyping analysis is shown.

Next, it was investigated whether there is a shift in the infiltration of CD4+ T cells as well as Th1 (IFNγ), Th2 (IL4) or Th17 (IL17A) subtype in the cardiac tissue of mice treated with the blocking Ab or the isotype control.

When analyzing flow cytometry data, no difference was observed in the composition of CD4+ T cells as well as Th1, Th2 and Th17 subtype in the cardiac tissue of mice treated with the IFNAR blocking Ab or the isotype control. However, a significant higher infiltration of CD4+ T cells into the cardiac tissue of IFNAR blocking treated mice compared to isotype-treated mice was observed (Fig 4-12A).

The number of IL4+ Th2 cells and IL17+ Th17 cells was increased in IFNAR blocking mice, whereas mice treated with the isotype showed reduced numbers of IL17+ cells and IL4+ cells. Sham-treated mice showed hardly any infiltration of T cell subtypes (Fig 4-12B).

Data from the flow cytometry illustrated that mice treated with the blocking IFNAR Ab showed a higher number of Th2 and Th17 CD4+ subtypes on day 14.

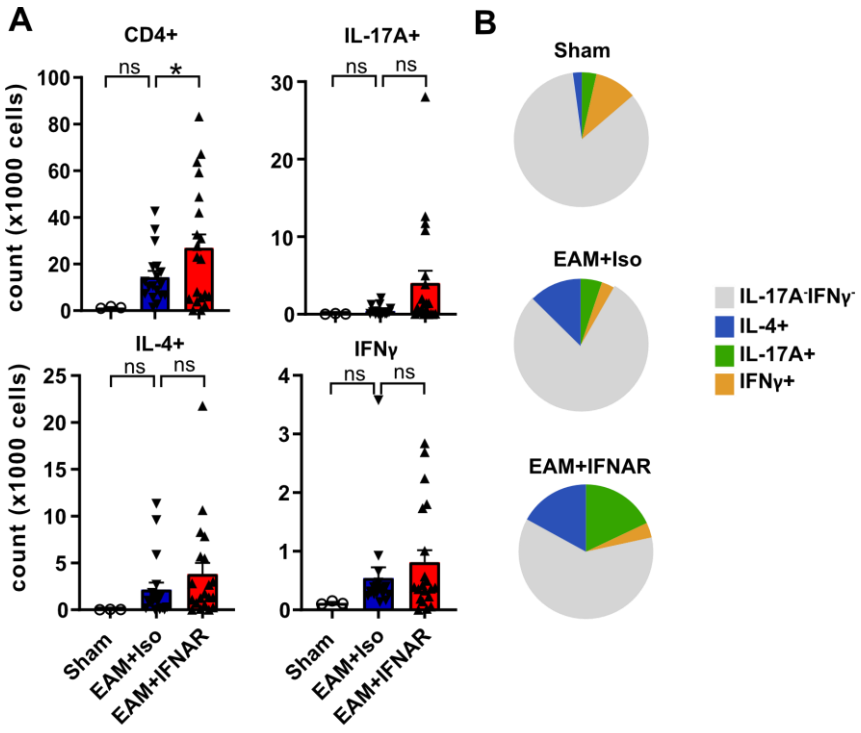

Figure 4-12 Quantitative analysis of infiltrating T cells into the cardiac tissue on day 14. Mice were immunized and treated with an IFNAR blocking Ab from day 8 until day 14. A) Flow cytometry analysis of the composition of T cell infiltrating cells in the cardiac tissue. B) Graphical presentation of the number of infiltrating T cells into the cardiac tissue, depicted by the size of the quadrant. n=10 for Sham, n= 20 for EAM+ isotype and n=20 for EAM+ IFNAR Ab. To determine P values, an ANOVA on ranks with Dunn´s multiple comparison test was performed. For all panels, *p<0.05; n.s. not significant. Data are presented as mean ± SEM.

To explore the expression profile of cytokines in the serum of mice treated with the IFNAR blocking Ab or the isotype control, a multiplex immunoassay was performed. To assess the effect of IFN, mice were treated with the blocking Ab. The results from the serum of mice on day 14 revealed that blocking IFNAR from day 8 until day 14 significantly reduced the amount of IFNα and IFNβ concentration in the serum of mice compared to sham-treated control mice and immunized mice treated with the isotype control (Fig 4-13 A, B). IFN was able to induce the production of IL-6 and CXCL10, but not IL-1β (Fig 4-13C-E) during EAM compared IFNAR Ab-treated mice. However, no difference was observed in the concentration of IL-1β in mice treated with the blocking Ab compared to isotype treated control mice (Fig 4-13 E).

Observations so far suggested, that blocking IFNAR increases CD4+ T cell infiltration into the cardiac tissue on day 14. However, none of the other leukocyte subsets were altered on day 14 after blocking IFNAR. Furthermore, blocking IFNAR reduced IFN-I, CXCL10 and IL-6 serum concentration.

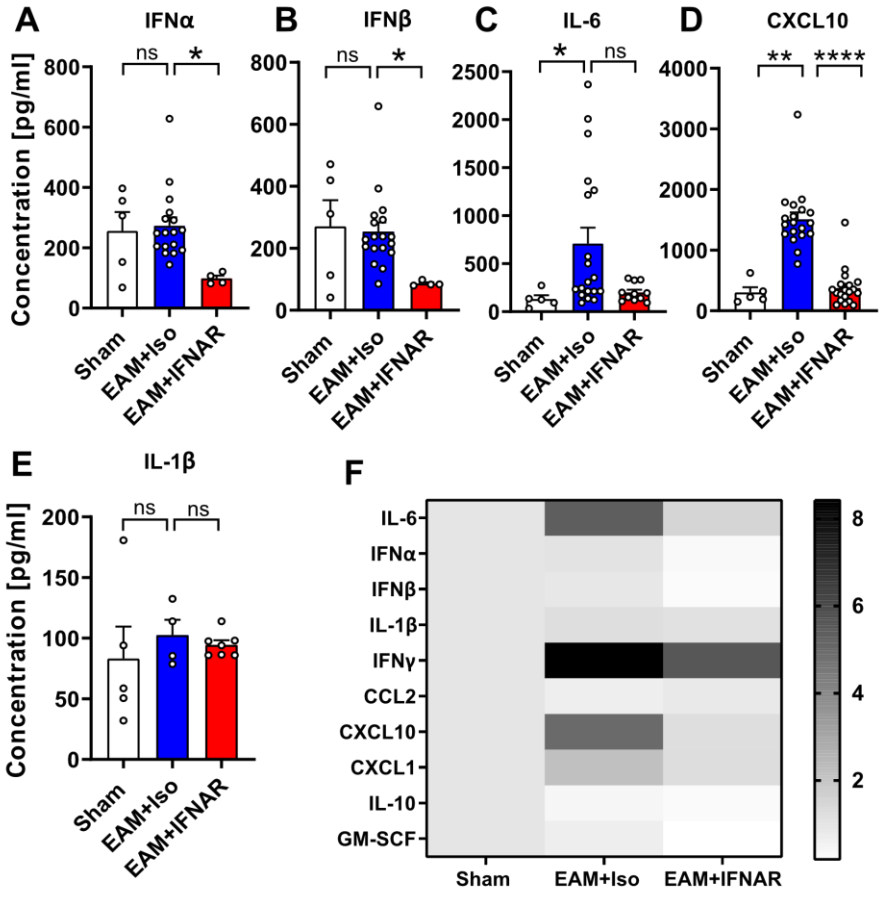

Figure 4-13 Quantification of cytokines in the serum after blocking IFNAR on day 14 after the induction of EAM. A-E) Analysis of cytokines in the serum of mice after IFNAR blocking on day 14 after the induction of EAM F) Heat map analysis of serum of mice after blocking IFNAR. n=10 for sham, n= 20 for EAM+ isotype and n=20 for EAM+IFNAR Ab. To determine P values, an ANOVA on ranks with Dunn´s multiple comparison test was performed. For all panels, *p<0.05; n.s. not significant. Data are presented as mean ± SEM.

4.4.4 Blocking IFNAR reduced infiltration of leukocytes into the cardiac tissue on day 21 after the onset of EAM

Since day 21 showed an upregulation of genes involved in the interferon pathway (Fig 4-7), the impact of IFN-I was elucidated on the acute phase of myocarditis on day 21.

Therefore, Balb/c mice were treated with the IFNAR Ab or the isotype control from day 8 until day 21 after the induction of EAM. The treatment consisted of three consecutive injections daily with 500µg per mouse followed by 500µg three times a week with either IFNAR Ab or isotype control until day 21 (Fig 4-14A).

Each group gained weight from day 0 until day 7 when analyzing the BW in relation to the initial BW. After the second immunization on day 7, mice receiving the isotype control showed a significant reduced BW compared to sham-treated control mice. This significant discrepancy of the BW between both groups remained until the end

of the experiment. Mice treated with the IFNAR blocking Ab showed a reduced BW compared to sham control mice. Additionally, mice treated with the IFNAR blocking Ab showed improved BW compared to isotype-treated mice indicating that IFN-I may play a role in EAM induced loss of BW (Fig 4-14B).

Next, HW/BW ratio of mice was analyzed on day 21. As for day 14, a significant increased HW/BW ratio was observed for the hearts of isotype-treated control mice compared to sham-treated mice. However, no difference was detected for the IFNAR Ab-treated group in comparison to the isotype-treated group (Fig 4-14C).

Additionally, data from the analysis of spleen and HW were obtained on day 21. As for the HW/BW ratio, a significant change in spleen and HW was observed for the isotype-treated group compared to sham-treated control mice. However, the data showed no changes in the organ weight for heart and spleen in the IFNAR Ab- or isotype-treated group (Fig 4-14D, E).

To sum up, isotype-treated mice showed changes in the HW, spleen weight and the HW/BW ratio compared to sham-treated mice on day 21. However, no change for this parameter was observed in the IFNAR Ab-treated mice on day 21.

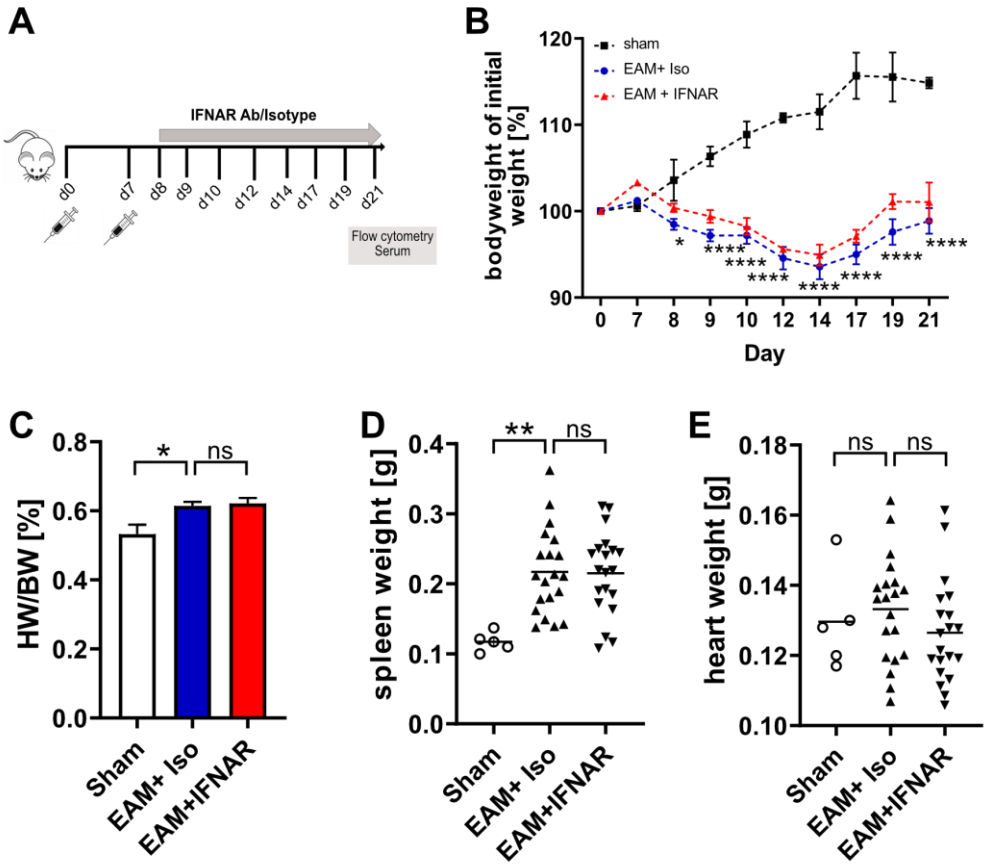

Figure 4-14 Blocking IFNAR from day 7 until 21 has no impact on the outcome of myocarditis. A) 500 µg of either control or IFNAR blocking antibody (Ab) were injected three days in a row followed by three times per week until day 21. B) Body weight of mice was measured over 14 days. C) Evaluation of the Heart/ body weight ratio, D) spleen weight and E) heart weight at day 14 after induction of EAM or sham-treated mice. n=10 for Sham, n= 20 for EAM+ isotype and n=20 for EAM+IFNAR Ab. To determine P values, a 2-way ANOVA was performed for B and ANOVA on ranks with Dunn´s multiple comparison test for C-E. For all panels, *p<0.05, **p<0.01; n.s. not significant. Data are presented as mean ± SEM.

To study whether the infiltration of specific leukocytes into the cardiac tissue was affected by IFNAR Ab or isotype application in EAM mice, the surface expression of CD45, Ly6G, TCRβ, SiglecH, B220 and CD69 was analyzed using flow cytometry on day 21 after induction of EAM. Analysis of the count of cells expressing the surface markers revealed a significant reduced infiltration of all leukocytes (CD45+) into the cardiac tissue of mice treated with the IFNAR Ab compared to isotype-treated mice (Fig 4-15A). Compared to isotype-treated control animals, the blockade of IFNAR resulted in a significant reduction in the number of CD45+Ly6G+ cells into the heart (Fig 4-15B). By staining TCRβ, it could be confirmed that the infiltration of CD45+TCRβ was significantly diminished after IFNAR application compared to isotype-treated control mice (Fig 4-15C). Administration of IFNAR Ab significantly reduced the number of CD45+SiglecH+B220+ cells compared to the isotype control

(Fig 4-15D). Staining the activation marker CD69 showed a significantly reduced infiltration of TCRβ CD69+ and SiglecH+B220+CD69+ after IFNAR blockade compared to isotype-treated control mice (Fig 4-15E, F).

Data from the multi-channel flow cytometry illustrated that blocking IFNAR led to a significant reduction of all leukocytes in the cardiac tissue, thus interfering with the infiltration of immune cells. This significantly diminished infiltration of immune cells highlights the importance of IFN-I during the pathogenesis of cardiac inflammation during the acute phase.

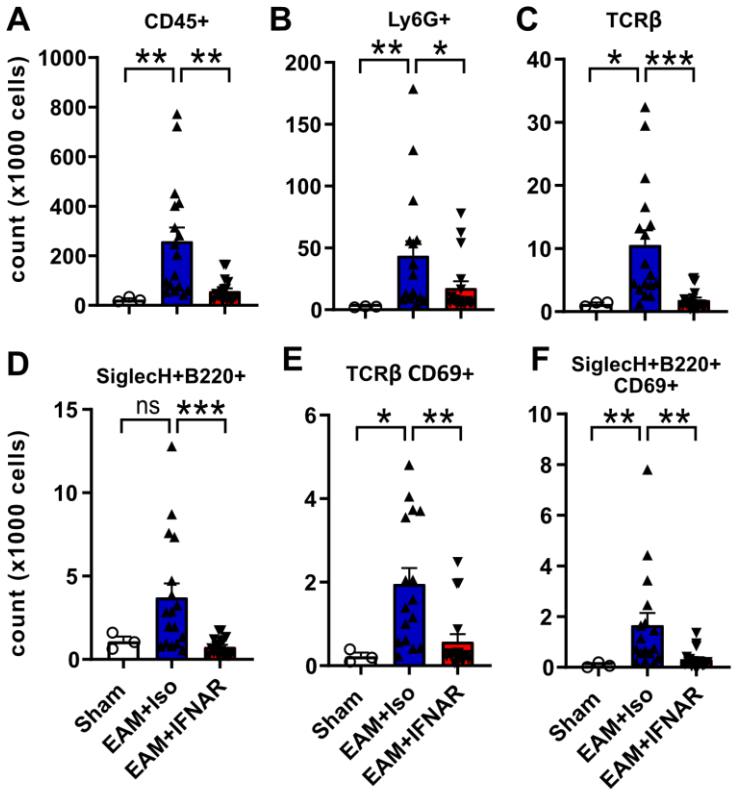

Figure 4-15 Targeting the interferon receptor (IFNAR) reduces leukocyte infiltration into the cardiac tissue on day 21. EAM was induced and mice were treated with an IFNAR blocking Ab or isotype from day 8 until day 21. Mice were sacrificed 21 days after Immunization. (A-F) Flow cytometry analysis of the composition of heart infiltrating inflammatory cells. A) Total cell number of intracardiac CD45+ leukocytes, B) Intracardiac CD45+Ly6G+ neutrophils, C) intracardiac TCRβ+ T cells, D) SiglecH+B220+ pDCs and E+F) activated T cells and pDCs. n=10 for Sham, n=20 for EAM+ isotype and n=20 for EAM+IFNAR Ab. To determine P values, an ANOVA on ranks with Dunn´s multiple comparison test was performed. For all panels, *p<0.05, **p<0.01, ***p<0.001; n.s. not significant. Data are presented as mean ± SEM.

To determine the frequency of lymphocyte subsets in the cardiac tissue intracellular staining of heart infiltrating leukocytes was performed. Therefore, hearts of mice treated with the IFNAR Ab or the isotype control were analyzed during EAM on day 21.

Flow cytometry data revealed an altered number of CD4+ T cells and subtypes between sham-treated and isotype-treated EAM mice. The number of infiltrated CD4+ T cells was upregulated and a significantly increased infiltration of CD4+ IFNγ (Th1), CD4+ IL4 (Th2) and CD4+ IL-17+ (Th17) cells was observed in isotype-treated EAM mice compared to sham-treated control mice (Fig 4-16A). Interestingly, the number of CD4+ T cells as well as CD4+ IFNγ+, CD4+IL4 and CD4+IL17+ cells were significantly diminished in the cardiac tissue of mice treated with the IFNAR blocking Ab in comparison to the isotype-treated control mice on day 21 (Fig 4-16A).

A different immune cell composition could be observed in the cardiac tissue of sham-treated mice compared to isotype or IFNAR Ab-treated animals. Here, the absolute number of CD4+ IL4 cells and CD4+ IL17+ cells was higher in IFNAR Ab-treated mice, whereas mice treated with the isotype control showed reduced numbers of IL17+ cells and IL4 cells on day 21. Sham-treated mice showed hardly any infiltration of CD4+ T cell subtypes (Fig 4-16B).

In summary, a significantly increased infiltration of leukocytes was observed in the EAM mice group treated with the isotype on day 21. Blocking IFNAR showed a significantly reduced infiltration of immune cells into the cardiac tissue compared to isotype-treated control mice on day 21 indicating that IFN-I may have an impact on the infiltration and recruitment of leukocytes into the heart after the onset of EAM on day 21. All of these findings further confirmed that IFN-I may be a potential therapeutic target with its involvement in cardiac inflammation.

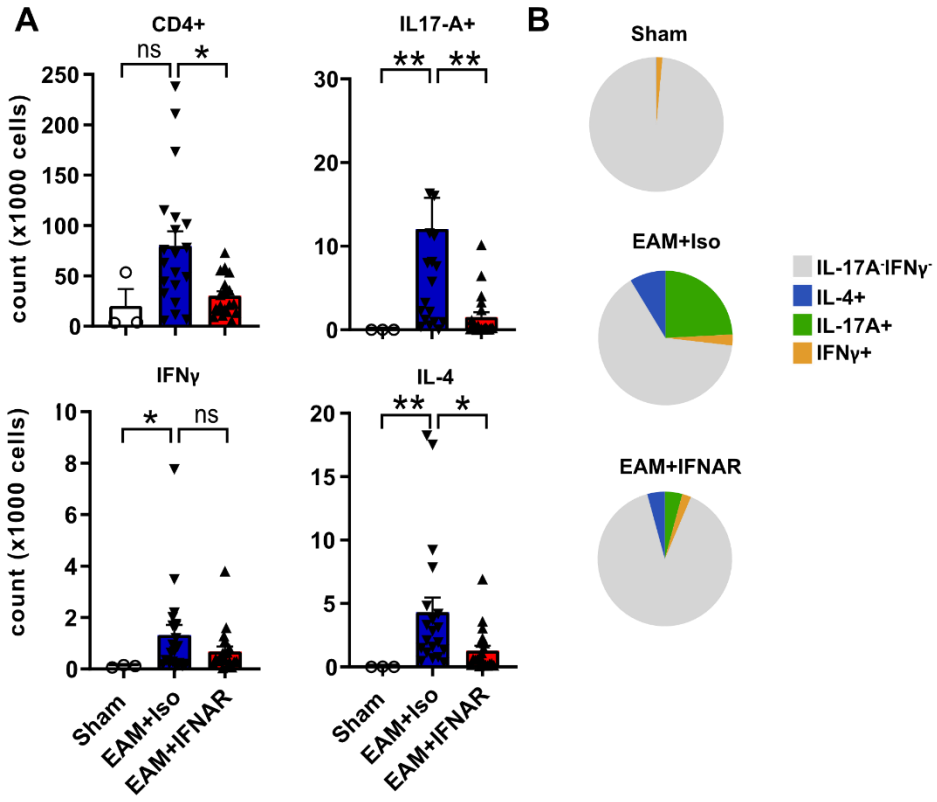

Figure 4-16 Quantitative analysis of infiltrating T cells into the cardiac tissue on day 21. Mice were immunized and treated with an IFNAR blocking antibody from day 8 until day 21. A) Flow cytometry analysis of the composition of T cell infiltrating cells in the cardiac tissue. B) Graphical presentation of the number of infiltrating T cells into the cardiac tissue, depicted by the size of the quadrant. n=10 for Sham, n= 20 for EAM+ isotype and n=20 for EAM+ IFNAR Ab. To determine P values, an ANOVA on ranks with Dunn´s multiple comparison test was performed. For all panels, *p<0.05, **p<0.01; n.s. = not significant. Data are presented as mean ± SEM.

5. Discussion

Over the past years the pathogenesis of myocarditis has been widely researched mainly focusing on the adaptive immune system rather than on the innate immunity. For this reason, the role of neutrophils and pDCs remains largely elusive. In the present study, the importance of neutrophils, pDCs and IFN-I for the pathogenesis during cardiac inflammation was analyzed *in vitro* and *in vivo*. It could be shown that the cytokine MK is upregulated on day 21 after the induction of EAM and that its receptor LRP1 is critical for the pathogenesis of EAM. In neutrophil-derived Hoxb8 cells i*n vitro*, we showed that MK-mediated NET formation is LRP1 dependent. Furthermore, our *in vivo* experiments unravel a crucial role of pDCs and the IFN-I pathway for the development of EAM.

5.1 EAM model

To investigate the pathology of myocarditis in humans, mouse models represent an excellent translational animal model in many biomedical fields[161]. In previous studies, a murine model of EAM was successfully established to investigate the pathogenesis of cardiac inflammation *in vivo*[168,232]. To induce EAM successfully, the adjuvant CFA is required. If CFA is applied together with an appropriate antigen, such as cardiac myosin, it provides the required immune activation to initiate EAM development and disease progression[170,233–235]. According to the protocol the Balb/c mice had to undergo two doses of CFA emulsified with cardiac myosin seven days apart for the development of EAM whereas other combinations of adjuvants were not sufficient[168,235]. In our study, we could confirm the validity of this mouse model for further experiments by injecting two doses of CFA emulsified with cardiac myosin seven days apart causing severe development of cardiac inflammation until day 21 (**Fig 4-1**).

First, we gained results to evaluate the degree of inflammation using H&E stained cross sections of mouse hearts by a semiquantitative score (EAM Score) on day 21. This time point is characterized by a massive infiltration of leukocytes and different subsets of leukocytes in the EAM model[174,180]. Here, we could show that mice immunized with myosin showed significantly increased leukocyte infiltration compared to sham-treated control animals. It was observed that EAM mice had inflammatory lesions and excessive infiltration of leukocytes into the myocardium on day 21. This is in line with studies that myeloid cells in CFA immunized mice infiltrate the heart at day 21[235]. Furthermore, the HW/BW ratio of EAM mice was significantly increased indicating a strongly pronounced inflammatory reaction in the myocardium in EAM

mice compared to sham-treated control mice. The effect of an increased HW/BW ratio in immunized mice compared to sham-treated mice has been described previously and is due to compensatory hypertrophy of the inflamed heart[224].

CFA has the ability to enhance the immune response to a presented antigen by stimulating and activating the immune system. It starts an immune response with an intense inflammatory reaction at the site of injection. This results in the damage of the tissue leading to an inflammation[236]. Our data show that total leukocyte numbers as well as the number of neutrophils, monocytes and lymphocytes were altered in the circulation in mice treated with the peptide on day 21. A study showed that neutrophils infiltrate the inflamed skin of mice 3h after CFA injection in an inflammation model and are also found 14 days later in the skin whereas T cells are found on day 7 in the skin[237]. This indicates that in our model an inflammation process took place, too. The fact that myosin induced mice lost weight from day 7 until day 21 indicates that these mice show a strong inflammatory process taking place within the whole body. Weight loss is an indicator for the progression of illness and is accompanied by decrease in BW due to decreased appetite as a consequence of distress, fear or pain[238,239].

We showed that spleen weight was significantly increased in EAM mice compared to control ones. This corresponds well with results from enlarged spleens during inflammation models[232,240,241]. CFA stimulates an inflammatory environment in the spleen at day 21[235] which could lead to the enlarged spleen in our model.

Here, we demonstrate that WT Balb/c mice are susceptible to the EAM model and the EAM model is a perfect model to study the pathogenesis of myocarditis *in vivo*.

5.2 MK-LRP1 axis plays a role during EAM

MK is a growth factor that mediates mid-gestational development and increased MK expression is associated with different diseases such as cancer, pathological kidney conditions, autoimmune diseases such as RA or cardiac pathologies such as myocardial infarction and heart failure[207,242]. Therefore, we analyzed whether MK, which is restrictively expressed under physiological conditions[243], is also expressed in the heart and kidney during cardiac inflammation. MK gene expression was analyzed on day 21 marking the peak of inflammation in EAM mice compared to sham-treated control mice. Our results augment these findings by showing that MK gene expression was significantly upregulated in the heart and kidney during cardiac inflammation indicating that MK plays a crucial role during cardiac inflammation (**Fig. 4-2**). We recently found that blocking MK using a neutralizing Ab from day one to 21 reduced leukocyte infiltration in EAM mice compared to sham-treated control mice[51].

MK might attract neutrophils to the site of inflammation during cardiac inflammation *in vivo*. The assumption that MK has a direct influence on the recruitment of PMN is supported by the observations of Weckbach et al. Here, MK could be shown to be critical for PMN adhesion and recruitment during the inflammatory process[225]. $MK^{-/-}$ mice showed reduced numbers of adherent neutrophils and extravasation[225]. Interestingly, only MK bound to the endothelium is able to initialize the recruitment of PMN[219] and studies showed that MK binds to the endothelium via its heparin-binding sites[244]. Immobilized MK leads to the adhesion and transmigration of PMN to the endothelium during inflammatory processes by leading to the high affinity conformation of β2 integrins (**Fig 5-1**).

LRP1 has been shown to be one of the receptors binding its ligand MK[215]. Other studies could show a role of the MK-LRP1 axis, where MK binds LRP1 and mediates neural cell survival[216]. Previously, LRP1 has been described to associate with the alpha chain of the β2 Integrin macrophage antigen-1 (MAC-1)[217] and regulating β2 integrin-mediated leukocyte adhesion[218]. Furthermore, blocking LRP1 impaired MK binding to PMN *in vitro*[225]. Therefore, MK may promote leukocyte infiltration in the EAM model acting via LRP1 (**Fig 5-1**). To investigate the functional role of LRP1 during myocarditis we inhibited LRP1 with RAP, which blocks all members of the LDL receptor family. Blocking LRP1 reduced leukocyte infiltration during EAM (**Fig 4-3**). Leukocyte adhesion and extravasation were substantially diminished in the absence of LRP1[51], indicating that LRP1 is critically involved in mediating adhesion. These results were similar to the data in $MK^{-/-}$ mice[225]. However, it cannot be excluded that the blockade of LDL receptor family members other than LRP1 contributed to our findings. However, different experimental procedures, including using $LRP1^{fl/fl}vav^{cre}$ and $MK^{-/-}$ mice, would be required to reveal the underlying mechanism of the MK-LRP1 axis attracting neutrophils to the site of inflammation during myocarditis.

5.3 MK mediates NET formation via LRP1 *in vitro*

In 2004, the group of A. Zychlinsky, discovered a new antimicrobial mechanism of activated neutrophils, called extracellular traps (NETs)[64]. Neutrophils maintain inflammation by releasing NETs where they play a role in autoimmune diseases such as RA or SLE[245,246]. As we showed that the MK-LRP1 axis plays a role during EAM, we wanted to elucidate whether the MK-LRP1 axis leads to the formation of NETs in PMN during myocarditis. In recent experiments, it could be shown that blocking MK reduced NET formation *in vivo* and MK mediated NET formation *in vitro*[51]. Therefore, we wanted to investigate whether binding of MK to its receptor LRP1 mediates NET formation *in vitro*. NET formation was studied *in vitro* using Hoxb8 cells lacking the

LRP1 receptor (Hoxb8LRP1^{ko}) and LRP1 WT cells (Hoxb8LRP1^{Wt}) as control. Here, LRP1 WT and KO cells were incubated either with PMA, MK or left untreated. Since the untreated control showed no decondensation of the cell nucleus, WT cells stimulated with MK showed NET formation with expelled traps (**Fig 4-4**). The stimulation with PMA as positive control showed NET formation regardless of LRP1. Here, we could show a proposed mechanism by which binding of MK to its receptor LRP1 promotes the induction of NETs. NET formation is one of the main functions of PMN to fight pathogens[64]. However, NETs are known to play a crucial role in many autoimmune diseases without any detectable pathogens and blocking the formation of NETs might be the solution[247]. Here, NETs not only eliminate the pathogen but also provide a novel source of autoantigens initiating or enhancing autoimmune diseases. The role of NETs during myocarditis is less known. Recently it could be shown that blocking NETs during the acute phase of EAM reduced cardiac inflammation[51]. I could show that LRP1 and MK play a crucial role during EAM indicating that MK binds LRP1 to produce NETs during cardiac inflammation.

A double-edged sword mechanism for the MK-LRP1-NET axis is proposed. Weckbach et al. showed that immobilized MK interacts with LRP1 leading to the adhesion of PMN[219]. Whereas we showed that binding of MK to LRP1 additionally induced NET formation *in vitro*. Binding of MK to LRP1 may lead to the adhesion and extravasation of PMN to the endothelium and might lead to NET formation in the cardiac tissue during myocarditis *in vivo*. This proposed mechanism is supported by the fact that blocking MK led to a reduced infiltration of PMN and the infiltrated PMN showed reduced NET formation[51]. Recruiting neutrophils and NET formation are beneficial to get rid of pathogens, however the fact that NETs also produce autoantigens leading to an immune response against itself, marks the MK-LRP1 axis as a double-edged sword. Further experiments are needed to prove the MK-LRP1-NET axis during myocarditis using different deficient mouse models.

5.4 Blocking NETs has no therapeutic intervention

PMN maintain inflammation by expelling NETs coated with their own DNA and antimicrobial proteins[64]. Furthermore, several reports by independent groups showed a role of NETs in autoimmune diseases. Excessive NET formation can have a worse impact on the heart. In recent experiments our group showed for the first time NETs in the cardiac tissue of patients with acute myocarditis and we demonstrated reduced leukocyte infiltration into the heart and reduced cardiac inflammation by blocking NETs with DNase and Cl-Amid during the acute phase[51]. Cl-Amid has been demonstrated to improve inflammatory disease phenotypes in autoimmune diseases

and it reduces the level of proinflammatory cytokines as well as the proliferation of CD4+ and CD8+ T cells[248]. All in all Cl-Amid treatment may lead to reduced inflammation caused by NETs.

Thus, we were interested whether blocking NETs has an impact on the outcome of myocarditis. To approach this, NETs were blocked with DNase and Cl-Amid from day 21 until day 63 during the chronic phase of myocarditis. How blocking NETs effects the further process of cardiac function and pathological reconstruction was assessed on day 63. Analysis of the cardiac function using ejection fraction and degree of fibrosis showed a marked limitation in EAM mice compared to sham-treated mice at this time point. Surprisingly, the outcome of myocarditis on day 63 in DNAse or Cl-Amid treated mice did not show any improvement of cardiac function nor cardiac tissue compared to EAM mice treated with PBS as control (**Fig 4-5**). Since the animals are housed in common rooms with many people entering, we cannot exclude that animals were under stress, providing potential explanation for this observation. Nonetheless we did not observe a difference in the outcome of Cl-Amid or DNAse and PBS-treated EAM mice, abrogating a potential effect of this treatment. It is still possible that the application time point on day 21 was too late. As we started the treatment at day 21, which is the time point patients usually go to see the doctor, chronic elevation of NET components in the tissue may have already led to repeated injury and the formation of excess matrix, affecting heart function over time. Here, NETs could be involved in the fibrosis process as it was shown for patients with fibrotic lung disease[249]. Other groups could show that mice receiving DNAse had improved cardiac function at the time sufficient for development of cardiac fibrosis to a similar extent as not expressing PAD4 in an experimental cardiac fibrosis mouse model[250]. However, the different outcome may be due to the different mouse models used or the inhibition in our model was not complete, hence NET formation was able to induce further fibrosis. Until now, genetic or pharmacological abrogation of PAD4 activity is the only way to clear NETs completely resulting in beneficial effects in various disease models, including thrombosis[251], fibrosis[252] or SLE. However, genetic ablation is not the suitable mouse model to answer the question whether blocking NETs has a therapeutic intervention because NETs contribute to the outcome of myocarditis.

In summary, blocking NETs after the manifestation of myocarditis has no therapeutic intervention.

5.5 The IFN-I pathway plays a role during EAM

As described above, myocarditis is a T cell mediated process and emphasis was now put on the link between the innate and the adaptive immune system during myocarditis.

5.5.1 IFN-I pathway genes during EAM

Here, to the best of our knowledge, this was the first study to reveal that IFN-I and genes related to the IFN-I pathway play a role during autoimmune myocarditis which was unreported so far. Until now IFN-I is associated with a number of autoimmune diseases such as SLE. We hence sought to evaluate whether IFN or genes involved in the IFN pathway may play a role during myocarditis.

Therefore, we investigated gene expression in the cardiac tissue on day 7, 14 and 21 after the induction of EAM compared to sham-treated control mice. In the present study, we identified that IFN-I, IRF3, 7 and ISG15, IFIT1, IFIT3 are highly expressed in the heart of EAM mice compared to sham-treated mice (**Fig 4-7**). IRF7 is cell type specific with constitutive expression in pDCs[116] and therefore can mediate immediately large amounts of IFNα[117]. Once pDCs could get activated by NETs expelled from Neutrophils[84,147], IRF7 gets phosphorylated by the CTTP complex[131,134]. Phosphorylated IRF7 translocates to the nucleus to act as a transcription factor where it promotes IFN-I production and the expression of various inflammatory cytokines such as IL-6 and CXCL10. Based on this knowledge, it is likely that the upregulation of the IFNα/β, IRF7 and cytokines CXCL10 and IL-6 gene expression in the cardiac tissue at day 14 and day 21 after the induction of cardiac inflammation indicates a crucial role for the IFN-I pathway. Additionally, IFN-I acts via an autocrine and paracrine signaling by binding to the IFNAR receptor on most every cell. This induces the phosphorylation of IRF3 inducing the expression of IFIT1, IFIT3 and ISG15[123]. It is important to note, that recent studies identified important functions of the IRFs in cardiovascular diseases. In patients with dilated cardiomyopathy IRF4 was downregulated in heart samples[253]. King et al discovered recently an importance for the IRF3-IFN axis in the infarcted heart in mice[151]. In our study IRF3 and IFIT1, IFIT3 and ISG15 are significantly upregulated on day 14 and 21 compared to sham-treated control mice. We suggest that IFN-I generates a stable pattern of IFN I transcripts (IFN signature) over time. This IFN-I signature found in the cardiac tissue at day 21 could be maintained by NETs found in the cardiac tissue lately[51]. Moreover, *in vitro*, NETs activate pDCs to produce IFN, which might explain the IFN signature in EAM mice. Despite these observations, the role of IFN-producing cells during myocarditis needs to be clarified because a number of studies suggest that several cell types are

involved in IFN production. However, as pDCs are the main producers of IFN-I and are detectable in the cardiac tissue, we assume that pDCs may drive the IFN-I immune response in the cardiac tissue during EAM.

5.5.2 The role of pDCs for EAM

Dendritic cells play a major part in autoimmune myocarditis[254], however, the role for pDCs remains elusive. Under homeostatic conditions pDCs circulate the blood, whereas upon inflammation pDCs accumulate in the inflamed tissue[255]. They are known to play a role in numerous diseases such as SLE or psoriasis by inducing massive amounts of IFN-I[256]. However, the contribution of pDCs to the progression of myocarditis remains largely unknown. Since pDCs are immune cells that had been proposed to control innate and adaptive immunity through the massive secretion of IFN-I, we aimed to analyze whether pDCs accumulate in the heart in our mouse model.

Therefore, pDC infiltration was measured using flow cytometry analysis on day 21 after the induction of EAM. Using the specific marker for murine pDC´s, SiglecH, it could be demonstrated that activated pDCs (SiglecH+CD69+) infiltrated the cardiac tissue on day 21 in EAM mice compared to sham-treated control mice (**Fig 4-6**). This is in line with another study which described the presence of accumulated pDCs in the heart tissue in EAM mice on day 21[257]. The immunohistochemical staining of endomyocardial biopsies showed increased pDCs in human myocarditis as well as in murine heart sections[258]. In addition, the same group showed decreased numbers of circulating pDCs[258], hence leading to an increase of activated pDCs in the target organ, the heart. Furthermore pDCs are known to infiltrate inflamed tissue leading to disease progression by producing IFNα[149]. Migration into the inflamed tissue is reliable on CXCL10[101], which is upregulated in the cardiac tissue in EAM mice on day 21 in our study. Furthermore, upregulated gene expression of CXCL10 might derive from pDCs after IFNα activation[102] leading to further recruitment of immune cells. Another hint for the importance of pDCs is the upregulated IRF8 gene expression in the cardiac tissue on day 14 and 21 (**Fig 4-7**), which is an important transcription factor regulating the survival and function of pDCs[139,140]. This leads to the assumption that after the activation of pDCs, IFN-I leads to a positive forward loop inducing the production of ISGs and inflammatory cytokines in cells during cardiac inflammation.

Considering that two groups have shown the presence of pDCs in the cardiac tissue independently from each other and the role pDCs play in other diseases, the assumption was made that pDCs might also have a key role during EAM. Since IFN-I signature genes are upregulated and activated pDCs accumulate in the cardiac

tissue, it was suggested that pDCs may produce IFN-I locally in the cardiac tissue as it is already shown for SLE lesions[97]. Furthermore, the exact mechanism of pDC migration into the cardiac tissue remains to be investigated.

5.5.3 Role of IFN-I on leukocytes during EAM

The contribution of IFN-I signaling to myocarditis remains completely unknown. IFNs control a variety of cell functions by binding to its receptor IFNAR 1 and 2, which is ubiquitously expressed on almost every cell in the body[119]. An increasing number of studies have demonstrated that the IFN-I pathway is profoundly involved in the development of autoimmune diseases such as SLE[256,259]. With our study proof was provide of the role of IFN-I during cardiac inflammation. Accordingly, understanding of the pathway mechanism will provide a new strategy for the prevention and treatment of myocarditis in humans. In this thesis, the importance of IFN-I production for the development of cardiac inflammation was confirmed by showing that systemic administration of a blocking AB against IFNAR led to a reduced leukocyte infiltration into the cardiac tissue on day 21 after the induction of EAM (**Fig. 4-15, 4-16**).

An increased immune cell count, such as neutrophils, T cells and pDCs was observed in the cardiac tissue in EAM mice compared to Sham treated control mice on day 21, as shown in the literature[174,257]. However, after blocking IFNAR until day 14 mice treated with the isotype as well as mice treated with the IFNAR blocking Ab showed similar leukocyte counts except for neutrophils (**Fig 4-10, 4-11**). Interestingly, blocking IFNAR until day 21 showed reduced leukocyte numbers of all immune cells. The data obtained, indicate that the inflammation process is still in the beginning at day 14 as altered leukocyte counts were not observed. It is slowly reaching its peak on day 21 with massive infiltration of leukocytes in the cardiac tissue indicating that IFN-I might be necessary for the massive infiltration of immune cells into the cardiac tissue and might be the key player for developing and inducing myocarditis. Blocking IFNAR attenuates the immune response on day 21, which is in line with findings of a myocardial infarction model, where IFNAR Ab treatment ablated the IFN-I response[260]. The assumption that the IFN-I pathway has multiple functions on different immune cells is supported by several observations.

We could proof that blocking IFNAR was successful, since the concentration of IFN-I was significantly reduced in the serum of mice treated with the IFNAR blocking Ab on day 14. Blocking the IFN-I pathway led to a reduced infiltration of only neutrophils into the cardiac tissue of EAM mice on day 14 showing that neutrophils are the first cells at the site of inflammation[63]. Hence, showing that neutrophils are more susceptible to IFN-I signals during the acute state, thereby explaining the specific effect on

neutrophils and not on adaptive immune cells on day 14. Furthermore, reduced IFN-I levels and reduced neutrophil infiltration after blocking IFNAR at day 14, supports the fact that neutrophils get induced by IFN-I leading to vascular damage[112]. Lately, neutrophils were identified as an inducer and producer of IFN-I[112,113] and likely contribute to the IFN-I levels detected in the cardiac tissue on day 21. As we detected reduced counts of immune cells at day 21 after blocking IFNAR in the heart, this would support the hypothesis, that the ongoing IFN-I signature might lead to damage in the cardiac tissue attracting further immune cells to the site of inflammation resulting in a massive infiltration of pDCs, neutrophils and T cells in the heart on day 21. Additionally, neutrophils are known to play a central role during cardiac inflammation by producing NETs as shown in heart sections of mice after the induction of EAM on day 21[51]. Furthermore, the existence of NETs in patients with acute myocarditis disclosed that the inflamed cardiac tissue harbors NETs in humans[51]. These structures have been shown to be involved in the activation of pDCs[84,261], leading to the production of IFN-I during cardiac inflammation. However, by blocking IFNAR it could be demonstrated that less activated pDCs infiltrated the heart on day 21 suggesting that activated pDCs may produce IFN-I during the latter phase of the disease at day 21. Furthermore, as NETs are known to regulate IFN-I[83] and blocking NETs reduces cardiac inflammation[51], NETs may be indicated to stimulate the IFN-I pathway. Regarding this, autoantigens released from neutrophils and subsequent formation of immune complexes might contribute to a positive-feedback loop that favors NET induction. This ultimately leads to the release of NETs with the capacity to stimulate pDCs to produce IFNα.

Furthermore, we examined the effect of IFN-I on the presence of T cells in the cardiac tissues, as previous studies have shown that T cells play a crucial role for the development of cardiac inflammation[170]. Here, a massive infiltration of T cells into the cardiac tissue was observed, which might be induced by IFN-I acting as an immune adjuvant[262]. Apart from being activated via NETs and producing higher amounts of IFN-I, pDCs are also a major source of pro-inflammatory and antiviral cytokines and chemokines and thus can directly recruit immune cells, in particular T cells[90,263].

T cells could interact with pDCs and enhance the IFN response during cardiac inflammation. After activation pDCs could be able to attract T cells by producing chemokines such as CXCL10[104] leading to the differentiation of CD4+ T cells into effector T cells by IFN-I[256]. We observed that mainly IL-17+ T cell infiltration was reduced when blocking IFNAR until day 21. This reduced number of Th17 cells could result in the direct effect of IFN on T cell differentiation into Th17 cells[264]. *In vivo* studies have already demonstrated that IL-17 is essential for the development of

EAM[196], showing that IFN can interrupt T cell recruitment. Additionally, NETs can prime T cells by reducing the activation threshold[81], therefore tempting to obtain that IFN-I leads to the release of NETs which might contribute to the activation of T cells in the cardiac tissue. So far, studies have shown that patients with SLE have increased NET formation and NETs activate pDCs to produce high levels of IFNα in a TLR9 dependent manner[84,147].

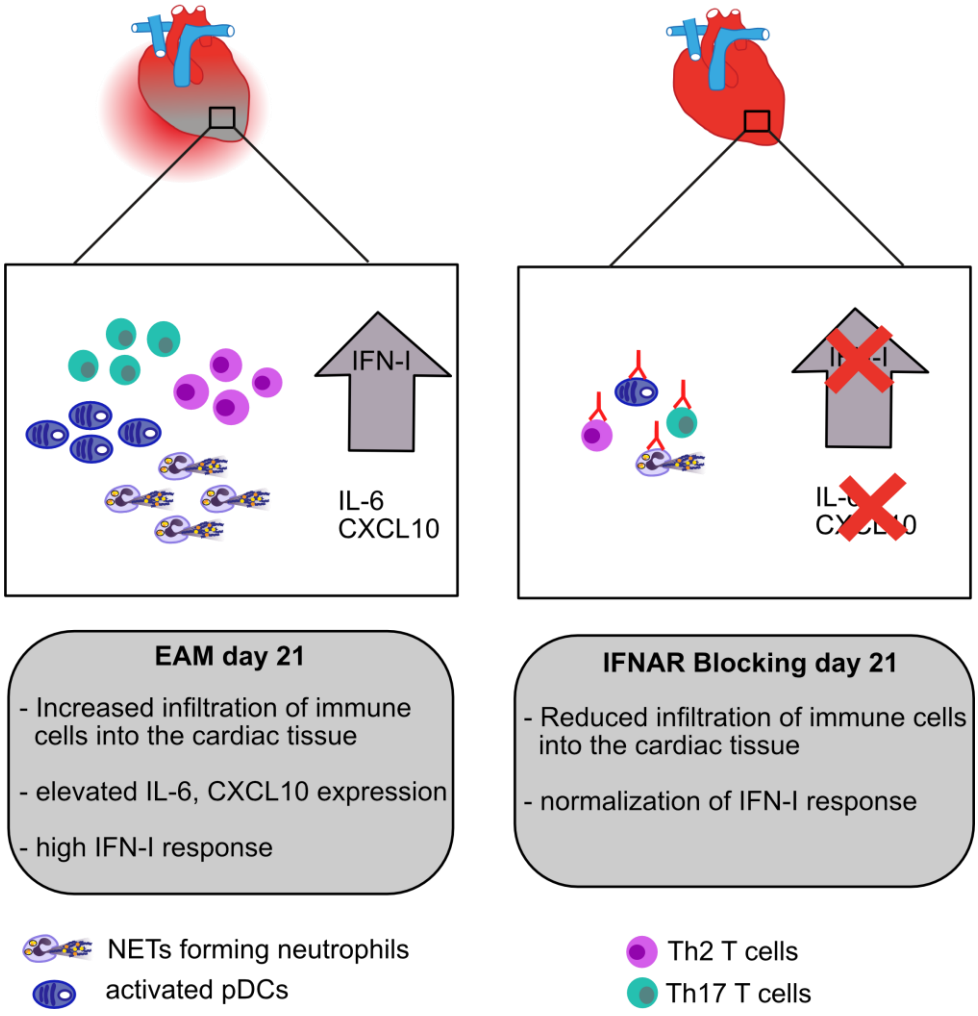

Figure 5-1 Mode of action of IFNAR blocking antibody on day 21. IFNAR reduced infiltration of immune cells and production of cytokines on day 21.

Here, it is demonstrated that several cell types are dependent on the IFN-I pathway with the important fact, that so far several cell types, once activated, can stimulate pDCs to produce IFN production. This identifies a new way in which pDCs and the IFN-I pathway connects the innate and adaptive immune response during myocarditis.

Altogether data from the multi-channel flow cytometry illustrated that inhibiting IFNAR until day 21 led to a significant reduction of neutrophils, pDCs and T cells in the cardiac tissue, thus interfering with the recruitment of immune cells. These findings further confirmed that IFN-I is a potential therapeutic target with its involvement in immune

cell trafficking. However, different experimental procedures, including using IFNAR$^{-/-}$ mice and depleting different immune cells, would be required to reveal the underlying mechanism of the IFN-I pathway during myocarditis.

5.5.4 Role of IFN-I for inflammatory cytokines

Another important factor which bridges the innate and the adaptive immune system is the pleiotropic IL-6. Studies showed that IL-6 is required for the pathogenesis of EAM and IL-6$^{-/-}$ mice showed reduced severity of myocarditis in the EAM model[195,196]. We observed significantly increased serum concentration of IL-6 in EAM mice on day 14 and upregulated gene expression on day 21 **(Fig 4-7, 4-13)**. This is in line with published data, that IL-6 is necessary for the induction of EAM[194]. Interestingly blocking IFNAR reduced IL-6 serum concentrations on day 14 and CD4+ IL-17 infiltrating cells on day 21. Lately it could be shown that IFNα enhances production of IL-6 by human neutrophils[265]. Furthermore, the upregulated IL-6 expression during cardiac inflammation on day 14 could be induced by NETs, as it was shown for RA neutrophils[245]. Therefore IFNα or NET could induce the production of IL-6 in the EAM model. IL-6 then mediates the induction of Th17 cells leading to EAM[196].

All in all, IFNAR blocking Ab application could reduce IL-6 levels and therefore the IFN-I pathway might have an impact on immune cells leading to ameliorated hearts.

5.5.5 Clinical relevance of the results

Until now there are no established treatment options so far for myocarditis. Although in up to 30% of the patients DCM occurs leading to heart failure and death. Our study gave first insights into the role of IFN-I and pDCs for myocarditis. To treat myocarditis specifically, the molecular mechanism behind it needs to be elucidated.

To our knowledge this is the first study showing a role of the IFN-I pathway during cardiac inflammation. Our observations could therefore be relevant for the understanding of the pathogenesis of autoimmune diseases such as myocarditis. Before selecting a therapeutic target for patients with myocarditis, different factors have to be kept in mind. First, the time when IFN-I is activated has to be considered. IFN-I mostly is activated during the early disease process, which we could also show in our mouse model. IFN-I genes and IFN-I protein expression is highly upregulated on day 14, whereas lower amounts are detected on day 21. Next, which IFNs are relevant in a specific patient? Here, due to the amount of subtypes of IFN, we only focused on α4 and β1 subunit. We could show that pDCs may be IFN-I producing cells during myocarditis, but to prove this, murine KO models should be used as well

as inhibiting other cells types. Last, the focus needs to be on the IFN target whether blocking IFNAR or signaling pathways is necessary.

With regard to clinical relevance, treatment with the IFNAR blocking Ab was considerably more effective at day 21 when initiated on day 8 after the induction of EAM. However, more studies are needed to fully elucidate the pathomechanism behind myocarditis.

6. Conclusion

In this work, first steps have been undertaken to disentangle the impacts of the immune system during myocarditis. Using experimental procedures such as a mouse model of EAM, we demonstrated that genes involved in the IFN-I pathway were upregulated during EAM, whereas leukocyte numbers (neutrophils, T cells, pDCs) in the heart were decreased after blocking IFNAR at day 21 after the induction of EAM. Here, an interplay between IFN-I and impaired recruitment could be observed. In summary the presented experimental data demonstrate for the first time that the IFN-I pathway plays a fundamental role during cardiac inflammation.

Despite these novel findings, which are summarized in **Figure 6-1**, this thesis identifies the knowledge gap in current research on myocarditis, especially regarding the link between the innate and adaptive immune system *in vivo*. However, this study demonstrates once more the complexity of this research field. Further efforts will be necessary to gain fundamental insights into how the immune system is regulated and works during cardiac inflammation.

The following action mode of IFN-I and immune cells during cardiac inflammation in the heart after exposure of hidden cardiac peptide and tissue damage of any cause to the immune system is proposed:

1. MK is highly expressed on the endothelium during cardiac inflammation
2. Neutrophils adhere to the inflamed tissue via the MK-LRP1 axis
3. MK induces NET formation via LRP1 in the cardiac tissue
4. NETs activate infiltrated pDCs to produce large amounts of IFN-I and pro-inflammatory cytokines (CXCL10, IL-6)
5. These attract further immune cells such as T cells (autoreactive against the cardiac peptide), more neutrophils and pDCs to migrate to the inflamed tissue
6. In a positive forward loop IFN-I activates more immune cells to produce more IFNα and stimulating neutrophils to produce further NETs
7. NETs further activate T cells and their differentiation into Th17 subtype
8. This leads to cardiac damage and a massive infiltration on day 21

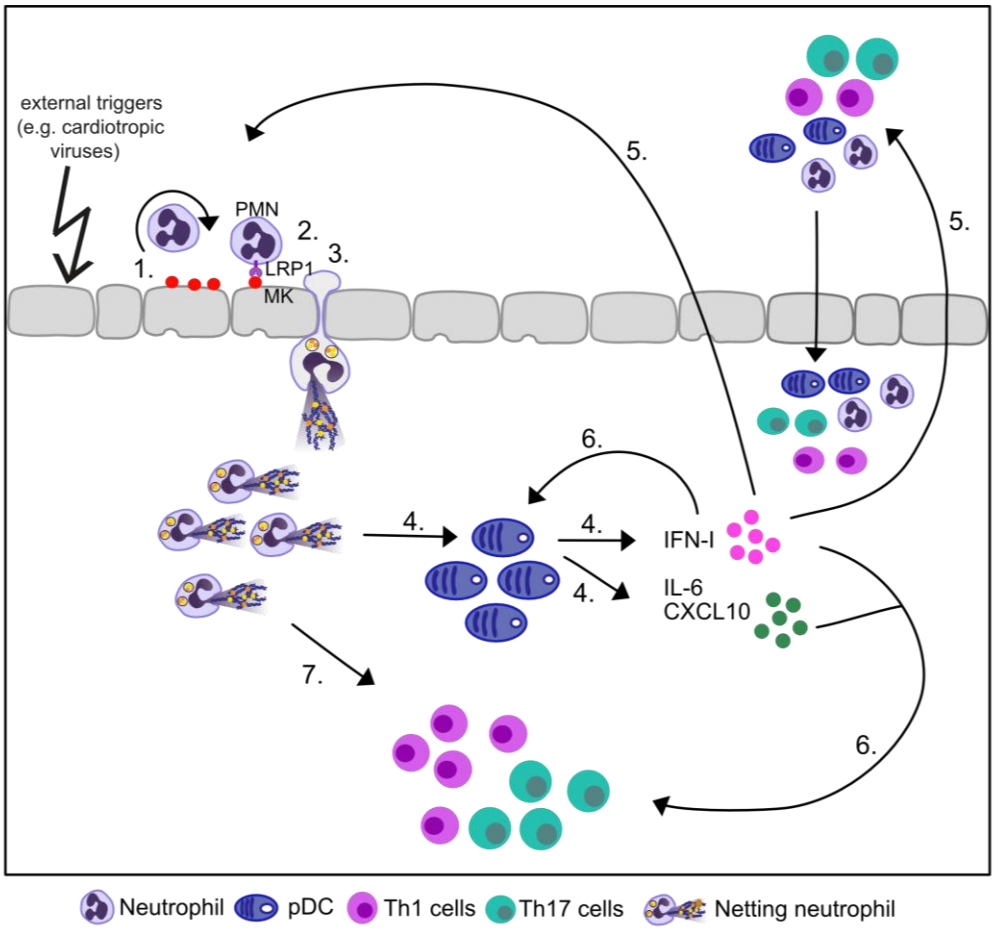

Figure 6-1 Proposed mechanism of IFN-I and immune cells during myocarditis. 1) MK is highly expressed on the endothelium during cardiac inflammation. 2) Neutrophils adhere on the inflamed tissue via the MK-LRP1 axis. 3) MK induces NET formation via LRP1 in the cardiac tissue. 4) NETs activate infiltrated pDCs to produce large amount of IFN-I and pro-inflammatory cytokines (CXCL10, IL-6). 5) These attract further immune cells such as T cells, more neutrophils and pDCs to migrate to the inflamed tissue. 6) In a positive forward loop IFN activates more immune cells to produce more IFNα and stimulating neutrophils to produce further NETs. 7) NETs further activate T cells and their differentiation into Th17 subtype. 8) This leads to cardiac damage and a massive infiltration on day 21.

References

1. Richardson P, McKenna RW, Bristow M, et al. Report of the 1995 World Health Organization/International Society and Federation of Cardiology Task Force on the definition and classification of cardiomyopathies. *Circulation*. 1996;93(5):841-842. doi:10.1161/01.CIR.93.5.841

2. Feldman AM, McNamara D. Myocarditis. *N Engl J Med*. 2000;343(19):1388-1398. doi:10.1056/NEJM200011093431908

3. Caforio ALP, Marcolongo R, Jahns R, Fu M, Felix SB, Iliceto S. Immune-mediated and autoimmune myocarditis: clinical presentation, diagnosis and management. *Heart Fail Rev*. 2013;18(6):715-732. doi:10.1007/s10741-012-9364-5

4. Caforio ALP, Pankuweit S, Arbustini E, et al. Current state of knowledge on aetiology, diagnosis, management, and therapy of myocarditis: A position statement of the European Society of Cardiology Working Group on Myocardial and Pericardial Diseases. *Eur Heart J*. 2013;34(33):2636-2648. doi:10.1093/eurheartj/eht210

5. Schultheiss HP, Khl U, Cooper LT. The management of myocarditis. *Eur Heart J*. 2011;32(21):2616-2625. doi:10.1093/eurheartj/ehr165

6. Kindermann I, Barth C, Mahfoud F, et al. Update on myocarditis. *J Am Coll Cardiol*. 2012;59(9):779-792. doi:10.1016/j.jacc.2011.09.074

7. Yilmaz A, Klingel K, Kandolf R, Sechtem U. A Geographical Mystery: Do Cardiotropic Viruses Respect National Borders? *J Am Coll Cardiol*. 2008;52(1):82. doi:10.1016/j.jacc.2008.01.072

8. Andréoletti L, Ventéo L, Douche-Aourik F, et al. Active Coxsackieviral B Infection Is Associated With Disruption of Dystrophin in Endomyocardial Tissue of Patients Who Died Suddenly of Acute Myocardial Infarction. *J Am Coll Cardiol*. 2007;50(23):2207-2214. doi:10.1016/j.jacc.2007.07.080

9. Pankuweit S. Prevalence of the parvovirus B19 genome in endomyocardial biopsy specimens. *Hum Pathol*. 2003;34(5):497-503. doi:10.1016/S0046-8177(03)00078-9

10. Pankuweit S, Lamparter S, Schoppet M, Maisch B. Parvovirus B19 Genome in Endomyocardial Biopsy Specimen. *Circulation*. 2004;109(14). doi:10.1161/01.CIR.0000124881.00415.59

11. Mahrholdt H, Wagner A, Deluigi CC, et al. Presentation, Patterns of Myocardial

Damage, and Clinical Course of Viral Myocarditis. *Circulation*. 2006;114(15):1581-1590. doi:10.1161/CIRCULATIONAHA.105.606509

12. Bonney KM, Engman DM. Autoimmune pathogenesis of chagas heart disease: Looking back, looking ahead. *Am J Pathol*. 2015;185(6):1537-1547. doi:10.1016/j.ajpath.2014.12.023

13. Fung G, Luo H, Qiu Y, Yang D, McManus B. Myocarditis. *Circ Res*. 2016;118(3):496-514. doi:10.1161/CIRCRESAHA.115.306573

14. Jefferies JL, Towbin JA. Dilated cardiomyopathy. *Lancet*. 2010;375(9716):752-762. doi:10.1016/S0140-6736(09)62023-7

15. Kang M, Chippa V, An J. *Viral Myocarditis*.; 2023. http://www.ncbi.nlm.nih.gov/pubmed/30740183

16. Dai H, Lotan D, Much AA, et al. Global, Regional, and National Burden of Myocarditis and Cardiomyopathy, 1990–2017. *Front Cardiovasc Med*. 2021;8. doi:10.3389/fcvm.2021.610989

17. Vos T, Barber RM, Bell B, et al. Global, regional, and national incidence, prevalence, and years lived with disability for 301 acute and chronic diseases and injuries in 188 countries, 1990–2013: a systematic analysis for the Global Burden of Disease Study 2013. *Lancet*. 2015;386(9995):743-800. doi:10.1016/S0140-6736(15)60692-4

18. Golpour A, Patriki D, Hanson PJ, McManus B, Heidecker B. Epidemiological Impact of Myocarditis. *J Clin Med*. 2021;10(4):603. doi:10.3390/jcm10040603

19. Wang YWY, Liu RB, Huang CY, et al. Global, regional, and national burdens of myocarditis, 1990–2019: systematic analysis from GBD 2019. *BMC Public Health*. 2023;23(1):714. doi:10.1186/s12889-023-15539-5

20. Fairweather D, Cooper LT, Blauwet LA. Sex and Gender Differences in Myocarditis and Dilated Cardiomyopathy. *Curr Probl Cardiol*. 2013;38(1):7-46. doi:10.1016/j.cpcardiol.2012.07.003

21. Kytö V, Sipilä J, Rautava P. The effects of gender and age on occurrence of clinically suspected myocarditis in adulthood. *Heart*. 2013;99(22):1681-1684. doi:10.1136/heartjnl-2013-304449

22. Maron BJ, Udelson JE, Bonow RO, et al. Eligibility and Disqualification Recommendations for Competitive Athletes With Cardiovascular Abnormalities: Task Force 3: Hypertrophic Cardiomyopathy, Arrhythmogenic Right Ventricular Cardiomyopathy and Other Cardiomyopathies, and

Myocarditis. *Circulation*. 2015;132(22). doi:10.1161/CIR.0000000000000239

23. Schultheiss HP, Baumeier C, Aleshcheva G, Bock CT, Escher F. Viral myocarditis—from pathophysiology to treatment. *J Clin Med*. 2021;10(22):1-25. doi:10.3390/jcm10225240

24. Ammirati E, Moslehi JJ. Diagnosis and Treatment of Acute Myocarditis. *JAMA*. 2023;329(13):1098. doi:10.1001/jama.2023.3371

25. Soongswang J, Durongpisitkul K, Nana A, et al. Cardiac Troponin T: A Marker in the Diagnosis of Acute Myocarditis in Children. *Pediatr Cardiol*. 2005;26(1):45-49. doi:10.1007/s00246-004-0677-6

26. Thomas Aretz H. Diagnosis of Myocarditis by Endomyocardial Biopsy. *Med Clin North Am*. 1986;70(6):1215-1226. doi:10.1016/S0025-7125(16)30893-8

27. Baughman KL. Diagnosis of Myocarditis. *Circulation*. 2006;113(4):593-595. doi:10.1161/CIRCULATIONAHA.105.589663

28. Maisch B, Alter P. Treatment options in myocarditis and inflammatory cardiomyopathy: Focus on i. v. immunoglobulins. *Herz*. 2018;43(5):423-430. doi:10.1007/s00059-018-4719-x

29. McMurray JJ V., Adamopoulos S, Anker SD, et al. ESC Guidelines for the diagnosis and treatment of acute and chronic heart failure 2012: The Task Force for the Diagnosis and Treatment of Acute and Chronic Heart Failure 2012 of the European Society of Cardiology. Developed in collaboration with the Heart. *Eur Heart J*. 2012;33(14):1787-1847. doi:10.1093/eurheartj/ehs104

30. Kühl U, Pauschinger M, Schwimmbeck PL, et al. Interferon-β Treatment Eliminates Cardiotropic Viruses and Improves Left Ventricular Function in Patients With Myocardial Persistence of Viral Genomes and Left Ventricular Dysfunction. *Circulation*. 2003;107(22):2793-2798. doi:10.1161/01.CIR.0000072766.67150.51

31. Kühl U, Lassner D, von Schlippenbach J, Poller W, Schultheiss HP. Interferon-Beta Improves Survival in Enterovirus-Associated Cardiomyopathy. *J Am Coll Cardiol*. 2012;60(14):1295-1296. doi:10.1016/j.jacc.2012.06.026

32. Mirić M, Vasiljević J, Bojić M, Popović Z, Keserović N, Pešić M. Long-term follow up of patients with dilated heart muscle disease treated with human leucocytic interferon alpha or thymic hormones: Initial results. *Heart*. 1996;75(6):596-601. doi:10.1136/hrt.75.6.596

33. Schultheiss HP, Piper C, Sowade O, et al. Betaferon in chronic viral

cardiomyopathy (BICC) trial: Effects of interferon-β treatment in patients with chronic viral cardiomyopathy. *Clin Res Cardiol*. 2016;105(9):763-773. doi:10.1007/s00392-016-0986-9

34. Sagar S, Liu PP, Cooper LT. Myocarditis. *Lancet*. 2012;379(9817):738-747. doi:10.1016/S0140-6736(11)60648-X

35. Blauwet LA, Cooper LT. Myocarditis. *Prog Cardiovasc Dis*. 2010;52(4):274-288. doi:10.1016/j.pcad.2009.11.006

36. D'Ambrosio A. The fate of acute myocarditis between spontaneous improvement and evolution to dilated cardiomyopathy: a review. *Heart*. 2001;85(5):499-504. doi:10.1136/heart.85.5.499

37. Maron BJ, Towbin JA, Thiene G, et al. Contemporary Definitions and Classification of the Cardiomyopathies. *Circulation*. 2006;113(14):1807-1816. doi:10.1161/CIRCULATIONAHA.106.174287

38. Pollack A, Kontorovich AR, Fuster V, Dec GW. Viral myocarditis-diagnosis, treatment options, and current controversies. *Nat Rev Cardiol*. 2015;12(11):670-680. doi:10.1038/nrcardio.2015.108

39. Bracamonte-Baran W, Čiháková D. Cardiac Autoimmunity: Myocarditis. In: ; 2017:187-221. doi:10.1007/978-3-319-57613-8_10

40. Cooper LT, Keren A, Sliwa K, Matsumori A, Mensah GA. The global burden of myocarditis: Part 1: A systematic literature review for the global burden of diseases, injuries, and risk factors 2010 study. *Glob Heart*. 2014;9(1):121-129. doi:10.1016/j.gheart.2014.01.007

41. Rose NR. Myocarditis: Infection Versus Autoimmunity. *J Clin Immunol*. 2009;29(6):730-737. doi:10.1007/s10875-009-9339-z

42. Caforio ALP, Mahon NJ, Tona F, McKenna WJ. Circulating cardiac autoantibodies in dilated cardiomyopathy and myocarditis: pathogenetic and clinical significance. *Eur J Heart Fail*. 2002;4(4):411-417. doi:10.1016/S1388-9842(02)00010-7

43. Neumann DA, Lynne Burek C, Baughman KL, Rose NR, Herskowitz A. Circulating heart-reactive antibodies in patients with myocarditis or cardiomyopathy. *J Am Coll Cardiol*. 1990;16(4):839-846. doi:10.1016/S0735-1097(10)80331-6

44. Swirski FK, Nahrendorf M. Cardioimmunology: the immune system in cardiac homeostasis and disease. *Nat Rev Immunol*. 2018;18(12):733-744.

doi:10.1038/s41577-018-0065-8

45. Kawai C. From Myocarditis to Cardiomyopathy : Mechanisms of Inflammation and Cell Death. *Heart*. 1999;99:1091-1100.

46. Elamm C, Fairweather DL, Cooper LT. Pathogenesis and diagnosis of myocarditis. *Heart*. 2012;98(11):835-840. doi:10.1136/heartjnl-2012-301686

47. Martino TA, Liu P, Petric M, Sole MJ. Enteroviral Myocarditis and Dilated Cardiomyopathy: a Review of Clinical and Experimental Studies. In: *Human Enterovirus Infections*. ASM Press; 1995:291-351. doi:10.1128/9781555818326.ch14

48. Liu PP, Opavsky MA. Viral Myocarditis. *Circ Res*. 2000;86(3):253-254. doi:10.1161/01.RES.86.3.253

49. Tschöpe C, Ammirati E, Bozkurt B, et al. Myocarditis and inflammatory cardiomyopathy: current evidence and future directions. *Nat Rev Cardiol*. 2021;18(3):169-193. doi:10.1038/s41569-020-00435-x

50. Zhang P, Cox CJ, Alvarez KM, Cunningham MW. Cutting Edge: Cardiac Myosin Activates Innate Immune Responses through TLRs. *J Immunol*. 2009;183(1):27-31. doi:10.4049/jimmunol.0800861

51. Weckbach LT, Grabmaier U, Uhl A, et al. Midkine drives cardiac inflammation by promoting neutrophil trafficking and NETosis in myocarditis. *J Exp Med*. 2019;216(2):350-368. doi:10.1084/jem.20181102

52. Matsumori A, Yamada T, Suzuki H, Matoba Y, Sasayama S. Increased circulating cytokines in patients with myocarditis and cardiomyopathy. *Br Heart J*. 1994;72(6):561-566. doi:10.1136/hrt.72.6.561

53. Heymans S, Eriksson U, Lehtonen J, Cooper LT. The Quest for New Approaches in Myocarditis and Inflammatory Cardiomyopathy. *J Am Coll Cardiol*. 2016;68(21):2348-2364. doi:10.1016/j.jacc.2016.09.937

54. Pillay J, den Braber I, Vrisekoop N, et al. In vivo labeling with 2H2O reveals a human neutrophil lifespan of 5.4 days. *Blood*. 2010;116(4):625-627. doi:10.1182/blood-2010-01-259028

55. Minns D, Smith KJ, Findlay EG. Orchestration of Adaptive T Cell Responses by Neutrophil Granule Contents. *Mediators Inflamm*. 2019;2019. doi:10.1155/2019/8968943

56. Nourshargh S, Alon R. Leukocyte Migration into Inflamed Tissues. *Immunity*. 2014;41(5):694-707. doi:10.1016/j.immuni.2014.10.008

57. Bevilacqua MP, Pober JS, Wheeler ME, Cotran RS, Gimbrone MA. Interleukin 1 acts on cultured human vascular endothelium to increase the adhesion of polymorphonuclear leukocytes, monocytes, and related leukocyte cell lines. *J Clin Invest*. 1985;76(5):2003-2011. doi:10.1172/JCI112200

58. Mackay F, Loetscher H, Stueber D, Gehr G, Lesslauer W. Tumor necrosis factor alpha (TNF-alpha)-induced cell adhesion to human endothelial cells is under dominant control of one TNF receptor type, TNF-R55. *J Exp Med*. 1993;177(5):1277-1286. doi:10.1084/jem.177.5.1277

59. Mócsai A, Walzog B, Lowell CA. Intracellular signalling during neutrophil recruitment. *Cardiovasc Res*. 2015;107(3):373-385. doi:10.1093/cvr/cvv159

60. Schymeinsky J, Sperandio M, Walzog B. The mammalian actin-binding protein 1 (mAbp1): a novel molecular player in leukocyte biology. *Trends Cell Biol*. 2011;21(4):247-255. doi:10.1016/j.tcb.2010.12.001

61. McEver RP. Selectins: Initiators of leucocyte adhesion and signalling at the vascular wall. *Cardiovasc Res*. 2015;107(3):331-339. doi:10.1093/cvr/cvv154

62. Lefort CT, Ley K. Neutrophil arrest by LFA-1 activation. *Front Immunol*. 2012;3(JUN):1-10. doi:10.3389/fimmu.2012.00157

63. Rosales C. Neutrophil: A cell with many roles in inflammation or several cell types? *Front Physiol*. 2018;9(FEB):1-17. doi:10.3389/fphys.2018.00113

64. Brinkmann V. Neutrophil Extracellular Traps Kill Bacteria. *Science (80-)*. 2004;303(5663):1532-1535. doi:10.1126/science.1092385

65. Fuchs TA, Abed U, Goosmann C, et al. Novel cell death program leads to neutrophil extracellular traps. *J Cell Biol*. 2007;176(2):231-241. doi:10.1083/jcb.200606027

66. Brinkmann V, Zychlinsky A. Neutrophil extracellular traps: Is immunity the second function of chromatin? *J Cell Biol*. 2012;198(5):773-783. doi:10.1083/jcb.201203170

67. Li P, Li M, Lindberg MR, Kennett MJ, Xiong N, Wang Y. PAD4 is essential for antibacterial innate immunity mediated by neutrophil extracellular traps. *J Exp Med*. 2010;207(9):1853-1862. doi:10.1084/jem.20100239

68. Vossenaar ER, Zendman AJW, van Venrooij WJ, Pruijn GJM. PAD, a growing family of citrullinating enzymes: genes, features and involvement in disease. *BioEssays*. 2003;25(11):1106-1118. doi:10.1002/bies.10357

69. Wang Y, Li M, Stadler S, et al. Histone hypercitrullination mediates chromatin

decondensation and neutrophil extracellular trap formation. *J Cell Biol*. 2009;184(2):205-213. doi:10.1083/jcb.200806072

70. Papayannopoulos V, Metzler KD, Hakkim A, Zychlinsky A. Neutrophil elastase and myeloperoxidase regulate the formation of neutrophil extracellular traps. *J Cell Biol*. 2010;191(3):677-691. doi:10.1083/jcb.201006052

71. Sollberger G, Choidas A, Burn GL, et al. Gasdermin D plays a vital role in the generation of neutrophil extracellular traps. *Sci Immunol*. 2018;3(26). doi:10.1126/sciimmunol.aar6689

72. Urban CF, Reichard U, Brinkmann V, Zychlinsky A. Neutrophil extracellular traps capture and kill Candida albicans and hyphal forms. *Cell Microbiol*. 2006;8(4):668-676. doi:10.1111/j.1462-5822.2005.00659.x

73. Branzk N, Lubojemska A, Hardison SE, et al. Neutrophils sense microbe size and selectively release neutrophil extracellular traps in response to large pathogens. *Nat Immunol*. 2014;15(11):1017-1025. doi:10.1038/ni.2987

74. Jorch SK, Kubes P. An emerging role for neutrophil extracellular traps in noninfectious disease. *Nat Med*. 2017;23(3):279-287. doi:10.1038/nm.4294

75. Lee KH, Kronbichler A, Park DDY, et al. Neutrophil extracellular traps (NETs) in autoimmune diseases: A comprehensive review. *Autoimmun Rev*. 2017;16(11):1160-1173. doi:10.1016/j.autrev.2017.09.012

76. Döring Y, Soehnlein O, Weber C. Neutrophil extracellular traps in atherosclerosis and atherothrombosis. *Circ Res*. 2017;120(4):736-743. doi:10.1161/CIRCRESAHA.116.309692

77. Hakkim A, Fürnrohr BG, Amann K, et al. Impairment of neutrophil extracellular trap degradation is associated with lupus nephritis. *Proc Natl Acad Sci U S A*. 2010;107(21):9813-9818. doi:10.1073/pnas.0909927107

78. Carmona-Rivera C, Carlucci PM, Goel RR, et al. Neutrophil extracellular traps mediate articular cartilage damage and enhance cartilage component immunogenicity in rheumatoid arthritis. *JCI Insight*. 2020;5(13). doi:10.1172/jci.insight.139388

79. Kang L, Yu H, Yang X, et al. Neutrophil extracellular traps released by neutrophils impair revascularization and vascular remodeling after stroke. *Nat Commun*. 2020;11(1). doi:10.1038/s41467-020-16191-y

80. Cervantes-Luevano KE, Caronni N, Castiello MC, et al. Neutrophils drive type I interferon production and autoantibodies in patients with Wiskott-Aldrich

syndrome. *J Allergy Clin Immunol*. 2018;142(5):1605-1617.e4. doi:10.1016/j.jaci.2017.11.063

81. Tillack K, Breiden P, Martin R, Sospedra M. T Lymphocyte Priming by Neutrophil Extracellular Traps Links Innate and Adaptive Immune Responses. *J Immunol*. 2012;188(7):3150-3159. doi:10.4049/jimmunol.1103414

82. Lande R, Gregorio J, Facchinetti V, et al. Plasmacytoid dendritic cells sense self-DNA coupled with antimicrobial peptide. *Nature*. 2007;449(7162):564-569. doi:10.1038/nature06116

83. Blanco LP, Wang X, Carlucci PM, et al. RNA externalized by neutrophil extracellular traps promotes inflammatory pathways in endothelial cells. *Arthritis Rheumatol*. Published online May 13, 2021:art.41796. doi:10.1002/art.41796

84. Lande R, Ganguly D, Facchinetti V, et al. Neutrophils Activate Plasmacytoid Dendritic Cells by Releasing Self-DNA–Peptide Complexes in Systemic Lupus Erythematosus. 2012;3(73):1-20. doi:10.1126/scitranslmed.3001180.

85. Wang H, Li T, Chen S, Gu Y, Ye S. Neutrophil Extracellular Trap Mitochondrial DNA and Its Autoantibody in Systemic Lupus Erythematosus and a Proof-of-Concept Trial of Metformin. *Arthritis Rheumatol (Hoboken, NJ)*. 2015;67(12):3190-3200. doi:10.1002/art.39296

86. A ISAACS JL. Virus interference. I. The interferon. *Proc R Soc London Ser B - Biol Sci*. 1957;147(927):258-267. doi:10.1098/rspb.1957.0048

87. Naik SH, Sathe P, Park HY, et al. Development of plasmacytoid and conventional dendritic cell subtypes from single precursor cells derived in vitro and in vivo. *Nat Immunol*. 2007;8(11):1217-1226. doi:10.1038/ni1522

88. Liu K, Victora GD, Schwickert TA, et al. In Vivo Analysis of Dendritic Cell Development and Homeostasis. *Science (80-)*. Published online March 12, 2009. doi:10.1126/science.1170540

89. Guiducci C, Coffman RL, Barrat FJ. Signalling pathways leading to IFN-α production in human plasmacytoid dendritic cell and the possible use of agonists or antagonists of TLR7 and TLR9 in clinical indications. *J Intern Med*. 2009;265(1):43-57. doi:10.1111/j.1365-2796.2008.02050.x

90. Swiecki M, Colonna M. The multifaceted biology of plasmacytoid dendritic cells. *Nat Rev Immunol*. 2015;15(8):471-485. doi:10.1038/nri3865

91. Feldman SB, Milone MC, Kloser P, Fitzgerald-Bocarsly P. Functional

deficiencies in two distinct interferon α -producing cell populations in peripheral blood mononuclear cells from human immunodeficiency virus seropositive patients. *J Leukoc Biol*. 1995;57(2):214-220. doi:10.1002/jlb.57.2.214

92. Cella M, Jarrossay D, Facchetti F, et al. Plasmacytoid monocytes migrate to inflamed lymph nodes and produce large amounts of type I interferon. *Nat Med*. 1999;5(8):919-923. doi:10.1038/11360

93. Matsutani T, Tanaka T, Tohya K, et al. Plasmacytoid dendritic cells employ multiple cell adhesion molecules sequentially to interact with high endothelial venule cells - molecular basis of their trafficking to lymph nodes. *Int Immunol*. 2007;19(9):1031-1037. doi:10.1093/intimm/dxm088

94. Sozzani S, Vermi W, Del Prete A, Facchetti F. Trafficking properties of plasmacytoid dendritic cells in health and disease. *Trends Immunol*. 2010;31(7):270-277. doi:10.1016/j.it.2010.05.004

95. Krug A, Uppaluri R, Facchetti F, et al. Cutting Edge: IFN-Producing Cells Respond to CXCR3 Ligands in the Presence of CXCL12 and Secrete Inflammatory Chemokines upon Activation. Published online 2021. doi:10.4049/jimmunol.169.11.6079

96. Wendland M, Czeloth N, Mach N, et al. CCR9 is a homing receptor for plasmacytoid dendritic cells to the small intestine. *Proc Natl Acad Sci*. 2007;104(15):6347-6352. doi:10.1073/pnas.0609180104

97. Farkas L, Beiske K, Lund-Johansen F, Brandtzaeg P, Jahnsen FL. Plasmacytoid Dendritic Cells (Natural Interferon- α/β-Producing Cells) Accumulate in Cutaneous Lupus Erythematosus Lesions. *Am J Pathol*. 2001;159(1):237-243. doi:10.1016/S0002-9440(10)61689-6

98. de Vries HJC, Teunissen MBM, Zorgdrager F, Picavet D, Cornelissen M. Lichen planus remission is associated with a decrease of human herpes virus type 7 protein expression in plasmacytoid dendritic cells. *Arch Dermatol Res*. 2007;299(4):213-219. doi:10.1007/s00403-007-0750-0

99. Cavanagh LL, Boyce A, Smith L, et al. Rheumatoid arthritis synovium contains plasmacytoid dendritic cells. *Arthritis Res Ther*. 2005;7(2):R230-40. doi:10.1186/ar1467

100. Schulte DJ, Yilmaz A, Shimada K, et al. Involvement of Innate and Adaptive Immunity in a Murine Model of Coronary Arteritis Mimicking Kawasaki Disease. *J Immunol*. 2009;183(8):5311-5318. doi:10.4049/jimmunol.0901395

101. Vanbervliet B, Bendriss-Vermare N, Massacrier C, et al. The Inducible CXCR3

Ligands Control Plasmacytoid Dendritic Cell Responsiveness to the Constitutive Chemokine Stromal Cell–derived Factor 1 (SDF-1)/CXCL12. *J Exp Med*. 2003;198(5):823-830. doi:10.1084/jem.20020437

102. Decalf J, Fernandes S, Longman R, et al. Plasmacytoid dendritic cells initiate a complex chemokine and cytokine network and are a viable drug target in chronic HCV patients. *J Exp Med*. 2007;204(10):2423-2437. doi:10.1084/jem.20070814

103. Jego G, Palucka AK, Blanck J philippe, Chalouni C, Pascual V, Banchereau J. Plasma Cell Differentiation through Type I Interferon and Interleukin 6. 2003;19:225-234.

104. Megjugorac NJ, Young HA, Amrute SB, Olshalsky SL, Fitzgerald-Bocarsly P. Virally stimulated plasmacytoid dendritic cells produce chemokines and induce migration of T and NK cells. *J Leukoc Biol*. 2004;75(3):504-514. doi:10.1189/jlb.0603291

105. Agnello D, Lankford CSR, Bream J, et al. Cytokines and transcription factors that regulate T helper cell differentiation: new players and new insights. *J Clin Immunol*. 2003;23(3):147-161. doi:10.1023/a:1023381027062

106. Henry T, Kirimanjeswara GS, Ruby T, et al. Type I IFN Signaling Constrains IL-17A/F Secretion by γδ T Cells during Bacterial Infections. *J Immunol*. 2010;184(7):3755-3767. doi:10.4049/jimmunol.0902065

107. Villadangos JA, Young L. Antigen-Presentation Properties of Plasmacytoid Dendritic Cells. *Immunity*. 2008;29(3):352-361. doi:10.1016/j.immuni.2008.09.002

108. Colonna M, Trinchieri G, Liu YJ. Plasmacytoid dendritic cells in immunity. *Nat Immunol*. 2004;5(12):1219-1226. doi:10.1038/ni1141

109. Rönnblom L, Alm G V. Systemic lupus erythematosus and the type I interferon system. *Arthritis Res Ther*. 2003;5(2):68-75. doi:10.1186/ar625

110. Hardy MP, Owczarek CM, Jermiin LS, Ejdebäck M, Hertzog PJ. Characterization of the type I interferon locus and identification of novel genes☆. *Genomics*. 2004;84(2):331-345. doi:10.1016/j.ygeno.2004.03.003

111. Stetson DB, Medzhitov R. Type I Interferons in Host Defense. *Immunity*. 2006;25(3):373-381. doi:10.1016/j.immuni.2006.08.007

112. Denny MF, Yalavarthi S, Zhao W, et al. A Distinct Subset of Proinflammatory Neutrophils Isolated from Patients with Systemic Lupus Erythematosus

Induces Vascular Damage and Synthesizes Type I IFNs. *J Immunol*. 2010;185(6):3779-3779. doi:10.4049/jimmunol.1090082

113. Shirafuji N, Matsuda S, Ogura H, et al. Granulocyte colony-stimulating factor stimulates human mature neutrophilic granulocytes to produce interferon-α. *Blood*. 1990;75(1):17-19. doi:10.1182/blood.v75.1.17.17

114. Stanifer ML, Pervolaraki K, Boulant S. Differential regulation of type I and type III interferon signaling. *Int J Mol Sci*. 2019;20(6):1-22. doi:10.3390/ijms20061445

115. Ivashkiv LB, Donlin LT. Regulation of type I interferon responses. *Nat Rev Immunol*. 2014;14(1):36-49. doi:10.1038/nri3581

116. Izaguirre A, Barnes BJ, Amrute S, et al. Comparative analysis of IRF and IFN-alpha expression in human plasmacytoid and monocyte-derived dendritic cells. *J Leukoc Biol*. 2003;74(6):1125-1138. doi:10.1189/jlb.0603255

117. Decker T, Müller M, Stockinger S. The Yin and Yang of type I interferon activity in bacterial infection. *Nat Rev Immunol*. 2005;5(9):675-687. doi:10.1038/nri1684

118. Mogensen TH. IRF and STAT Transcription Factors - From Basic Biology to Roles in Infection, Protective Immunity, and Primary Immunodeficiencies. *Front Immunol*. 2019;9. doi:10.3389/fimmu.2018.03047

119. Trinchieri G. Type I interferon: Friend or foe? *J Exp Med*. 2010;207(10):2053-2063. doi:10.1084/jem.20101664

120. Monti M, Consoli F, Bugatti M, Vermi W. Human Plasmacytoid Dendritic Cells and Cutaneous Melanoma. Published online 2020:1-36.

121. Chistiakov DA, Orekhov AN, Sobenin IA, Bobryshev Y V. Plasmacytoid dendritic cells: Development, functions, and role in atherosclerotic inflammation. *Front Physiol*. 2014;5 JUL(July):1-17. doi:10.3389/fphys.2014.00279

122. Saas P, Varin A, Perruche S, Ceroi A. Recent insights into the implications of metabolism in plasmacytoid dendritic cell innate functions : Potential ways to control these functions Recent insights into the implications of metabolism in plasmacytoid dendritic cell innate functions : Potential. 2017;(April). doi:10.12688/f1000research.11332.1

123. Wang W, Xu L, Su J, Peppelenbosch MP, Pan Q. Transcriptional Regulation of Antiviral Interferon-Stimulated Genes. *Trends Microbiol*. 2017;25(7):573-

584. doi:10.1016/j.tim.2017.01.001

124. Patricia FB, Jihong D, Sukhwinder S. Plasmacytoid dendritic cells and type I IFN: 50 years of convergent history. *Cytokine Growth Factor Rev*. 2008;19(1):3-19.

125. Blasius AL, Colonna M. Sampling and signaling in plasmacytoid dendritic cells: the potential roles of Siglec-H. *Trends Immunol*. 2006;27(6):255-260. doi:10.1016/j.it.2006.04.005

126. Hornung V, Rothenfusser S, Britsch S, et al. Quantitative Expression of Toll-Like Receptor 1 − 10 mRNA in Cellular Subsets of Human Peripheral Blood Mononuclear Cells and Sensitivity to CpG Oligodeoxynucleotides. Published online 2021. doi:10.4049/jimmunol.168.9.4531

127. Fuchsberger M, Hochrein H, O'Keeffe M. Activation of plasmacytoid dendritic cells. *Immunol Cell Biol*. 2005;83(5):571-577. doi:10.1111/j.1440-1711.2005.01392.x

128. Lavine KJ, Mann DL. Recognition of self-DNA drives cardiac inflammation: why broken hearts fail. *Nat Med*. 2017;23(12):1400-1401. doi:10.1038/nm.4455

129. Musumeci A, Lutz K, Winheim E, Krug AB. What makes a PDC: Recent advances in understanding plasmacytoid DC development and heterogeneity. *Front Immunol*. 2019;10(MAY):1-7. doi:10.3389/fimmu.2019.01222

130. Gilliet M, Lande R. Antimicrobial peptides and self-DNA in autoimmune skin inflammation. *Curr Opin Immunol*. 2008;20(4):401-407. doi:10.1016/j.coi.2008.06.008

131. Honda K, Yanai H, Negishi H, et al. IRF-7 is the master regulator of type-I interferon-dependent immune responses. *Nature*. 2005;434(7034):772-777. doi:10.1038/nature03464

132. Bao M, Liu Y jun. Regulation of TLR7 / 9 signaling in plasmacytoid dendritic cells. 2013;4(1):40-52. doi:10.1007/s13238-012-2104-8

133. Kawai T, Sato S, Ishii KJ, et al. Interferon-α induction through Toll-like receptors involves a direct interaction of IRF7 with MyD88 and TRAF6. *Nat Immunol*. 2004;5(10):1061-1068. doi:10.1038/ni1118

134. Honda K, Yanai H, Mizutani T, et al. Role of a transductional-transcriptional processor complex involving MyD88 and IRF-7 in Toll-like receptor signaling. *Proc Natl Acad Sci*. 2004;101(43):15416-15421. doi:10.1073/pnas.0406933101

135. Honda K, Ohba Y, Yanai H, et al. Spatiotemporal regulation of MyD88–IRF-7 signalling for robust type-I interferon induction. *Nature*. 2005;434(7036):1035-1040. doi:10.1038/nature03547

136. Kawagoe T, Sato S, Matsushita K, et al. Sequential control of Toll-like receptor–dependent responses by IRAK1 and IRAK2. *Nat Immunol*. 2008;9(6):684-691. doi:10.1038/ni.1606

137. Liu YJ. IPC: Professional type 1 interferon-producing cells and plasmacytoid dendritic cell precursors. *Annu Rev Immunol*. 2005;23(3):275-306. doi:10.1146/annurev.immunol.23.021704.115633

138. Pelka K, Latz E. IRF5, IRF8, and IRF7 in human pDCs - the good, the bad, and the insignificant? *Eur J Immunol*. 2013;43(7):1693-1697. doi:10.1002/eji.201343739

139. Sichien D, Scott CL, Martens L, et al. IRF8 Transcription Factor Controls Survival and Function of Terminally Differentiated Conventional and Plasmacytoid Dendritic Cells, Respectively. *Immunity*. 2016;45(3):626-640. doi:10.1016/j.immuni.2016.08.013

140. Tamura T, Tailor P, Yamaoka K, et al. IFN Regulatory Factor-4 and -8 Govern Dendritic Cell Subset Development and Their Functional Diversity. *J Immunol*. 2005;174(5):2573-2581. doi:10.4049/jimmunol.174.5.2573

141. Takaoka A, Yanai H, Kondo S, et al. Integral role of IRF-5 in the gene induction programme activated by Toll-like receptors. *Nature*. 2005;434(7030):243-249. doi:10.1038/nature03308

142. Paun A, Reinert JT, Jiang Z, et al. Functional characterization of murine interferon regulatory factor 5 (IRF-5) and its role in the innate antiviral response. *J Biol Chem*. 2008;283(21):14295-14308. doi:10.1074/jbc.M800501200

143. Gilliet M, Cao W, Liu YJ. Plasmacytoid dendritic cells: sensing nucleic acids in viral infection and autoimmune diseases. *Nat Rev Immunol*. 2008;8(8):594-606. doi:10.1038/nri2358

144. Häcker H, Karin M. Regulation and function of IKK and IKK-related kinases. *Sci STKE*. 2006;2006(357). doi:10.1126/stke.3572006re13

145. Hirsch I. Cross Talk between inhibitory immunoreceptor Tyrosine-Based Activation Motif-Signaling and Toll-Like Receptor Pathways in Macrophages and Dendritic Cells. 2017;8(April):1-12. doi:10.3389/fimmu.2017.00394

146. Abbas A, Vu Manh TP, Valente M, et al. The activation trajectory of plasmacytoid dendritic cells in vivo during a viral infection. *Nat Immunol*. 2020;21(9):983-997. doi:10.1038/s41590-020-0731-4

147. Garcia-Romo GS, Caielli S, Vega B, et al. Netting Neutrophils Are Major Inducers of Type I IFN Production in Pediatric Systemic Lupus Erythematosus. *Sci Transl Med*. 2011;3(73):73ra20-73ra20. doi:10.1126/scitranslmed.3001201

148. Means TK, Latz E, Hayashi F, Murali MR, Golenbock DT, Luster AD. Human lupus autoantibody–DNA complexes activate DCs through cooperation of CD32 and TLR9. *J Clin Invest*. 2005;115(2):407-417. doi:10.1172/JCI23025

149. Nestle FO, Conrad C, Tun-Kyi A, et al. Plasmacytoid predendritic cells initiate psoriasis through interferon-α production. *J Exp Med*. 2005;202(1):135-143. doi:10.1084/jem.20050500

150. Heim A, Grumbach I, Pring-Åkerblom P, et al. Inhibition of coxsackievirus B3 carrier state infection of cultured human myocardial fibroblasts by ribavirin and human natural interferon-α. *Antiviral Res*. 1997;34(3):101-111. doi:10.1016/S0166-3542(97)01028-0

151. King KR, Aguirre AD, Ye YX, et al. IRF3 and type I interferons fuel a fatal response to myocardial infarction. *Nat Med*. 2017;23(12):1481-1487. doi:10.1038/nm.4428

152. Gall A, Treuting P, Elkon KB, et al. Autoimmunity Initiates in Nonhematopoietic Cells and Progresses via Lymphocytes in an Interferon-Dependent Autoimmune Disease. *Immunity*. 2012;36(1):120-131. doi:10.1016/j.immuni.2011.11.018

153. Kumar B V., Connors TJ, Farber DL. Human T Cell Development, Localization, and Function throughout Life. *Immunity*. 2018;48(2):202-213. doi:10.1016/j.immuni.2018.01.007

154. Allman D, Sambandam A, Kim S, et al. Thymopoiesis independent of common lymphoid progenitors. *Nat Immunol*. 2003;4(2):168-174. doi:10.1038/ni878

155. Murphy K, Weaver C. *Janeway Immunologie*. Springer Berlin Heidelberg; 2018. doi:10.1007/978-3-662-56004-4

156. Klein L, Hinterberger M, Wirnsberger G, Kyewski B. Antigen presentation in the thymus for positive selection and central tolerance induction. *Nat Rev Immunol*. 2009;9(12):833-844. doi:10.1038/nri2669

157. Boyd RL, Hugo P. Towards an integrated view of thymopoiesis. *Immunol Today*. 1991;12(2):71-79. doi:10.1016/0167-5699(91)90161-L

158. Zúñiga-Pflücker JC. T-cell development made simple. *Nat Rev Immunol*. 2004;4(1):67-72. doi:10.1038/nri1257

159. Germain RN. T-cell development and the CD4–CD8 lineage decision. *Nat Rev Immunol*. 2002;2(5):309-322. doi:10.1038/nri798

160. Hall BM. T Cells: Soldiers and Spies--The Surveillance and Control of Effector T Cells by Regulatory T Cells. *Clin J Am Soc Nephrol*. 2015;10(11):2050-2064. doi:10.2215/CJN.06620714

161. Perlman RL. Mouse models of human disease: An evolutionary perspective. *Evol Med public Heal*. 2016;2016(1):170-176. doi:10.1093/emph/eow014

162. Leuschner F, Katus HA, Kaya Z. Autoimmune myocarditis: Past, present and future. *J Autoimmun*. 2009;33(3-4):282-289. doi:10.1016/j.jaut.2009.07.009

163. Li HS, Ligons DL, Rose NR. Genetic complexity of autoimmune myocarditis. *Autoimmun Rev*. 2008;7(3):168-173. doi:10.1016/j.autrev.2007.11.010

164. Błyszczuk P. Myocarditis in Humans and in Experimental Animal Models. *Front Cardiovasc Med*. 2019;6. doi:10.3389/fcvm.2019.00064

165. Caforio AL, Mahon NJ, Mckenna WJ. Cardiac autoantibodies to myosin and other heart-specific autoantigens in myocarditis and dilated cardiomyopathy. *Autoimmunity*. 2001;34(3):199-204. doi:10.3109/08916930109007385

166. Molkentin J. α-myosin Heavy Chain Gene Regulation: Delineation and Characterization of the Cardiac Muscle-specific Enhancer and Muscle-specific Promoter. *J Mol Cell Cardiol*. 1996;28(6):1211-1225. doi:10.1006/jmcc.1996.0112

167. Neu N, Beisel KW, Traystman MD, Rose NR, Craig SW. Autoantibodies specific for the cardiac myosin isoform are found in mice susceptible to Coxsackievirus B3-induced myocarditis. *J Immunol*. 1987;138(8):2488-2492. http://www.ncbi.nlm.nih.gov/pubmed/3031159

168. Neu N, Rose NR, Beisel KW, Herskowitz A, Gurri-Glass G, Craig SW. Cardiac myosin induces myocarditis in genetically predisposed mice. *J Immunol*. 1987;139(11):3630-3636. http://www.ncbi.nlm.nih.gov/pubmed/3680946

169. Li HS, Ligons DL, Rose NR. Genetic complexity of autoimmune myocarditis. *Autoimmun Rev*. 2008;7(3):168-173. doi:10.1016/j.autrev.2007.11.010

170. Smith SC, Allen PM. Myosin-induced acute myocarditis is a T cell-mediated

disease. *J Immunol*. 1991;147(7):2141-2147. http://www.ncbi.nlm.nih.gov/pubmed/1918949

171. Smith SC, Allen PM. The Role of T Cells in Myosin-Induced Autoimmune Myocarditis. *Clin Immunol Immunopathol*. 1993;68(2):100-106. doi:10.1006/clin.1993.1103

172. Neumann DA, Lane JR, Wulff SM, et al. In vivo deposition of myosin-specific autoantibodies in the hearts of mice with experimental autoimmune myocarditis. *J Immunol*. 1992;148(12):3806-3813. http://www.ncbi.nlm.nih.gov/pubmed/1602130

173. Rose NR. Critical cytokine pathways to cardiac inflammation. *J Interf Cytokine Res*. 2011;31(10):705-710. doi:10.1089/jir.2011.0057

174. Afanasyeva M, Georgakopoulos D, Belardi DF, et al. Quantitative Analysis of Myocardial Inflammation by Flow Cytometry in Murine Autoimmune Myocarditis. *Am J Pathol*. 2004;164(3):807-815. doi:10.1016/S0002-9440(10)63169-0

175. Cihakova D, Rose NR. Chapter 4 Pathogenesis of Myocarditis and Dilated Cardiomyopathy. In: ; 2008:95-114. doi:10.1016/S0065-2776(08)00604-4

176. Barin JG, Čiháková D. Control of inflammatory heart disease by CD4+T cells. *Ann N Y Acad Sci*. 2013;1285(1):80-96. doi:10.1111/nyas.12134

177. Okuno M, Nakagawa M, Shimada M, Saito M, Hishinuma S, Yamauchi-Takihara K. Expressional patterns of cytokines in a murine model of acute myocarditis: Early expression of cardiotrophin-1. *Lab Investig*. 2000;80(3):433-440. doi:10.1038/labinvest.3780048

178. Fairweather D, Kaya Z, Shellam GR, Lawson CM, Rose NR. From Infection to Autoimmunity. *J Autoimmun*. 2001;16(3):175-186. doi:10.1006/jaut.2000.0492

179. Afanasyeva M, Georgakopoulos D, Rose NR. Autoimmune myocarditis: cellular mediators of cardiac dysfunction. *Autoimmun Rev*. 2004;3(7-8):476-486. doi:10.1016/j.autrev.2004.08.009

180. Afanasyeva M, Wang Y, Kaya Z, et al. Experimental autoimmune myocarditis in A/J mice is an interleukin-4-dependent disease with a Th2 phenotype. *Am J Pathol*. 2001;159(1):193-203. doi:10.1016/S0002-9440(10)61685-9

181. Korn T, Bettelli E, Oukka M, Kuchroo VK. IL-17 and Th17 Cells. *Annu Rev Immunol*. 2009;27(1):485-517. doi:10.1146/annurev.immunol.021908.132710

182. Baldeviano GC, Barin JG, Talor M V, et al. Interleukin-17A is dispensable for

myocarditis but essential for the progression to dilated cardiomyopathy. *Circ Res*. 2010;106(10):1646-1655. doi:10.1161/CIRCRESAHA.109.213157

183. Liu Y, Zhu H, Su Z, et al. Il-17 contributes to cardiac fibrosis following experimental autoimmune myocarditis by a PKCβ/Erk1/2/NF-κB-dependent signaling pathway. *Int Immunol*. 2012;24(10):605-612. doi:10.1093/intimm/dxs056

184. Wu L, Ong SF, Talor M V., et al. Cardiac fibroblasts mediate IL-17A-driven inflammatory dilated cardiomyopathy. *J Exp Med*. 2014;211(7):1449-1464. doi:10.1084/jem.20132126

185. Medzhitov R, Janeway C. Innate Immunity. Mackay IR, Rosen FS, eds. *N Engl J Med*. 2000;343(5):338-344. doi:10.1056/NEJM200008033430506

186. Fairweather D, Frisancho-Kiss S, Gatewood S, et al. Mast Cells and Innate Cytokines are Associated with Susceptibility to Autoimmune Heart Disease Following Coxsackievirus B3 Infection. *Autoimmunity*. 2004;37(2):131-145. doi:10.1080/0891693042000196200

187. Barin JG, Baldeviano GC, Talor M V., et al. Fatal Eosinophilic Myocarditis Develops in the Absence of IFN-γ and IL-17A. *J Immunol*. 2013;191(8):4038-4047. doi:10.4049/jimmunol.1301282

188. Reifenberg K, Lehr HA, Torzewski M, et al. Interferon-γ induces chronic active myocarditis and cardiomyopathy in transgenic mice. *Am J Pathol*. 2007;171(2):463-472. doi:10.2353/ajpath.2007.060906

189. Nindl V, Maier R, Ratering D, et al. Cooperation of Th1 and Th17 cells determines transition from autoimmune myocarditis to dilated cardiomyopathy. *Eur J Immunol*. 2012;42(9):2311-2321. doi:10.1002/eji.201142209

190. Afanasyeva M, Georgakopoulos D, Belardi DF, et al. Impaired up-regulation of CD25 on CD4+ T cells in IFN-γ knockout mice is associated with progression of myocarditis to heart failure. *Proc Natl Acad Sci U S A*. 2005;102(1):180-185. doi:10.1073/pnas.0408241102

191. Eriksson U, Kurrer MO, Bingisser R, et al. Lethal Autoimmune Myocarditis in Interferon-γ Receptor–Deficient Mice. *Circulation*. 2001;103(1):18-21. doi:10.1161/01.cir.103.1.18

192. Eriksson U, Kurrer MO, Sebald W, Brombacher F, Kopf M. Dual Role of the IL-12/IFN-γ Axis in the Development of Autoimmune Myocarditis: Induction by IL-12 and Protection by IFN-γ. *J Immunol*. 2001;167(9):5464-5469. doi:10.4049/jimmunol.167.9.5464

193. Kania G, Siegert S, Behnke S, et al. Innate signaling promotes formation of regulatory nitric oxide-producing dendritic cells limiting t-cell expansion in experimental autoimmune myocarditis. *Circulation*. 2013;127(23):2285-2294. doi:10.1161/CIRCULATIONAHA.112.000434

194. Eriksson U, Kurrer MO, Schmitz N, et al. Interleukin-6-deficient mice resist development of autoimmune myocarditis associated with impaired upregulation of complement C3. *Circulation*. 2003;107(2):320-325. doi:10.1161/01.CIR.0000043802.38699.66

195. Legault J, Baldeviano G, Barin J, et al. IL6 is necessary for the progression of experimental autoimmune myocarditis to dilated cardiomyopathy. *J Immunol*. 2012;188(1 Supplement):171.11 LP-171.11. http://www.jimmunol.org/content/188/1_Supplement/171.11.abstract

196. Yamashita T, Iwakura T, Matsui K, et al. IL-6-mediated Th17 differentiation through RORγt is essential for the initiation of experimental autoimmune myocarditis. *Cardiovasc Res*. 2011;91(4):640-648. doi:10.1093/cvr/cvr148

197. Lv HJ, Havari E, Pinto S, et al. Impaired thymic tolerance to α-myosin directs autoimmunity to the heart in mice and humans. *J Clin Invest*. 2011;121(4):1561-1573. doi:10.1172/JCI44583

198. Vdovenko D, Eriksson U. Regulatory Role of CD4 + T Cells in Myocarditis . *J Immunol Res*. 2018;2018:1-11. doi:10.1155/2018/4396351

199. Eriksson U, Ricci R, Hunziker L, et al. Dendritic cell–induced autoimmune heart failure requires cooperation between adaptive and innate immunity. *Nat Med*. 2003;9(12):1484-1490. doi:10.1038/nm960

200. Gil-Cruz C, Perez-Shibayama C, de Martin A, et al. Microbiota-derived peptide mimics drive lethal inflammatory cardiomyopathy. *Science (80-)*. 2019;366(6467):881-886. doi:10.1126/science.aav3487

201. Kadomatsu K, Tomomura M, Muramatsu T. cDNA cloning and sequencing of a new gene intensely expressed in early differentiation stages of embryonal carcinoma cells and in mid-gestation period of mouse embryogenesis. *Biochem Biophys Res Commun*. 1988;151(3):1312-1318. doi:10.1016/S0006-291X(88)80505-9

202. Muramatsu T. Midkine and pleiotrophin: two related proteins involved in development, survival, infammation and tumorigenesis. *J Biochem*. 2002;132(3):359-371.

203. Tomomura M, Kadomatsu K, Nakamoto M, et al. A retinoic acid responsive

gene, MK, produces a secreted protein with heparin binding activity. *Biochem Biophys Res Commun*. 1990;171(2):603-609. doi:10.1016/0006-291X(90)91189-Y

204. Kerzerho J, Adotevi O, Castelli FA, et al. The Angiogenic Growth Factor and Biomarker Midkine Is a Tumor-Shared Antigen. *J Immunol*. 2010;185(1):418-423. doi:10.4049/jimmunol.0901014

205. Muramatsu T. Midkine: A Promising Molecule for Drug Development to Treat Diseases of the Central Nervous System. *Curr Pharm Des*. 2011;17(5):410-423. doi:10.2174/138161211795164167

206. Weckbach LT, Groesser L, Borgolte J, et al. Midkine acts as proangiogenic cytokine in hypoxia-induced angiogenesis. *Am J Physiol Circ Physiol*. 2012;303(4):H429-H438. doi:10.1152/ajpheart.00934.2011

207. Weckbach LT, Muramatsu T, Walzog B. Midkine in Inflammation. *Sci World J*. 2011;11:2491-2505. doi:10.1100/2011/517152

208. Kosugi T, Yuzawa Y, Sato W, et al. Midkine is involved in tubulointerstitial inflammation associated with diabetic nephropathy. *Lab Investig*. 2007;87(9):903-913. doi:10.1038/labinvest.3700599

209. Shindo E, Nanki T, Kusunoki N, et al. The growth factor midkine may play a pathophysiological role in rheumatoid arthritis. *Mod Rheumatol*. 2017;27(1):54-59. doi:10.1080/14397595.2016.1179860

210. Wang J, Takeuchi H, Sonobe Y, et al. Inhibition of midkine alleviates experimental autoimmune encephalomyelitis through the expansion of regulatory T cell population. *Proc Natl Acad Sci U S A*. 2008;105(10):3915-3920. doi:10.1073/pnas.0709592105

211. Takeuchi H. Midkine and multiple sclerosis. *Br J Pharmacol*. 2014;171(4):931-935. doi:10.1111/bph.12499

212. Krzystek-Korpacka M, Neubauer K, Matusiewicz M. Circulating midkine in Crohn's disease: Clinical implications. *Inflamm Bowel Dis*. 2010;16(2):208-215. doi:10.1002/ibd.21011

213. Jones DR. Measuring midkine: the utility of midkine as a biomarker in cancer and other diseases. *Br J Pharmacol*. 2014;171(12):2925-2939. doi:10.1111/bph.12601

214. Jono H, Ando Y. Midkine: A novel prognostic biomarker for cancer. *Cancers (Basel)*. 2010;2(2):624-641. doi:10.3390/cancers2020624

215. Lillis AP, Van Duyn LB, Murphy-Ullrich JE, Strickland DK. LDL Receptor-Related Protein 1: Unique Tissue-Specific Functions Revealed by Selective Gene Knockout Studies. *Physiol Rev*. 2008;88(3):887-918. doi:10.1152/physrev.00033.2007

216. Chen S, Bu G, Takei Y, et al. Midkine and LDL-receptor-related protein 1 contribute to the anchorage-independent cell growth of cancer cells. *J Cell Sci*. 2007;120(22):4009-4015. doi:10.1242/jcs.013946

217. Ranganathan S, Cao C, Catania J, Migliorini M, Zhang L, Strickland DK. Molecular Basis for the Interaction of Low Density Lipoprotein Receptor-related Protein 1 (LRP1) with Integrin $\alpha_M \beta_2$. *J Biol Chem*. 2011;286(35):30535-30541. doi:10.1074/jbc.M111.265413

218. Spijkers PPEM, da Costa Martins P, Westein E, Gahmberg CG, Zwaginga JJ, Lenting PJ. LDL-receptor–related protein regulates β2-integrin–mediated leukocyte adhesion. *Blood*. 2005;105(1):170-177. doi:10.1182/blood-2004-02-0498

219. Weckbach LT, Gola A, Winkelmann M, et al. The cytokine midkine supports neutrophil trafficking during acute inflammation by promoting adhesion via b2 integrins (CD11/CD18). *Blood*. 2014;123(12):1887-1896. doi:10.1182/blood-2013-06-510875

220. Herter, J and Mayadas T. Comment: Midkine, a middle manager of B2 integrins. *Blood*. 2014;123(12):2-3.

221. Masuda T, Maeda K, Sato W, et al. Growth Factor Midkine Promotes Nuclear Factor of Activated T Cells–Regulated T-Cell–Activation and Th1 Cell Differentiation in Lupus Nephritis. *Am J Pathol*. 2017;0(0). doi:10.1016/j.ajpath.2016.12.006

222. Livak KJ, Schmittgen TD. Analysis of Relative Gene Expression Data Using Real-Time Quantitative PCR and the 2−ΔΔCT Method. *Methods*. 2001;25(4):402-408. doi:10.1006/meth.2001.1262

223. Pummerer CL, Luze K, Grässl G, et al. Identification of cardiac myosin peptides capable of inducing autoimmune myocarditis in BALB/c mice. *J Clin Invest*. 1996;97(9):2057-2062. doi:10.1172/JCI118642

224. Stull LB, DiIulio NA, Yu M, et al. Alterations in Cardiac Function and Gene Expression during Autoimmune Myocarditis in Mice. *J Mol Cell Cardiol*. 2000;32(11):2035-2049. doi:10.1006/jmcc.2000.1235

225. Weckbach LT, Gola A, Winkelmann M, et al. The cytokine midkine supports

neutrophil trafficking during acute inflammation by promoting adhesion via b2 integrins (CD11/CD18). *Blood*. 2014;123(12):1887-1896. doi:10.1182/blood-2013-06-510875.The

226. Prasad JM, Migliorini M, Galisteo R, Strickland DK. Generation of a potent low density lipoprotein receptor-related protein 1 (LRP1) antagonist by engineering a stable form of the receptor-associated protein (RAP) D3 domain. *J Biol Chem*. 2015;290(28):17262-17268. doi:10.1074/jbc.M115.660084

227. Redecke V, Wu R, Zhou J, et al. Hematopoietic progenitor cell lines with myeloid and lymphoid potential. *Nat Methods*. 2013;10(8):795-803. doi:10.1038/nmeth.2510

228. Wang GG, Calvo KR, Pasillas MP, Sykes DB, Häcker H, Kamps MP. Quantitative production of macrophages or neutrophils ex vivo using conditional Hoxb8. *Nat Methods*. 2006;3(4):287-293. doi:10.1038/nmeth865

229. Meng W, Paunel-Görgülü A, Flohé S, et al. Deoxyribonuclease is a potential counter regulator of aberrant neutrophil extracellular traps formation after major trauma. *Mediators Inflamm*. 2012;2012. doi:10.1155/2012/149560

230. Yuan L, Kyouhei A, Monica B, et al. Inhibitors and Inactivators of Protein Arginine Deiminase 4: Functional and Structural Characterization. *Biochemistry*. 2006;45(39):11727–11736.

231. Lande R, Gilliet M. Plasmacytoid dendritic cells: key players in the initiation and regulation of immune responses. *Ann N Y Acad Sci*. 2010;1183(1):89-103. doi:10.1111/j.1749-6632.2009.05152.x

232. Kang J, Zhang HY, Feng GD, Feng DY, Jia HG. Development of an improved animal model of experimental autoimmune myositis. *Int J Clin Exp Pathol*. 2015;8(11):14457-14464.

233. Neu N, Ploier B. Experimentally-Induced Autoimmune Myocarditis: Production of Heart Myosin-Specific Autoantibodies Within the Inflammatory Infiltrate. *Autoimmunity*. 1991;8(4):317-322. doi:10.3109/08916939109007639

234. Čiháková D, Sharma RB, Fairweather D, Afanasyeva M, Rose NR. Animal Models for Autoimmune Myocarditis and Autoimmune Thyroiditis. In: *Autoimmunity*. Humana Press; :175-194. doi:10.1385/1-59259-805-6:175

235. Fontes JA, Barin JG, Talor M V., et al. Complete Freund's adjuvant induces experimental autoimmune myocarditis by enhancing IL-6 production during initiation of the immune response. *Immun Inflamm Dis*. 2017;5(2):163-176. doi:10.1002/iid3.155

236. Stills HF. Adjuvants and antibody production: Dispelling the myths associated with Freund's complete and other adjuvants. *ILAR J*. 2005;46(3):280-293. doi:10.1093/ilar.46.3.280

237. Ghasemlou N, Chiu IM, Julien JP, Woolf CJ. CD11b+Ly6G- myeloid cells mediate mechanical inflammatory pain hypersensitivity. *Proc Natl Acad Sci U S A*. 2015;112(49):E6808-E6817. doi:10.1073/pnas.1501372112

238. Andermann ML, Lowell BB. Toward a Wiring Diagram Understanding of Appetite Control. *Neuron*. 2017;95(4):757-778. doi:10.1016/j.neuron.2017.06.014

239. Hankenson FC, Ruskoski N, van Saun M, Ying GS, Oh J, Fraser NW. Weight loss and reduced body temperature determine humane endpoints in a mouse model of ocular herpesvirus infection. *J Am Assoc Lab Anim Sci*. 2013;52(3):277-285. http://www.ncbi.nlm.nih.gov/pubmed/23849410

240. Campbell IK, O'Donnell K, Lawlor KE, Wicks IP. Severe inflammatory arthritis and lymphadenopathy in the absence of TNF. *J Clin Invest*. 2001;107(12):1519-1527. doi:10.1172/JCI12724

241. Ismahil MA, Hamid T, Bansal SS, Patel B, Kingery JR, Prabhu SD. Remodeling of the Mononuclear Phagocyte Network Underlies Chronic Inflammation and Disease Progression in Heart Failure. *Circ Res*. 2014;114(2):266-282. doi:10.1161/CIRCRESAHA.113.301720

242. Woulfe KC, Sucharov CC. Midkine's Role in Cardiac Pathology. *J Cardiovasc Dev Dis*. 2017;4(4):13. doi:10.3390/jcdd4030013

243. Muramatsu T, Kadomatsu K. Midkine: An emerging target of drug development for treatment of multiple diseases. *Br J Pharmacol*. 2014;171(4):811-813. doi:10.1111/bph.12571

244. Novotny WF, Maffi T, Mehta RL, Milner PG. Identification of novel heparin-releasable proteins, as well as the cytokines midkine and pleiotrophin, in human postheparin plasma. *Arterioscler Thromb A J Vasc Biol*. 1993;13(12):1798-1805. doi:10.1161/01.ATV.13.12.1798

245. Khandpur R, Carmona-Rivera C, Vivekanandan-Giri A, et al. NETs Are a Source of Citrullinated Autoantigens and Stimulate Inflammatory Responses in Rheumatoid Arthritis. *Sci Transl Med*. 2013;5(178):178ra40-178ra40. doi:10.1126/scitranslmed.3005580

246. van der Linden M, van den Hoogen LL, Westerlaken GHA, et al. Neutrophil extracellular trap release is associated with antinuclear antibodies in systemic

lupus erythematosus and anti-phospholipid syndrome. *Rheumatol (United Kingdom)*. 2018;57(7):1228-1234. doi:10.1093/rheumatology/key067

247. Knight JS, Zhao W, Luo W, et al. Peptidylarginine deiminase inhibition is immunomodulatory and vasculoprotective in murine lupus. *J Clin Invest*. 2013;123(7):2981-2993. doi:10.1172/JCI67390

248. Jang B, Kim HW, Kim JS, et al. Peptidylarginine deiminase inhibition impairs Toll-like receptor agonist-induced functional maturation of dendritic cells, resulting in the loss of T cell-proliferative capacity: a partial mechanism with therapeutic potential in inflammatory settings. *J Leukoc Biol*. 2015;97(2):351-362. doi:10.1189/jlb.3A0314-142RR

249. Chrysanthopoulou A, Mitroulis I, Apostolidou E, et al. Neutrophil extracellular traps promote differentiation and function of fibroblasts. *J Pathol*. 2014;233(3):294-307. doi:10.1002/path.4359

250. Chirivi RGS, van Rosmalen JWG, van der Linden M, et al. Therapeutic ACPA inhibits NET formation: a potential therapy for neutrophil-mediated inflammatory diseases. *Cell Mol Immunol*. 2020;(June 2019). doi:10.1038/s41423-020-0381-3

251. Gollomp K, Kim M, Johnston I, et al. Neutrophil accumulation and NET release contribute to thrombosis in HIT. *JCI Insight*. 2018;3(18). doi:10.1172/jci.insight.99445

252. Martinod K, Witsch T, Erpenbeck L, et al. Peptidylarginine deiminase 4 promotes age-related organ fibrosis. *J Exp Med*. Published online 2016:jem.20160530. doi:10.1084/jem.20160530

253. Jiang DS, Bian ZY, Zhang Y, et al. Role of Interferon Regulatory Factor 4 in the Regulation of Pathological Cardiac Hypertrophy. *Hypertension*. 2013;61(6):1193-1202. doi:10.1161/HYPERTENSIONAHA.111.00614

254. Van der Borght K, Lambrecht BN. Heart macrophages and dendritic cells in sickness and in health: A tale of a complicated marriage. *Cell Immunol*. 2018;330:105-113. doi:10.1016/j.cellimm.2018.03.011

255. Arimura K, Takagi H, Uto T, et al. Crucial role of plasmacytoid dendritic cells in the development of acute colitis through the regulation of intestinal inflammation. *Mucosal Immunol*. 2017;10(4):957-970. doi:10.1038/mi.2016.96

256. Rönnblom L, Leonard D. Interferon pathway in SLE: One key to unlocking the mystery of the disease. *Lupus Sci Med*. 2019;6(1):1-11. doi:10.1136/lupus-2018-000270

257. Anzai A, Mindur JE, Halle L, et al. Self-reactive CD4 + IL-3 + T cells amplify autoimmune inflammation in myocarditis by inciting monocyte chemotaxis. 2019;216(2):369-383.

258. Pistulli R, Andreas E, König S, et al. Characterization of dendritic cells in human and experimental myocarditis. *ESC Hear Fail*. 2020;7(5):2305-2317. doi:10.1002/ehf2.12767

259. Crow MK. Type I Interferon in the Pathogenesis of Lupus Systemic Lupus Erythematosus. *J Immunol*. 2014;192(12):5459-5468. doi:10.4049/jimmunol.1002795.Type

260. King KR, Aguirre AD, Ye YX, et al. +. *Nat Med*. 2017;23(12):1481-1487. doi:10.1038/nm.4428

261. Arai Y, Yamashita K, Kuriyama K, et al. Plasmacytoid Dendritic Cell Activation and IFN-α Production Are Prominent Features of Murine Autoimmune Pancreatitis and Human IgG4-Related Autoimmune Pancreatitis. *J Immunol*. 2015;195(7):3033-3044. doi:10.4049/jimmunol.1500971

262. Attallah AM, Strong DM. Differential Effects of Interferon on the MHC Expression of Human Lymphocytes. *Int Arch Allergy Immunol*. 1979;60(1):101-105. doi:10.1159/000232328

263. Barrat FJ, Su L. A pathogenic role of plasmacytoid dendritic cells in autoimmunity and chronic viral infection. *J Exp Med*. 2019;216(9):1974-1985. doi:10.1084/jem.20181359

264. Yu CF, Peng WM, Oldenburg J, et al. Human Plasmacytoid Dendritic Cells Support Th17 Cell Effector Function in Response to TLR7 Ligation. *J Immunol*. 2010;184(3):1159-1167. doi:10.4049/jimmunol.0901706

265. Zimmermann M, Arruda-Silva F, Bianchetto-Aguilera F, et al. IFNα enhances the production of IL-6 by human neutrophils activated via TLR8. *Sci Rep*. 2016;6(December 2015):1-13. doi:10.1038/srep19674

Acknowledgements

This work could not have been completed without the help and support of various people.

First, and foremost, I would like to thank Prof. Dr. Alexander Bartelt for making it possible for me to still submit the work. I am very grateful for taking over my supervision. Thank you for your support and time! I would also like to say thank you to Prof. Dr. Barbara Walzog and Dr. med Ludwig Weckbach for giving me the opportunity to work on this fascinating project in their lab.

I also would like to acknowledge the SFB914 for funding my project and the associated IRTG for all the excellent professional training opportunities. A special thanks to Dr. Verena Kochan, for helping whenever necessary. I am also thankful to all the members of the Walter Brendel Center for a great working atmosphere.

I am grateful for the generous help of all current and former members of the Walzog and Weckbach group providing constructive criticism, advice on experimental techniques, and a great working atmosphere. In this respect I would like to mention Judith Arcifa and Andreas Uhl in particular. Thank you for your outstanding advisory and technical support. Additionally, I would like to thank Dr. Susanne Stutte for her advisory and technical support and the outstanding discussions in the lab about pDCs. Also thanks to the rest of the Walzog lab for the good atmosphere and support, on both professional and personal levels: Annette Zehrer, Jennifer Truong, Melanie Salvermoser, Ann-Cathrin Werner and Anna-Karina Becker.

Special thanks to colleagues who became friends during this time. Without them my time as a doctoral student would have been much harder to endure.

This exciting phase of my life was only possible by the emotional support and love of my family and friends. I would like to thank my beloved friends and family, especially my mom, for their endless support, love and patience throughout all these years of hard work, scientific challenges, emotional ups and downs and endless emotional talks and support that enabled me to submit this PhD thesis. Your endless understanding and faith in me gave me so much energy. I am beyond grateful and could have never done this without any single one of you!

Special thanks to Sophia and Juli for pushing me beyond my limits in the very last phase, when I almost gave up on the work, and tirelessly pushed me not to give up and fight.

I wish I could give you all back the double of everything you did and still do for me!

DANKE!

Publications

List of publications

Parts of the following data are published in *the Journal of Experimental Medicine*: Weckbach LT, Grabmaier U, Uhl A, Gess S, **Boehm F**, Zehrer A, Pick R, Salvermoser M, Czermak T, Pircher J, Sorrelle N, Migliorini M, Strickland DK, Klingel K, Brinkmann V, Abu Abed U, Eriksson U, Massberg S, Brunner S, Walzog B. Midkine drives cardiac inflammation by promoting neutrophil trafficking and NETosis in myocarditis*. J Exp Med*. 2019 Feb 4;216(2):350-368[51].

Additional publications

Weckbach LT, Uhl A, **Boehm F**, Seitelberger V, Huber BC, Kania G, Brunner S, Grabmaier U. Blocking LFA-1 Aggravates Cardiac Inflammation in Experimental Autoimmune Myocarditis. *Cells*. 2019 Oct 17;8(10):1267.

Wolf K, Kühn H, **Boehm F**, Gebhardt L, Glaudo M, Agelopoulos K, Ständer S, Ectors P, Zahn D, Riedel YK, Thimm D, Müller CE, Kretschmann S, Kremer AN, Chien D, Limjunyawong N, Peng Q, Dong X, Kolkhir P, Scheffel J, Søgaard ML, Weigmann B, Neurath MF, Hawro T, Metz M, Fischer MJM, Kremer AE. A group of cationic amphiphilic drugs activates MRGPRX2 and induces scratching behavior in mice. *J Allergy Clin Immunol.* 2021 Feb 20:S0091-6749(21)00229-3.

Scientific presentations & Conference attendances:

02/2020 Interact, Munich, Germany

11/2019 Annual Retreat of the IRTG of the SFB 914, Herrsching, Germany (oral presentation)

05/2019 53rd Annual Meeting oft he European Society for clinical Investigation (ESCI), Coimbra, Portugal

11/2018 Annual Retreat of the IRTG of the SFB 914, Günzburg, Germany (poster presentation)

05/2018 5th Midkine Symposium, Munich, Germany

03/2018 2nd International Conference on Leukocyte Trafficking, Munich, Germany

Affidavit

Affidavit

Böhm, Felicitas

Surname, first name

Street

Zip code, town, country

I hereby declare, that the submitted thesis entitled

The molecular insights into the pathogenesis of myocarditis

is my own work. I have only used the sources indicated and have not made unauthorized use of services of a third party. Where the work of others has been quoted or reproduced, the source is always given.

I further declare that the submitted thesis or parts thereof have not been presented as part of an examination degree to any other university.

München, 10.08.2023

Place, date

Felicitas Böhm

Signature doctoral candidate